August 2015

Structure-Property Relationships at the Nano-Bio Interface: Engineering the Nanoparticle Surface for Immunomodulation

Daniel Fernando Moyano Marino
University of Massachusetts Amherst

STRUCTURE-PROPERTY RELATIONSHIPS AT THE NANO-BIO INTERFACE: ENGINEERING THE NANOPARTICLE SURFACE FOR IMMUNOMODULATION

Dissertation Presented

by

DANIEL F. MOYANO-MARIÑO

Submitted to the Graduate School of the
University of Massachusetts Amherst
in partial fulfillment of the requirements for the degree of

DOCTOR OF PHILOSOPHY

May 2015

Chemistry

STRUCTURE-PROPERTY RELATIONSHIPS AT THE
NANO-BIO INTERFACE: ENGINEERING THE NANOPARTICLE
SURFACE FOR IMMUNOMODULATION

Dissertation Presented
by
DANIEL F. MOYANO-MARIÑO

Approved as to style and content by:

_____
Vincent M. Rotello, Chair

_____
Lynmarie K. Thompson, Member

_____
Michael J. Knapp, Member

_____
Sam R. Nugen, Member

_____
Craig T. Martin,
Department Head Department of Chemistry

“A veces me pregunto qué razones
Me mueven a estudiar sin esperanza
De precisión, mientras mi noche avanza,
La lengua de los ásperos sajones.

Gastada por los años la memoria
Deja caer la en vano repetida
Palabra y es así como mi vida
Teje y desteje su cansada historia.

Será (me digo entonces) que de un modo
Secreto y suficiente el alma sabe
Que es inmortal y que su vasto y grave
Círculo abarca todo y puede todo.

Más allá de este afán y de este verso
Me queda inagotable el universo.”

Jorge Luis Borges
(Poem written in a copy of Beowulf)

A mi madre y a mi padre,
quienes me infundaron el insaciable deseo de aprender de este universo iridiscente.

ACKNOWLEDGEMENTS

I would like to express my gratitude to my advisor Prof. Vincent M. Rotello for his guidance and for the opportunity that he gave to explore my diverse scientific interests. He was a vital part of all my work, guiding aspects of both doing and communicating science. Likewise, I would like to thank Prof. Dan Peer whose help allowed this project to begin, and to Prof. Barbara Osborne for her guidance during my adventures in the world of immunology.

I would also like to thank my collaborators Krishnendu, Gyan, Yuanchang, Akash, Furkan, Gokhan, Rubul, Rui, Moumita, Xiaoning, Singyuk, Bo, Gülen, Tsukasa, Bradley, Meir, Rochelle, Oscar, and Subinoy, whose help was vital in the development of my scientific endeavors during and the work described in this thesis. Similarly, I would like to thank my committee members Prof. Michael Knapp, Prof. Lynmarie Thompson, and Prof. Sam Nugen for their advice and the valuable time that they dedicated to this work.

Now, I would like to take this opportunity to thank my Amherst friends NLe, Tsuki, Rui, Xiaoning, Ziwen, Dave, Cris, Andrea, Mario, Aleja, Moumis, Tülin, Meli, Diego and Ying for their friendship, I will always treasure the memories of our adventures in New England. Special thanks goes to my dear friend Luis for his invaluable friendship, to Krish a kind spirit and a true friend, and to Rubul for our philosophical debates.

I would like to thank my parents Pablo Moyano and Betty Mariño, and my brother German Moyano for their unconditional love and help, gracias por todo, simplemente gracias. Finally I would like to thank my wife, Diana Parra, for her humble love and vivid company that made my life happy. I hope we can continue to travel together in this and the other life.

ABSTRACT

STRUCTURE-PROPERTY RELATIONSHIPS AT THE NANO-BIO INTERFACE: ENGINEERING THE NANOPARTICLE SURFACE FOR IMMUNOMODULATION

MAY 2015

DANIEL F. MOYANO-MARIÑO,
B.Sc., NATIONAL UNIVERSITY OF COLOMBIA
Ph.D., UNIVERSITY OF MASSACHUSETTS AMHERST
Directed by: Professor Vincent M. Rotello

Each year, a variety of novel nanomaterials are being developed with the objective of treating different diseases. However, since nanomaterials are foreign to the human body, one of the principal factors that limit their use is the encounter with the first line of defense from the body: the immune system. If this interaction is not taken into account, an undesired recognition takes place and the efficiency of nanoparticle-based therapies is dramatically reduced. As such, understanding the rules that govern this recognition is of prime importance in the field of nanomedicine. Following this line of thoughts (the driving force), the work described in this dissertation takes a systematic approach to understand and use the relationship between immunological responses and the chemical nature of the nanoparticle surface. We first explored the chemical rules of the immunological recognition, to then re-engineer our materials based on the acquired knowledge, setting a final goal in the development of new nanomaterials capable of modulating immune responses. Our findings demonstrated not only the vast potential of nanomaterials for their use in immunotherapies, but also the power of Chemistry in the development of these systems.

TABLE OF CONTENTS

Page

LIST OF FIGURES

Figure Page

CHAPTER 1

THE NANOPARTICLE SURFACE CHEMISTRY AND ITS RELEVANCE FOR IMMUNOMODULATION

"In all the things of nature there is something of the marvelous"
- Aristotle, *De Partibus Animalium*

1.1. The nano-bio interface

The use of nanoparticles (NPs) in biological applications has increased exponentially during the last decade.[1] This is the result of the unique properties that nanomaterials offer compared to bulk materials and small molecules, such as high surface-to-volume ratio[2] and commensurate size with biomacromolecules.[3] These properties allow NPs to interact in multiple ways with proteins and other macromolecules relevant in cell biology, making them an ideal platform for a variety of biomedical applications, including imaging,[4] delivery[5] and sensing.[6] Nanomaterials can be synthesized in a variety of forms and sizes,[7] and can be coated with a diversity of ligands,[8] giving birth to an almost infinite variety of possibilities. By changing the size (from 1 nm to 200 nm), shape (spheres, cubes, stars, rods) and materials (polymers, metals, lipids) nanomaterials with different physical, chemical and biological properties can be obtained.[9] The art of engineering nanomaterials and understanding their interaction with biosystems is multiparametric in nature.

Despite this variety of properties, one of the most critical factors that influence the interaction of NPs with the outside world is the nature of the NP surface (Figure 1.1).[10] Understanding events that take place at the nano-bio interface is fundamentally important for the

use of these materials in therapy and diagnostics. For example, an understanding of how NPs interact with nucleic acids and proteins has allowed the use of NPs as delivery vehicles.[11] Similarly, by tuning the interaction of NPs with enzymes and proteins, a variety of sensors have been developed.[12] The work described in this dissertation aims to obtain clues on how NPs interact with the immune system, and how, by modifying chemical properties of the NP surface, control of those responses can be achieved. First, let us illustrate recent advances on the understanding of the interaction of NPs with different components of the immune system, and their importance in the context of nanomedicine.

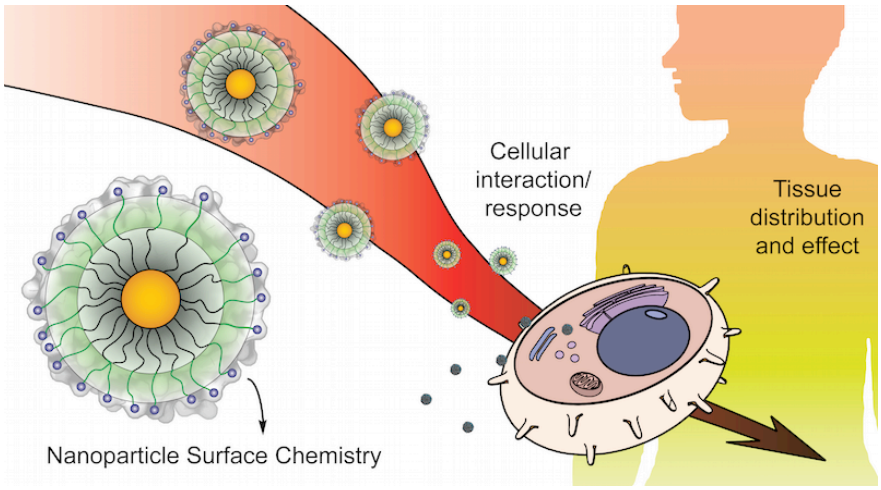

Figure 1.1. The chemical nature of the nanoparticle surface dictates the recognition and response of these materials at the cellular level, which in turn induces the desired physiological effects.

1.2. Nanoparticle in immunomodulation

As described before, the NP surface critically influences the activity of many biological systems, opening new avenues for the use of nanomaterials in therapeutic applications. One of these applications is the modulation of immunological responses, with important implications ranging from the prevention of different diseases (by the enhancement of vaccines and immuno-

therapies), to the development of new stealth delivery vehicles.[13] The immune system is the prime defense barrier that living organisms present when foreign entities try to gain access to the body. Depending on how the immune system recognizes the foreign entities (like NPs) different types of immunological responses are triggered.[14] It is clear that understanding the interaction between NPs and the immune system is of critical importance to both develop new NP-based therapies, and to understand the fundamental chemical rules that govern immune recognition. Many parameters of the nanoparticle surface chemistry influence the immunological fate of NPs.

Surface charge: The use of NPs as carriers for the delivery of therapeutic molecules is one of the major applications of nanomaterials in biological systems. A significant amount of research has been directed towards the development of carriers that have minimal interaction with the immune system to increase delivery efficiency. One of the properties that most delivery vehicles share is the presence of a net positive charge at the surface, often use for complementarity with the therapeutic molecule (i. e. nucleic acids and/or anionic proteins), or generated as a result of the surfactant that is used to create the NPs.[15] However, it has been observed that cationic systems induce the activation of inflammatory responses, even when used in concentrations below the cytotoxic threshold. For example, Peer et al. performed a systematic study of the effect of the NP charge in the expression of cytokines, a group of proteins that indicate the activation of an immune response.[16] They observed that positively-charged lipid NPs produced a strong immunological effect, 10-20 fold higher than that for neutral and anionic NPs. The study suggested that Toll-like Receptor 4, a surface receptor that is known to mediate the activation of inflammatory pathways in different cells of the immune system, may be involved in this recognition. Similarly, other receptors have been also identified as possible pathways for the recognition of charged systems, such as a variety of scavenger receptors.[17] However, this is not the only way by which the immune system can identify foreign charged systems. Another effect that needs to be taken into consideration is the non-specific adsorption of proteins over the NP surface, namely the formation of a protein corona. When NPs are injected in the mammalian

body, this corona often includes a series of proteins called opsonins (such as C1q and C3b) whose only function is to tag foreign bodies for their fast elimination.[18] The binding of these proteins to charged NP surfaces induces activation of the complement system and macrophage recruitment, initiating the cascade of immune responses that reduces the circulation time of these systems.

Poly(ethylene glycol) (PEG): PEGylation is one of the most successful approaches to control the stability of NPs in biological fluids that not only reduces non-specific protein adsorption, but also improves the circulation time of NPs. After PEG modification, nanoparticles can be decorated with different molecular structures such as antibodies, oligonucleotides, and peptides, allowing their use in active targeting and immunotherapy. However, despite its fame as the ideal non-fouling coating, PEG on its own seems to be recognized by the immune system. For example, Jiang et. al. demonstrated that PEGylated NPs could induce the secretion of anti-PEG antibodies, accelerating the blood clearance of these systems, while other non-fouling coatings, such as zwitterions, did not induce this effect (Figure 1.2a).[19] Likewise, reports on the recognition of PEG structures by proteins from the complement system (similar to cationic NPs) have been presented.[20] These studies suggested that the density and chain length of PEG are crucial parameters for the immunogenicity of these systems, as these parameters influence cellular binding, uptake, and degradation. It is important to note that these effects might compromise the efficacy and safety of the use of PEG in biomedical applications. As an example, *in vivo* studies showed that PEG (5000)-coated NPs induced acute inflammation and apoptosis in the liver of mice.[21]

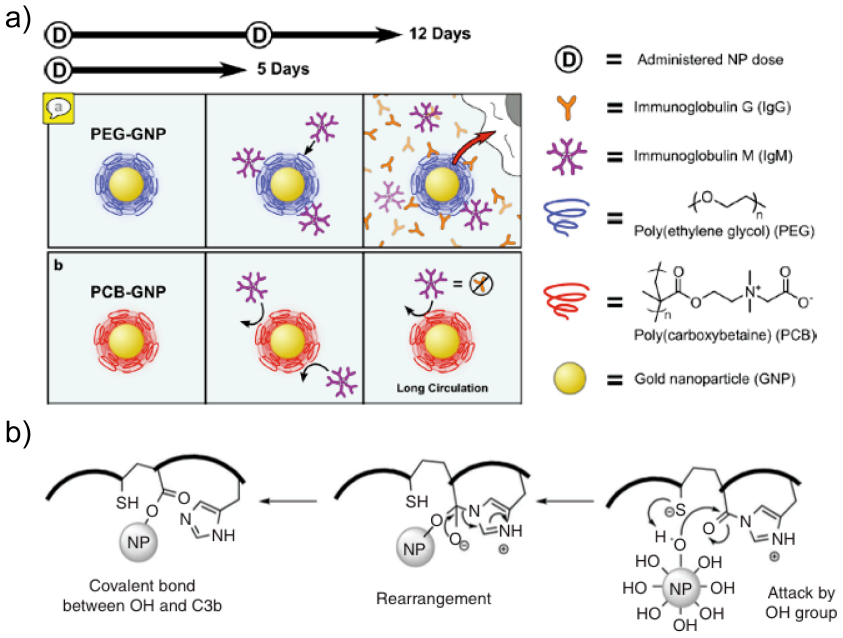

Figure 1.2. a) Schematic illustration of the sequence of events after PEG-AuNPs and zwitterionic-AuNPs enter the blood stream. b) Proposed mechanism of the binding of PEG-NPs with proteins of the complement system. Reproduced with permission from references 19 and 22 respectively.

These properties, however, can also be tailored for their use in therapy. As an example, Hubbell et al. used PEG modified NPs as a platform to both deliver and boost the recognition of a specific antigen.[22] By inverse emulsion polymerization, PEG and poly(propylene glycol) (PPG) were copolymerized to achieve NPs that were efficiently and quickly taken and transported to the lymph node, achieving the intended delivery to the lymph node resident dendritic cells. The study suggests that the presence of PEG is crucial for this process as the binding of hydroxyl terminal groups with the exposed thioester of the complement protein C3b initiates complement activation and induced maturation of dendritic cells (Figure 1.2b). As a result, the PEG-NPs induced a strong adjuvant activity when conjugated with ovalbumin, up-regulating both humoral and cellular immunity, and producing strong levels of anti-ovalbumin immunoglobulin.

Aliphatic chains (hydrophobic portions): Hydrophobic portions, such as aliphatic and aromatic residues, have been also hypothesized to be involved in the activation of the immune system. This idea comes from the fact that the immune system needs to recognize molecular patterns that indicate damage at the cellular level to activate the repair machinery. These markers, term as damaged-associated molecular patterns, and commonly known as "danger signals", consist of structural motifs that under normal conditions would not be exposed to the extracellular environment, but get released when cellular damage occurs.[23] As such, it is considered that hydrophobic portions that are normally hidden inside the cellular membrane may serve as one such danger signal. As will be discussed in Chapter 2, we functionalized NPs with different degrees of hydrophobicity by the use of different aliphatic residues, and measured cytokine expression after exposing splenocytes to the NPs. Our findings showed a direct correlation between the hydrophobicity of NPs and cytokine expression, while other functionalities such as H-bond donors/acceptors did not affect the response. Interestingly, this effect was observed for pro- and anti-inflammatory cytokines both *in vitro* and *in vivo*. Similar results were observed by the Santos group by the use of thermally hydrocarbonized porous silicon NPs, reporting not only an increase in the cytokine expression, but also the increase the maturation of dendritic cells.[24] Likewise, other studies using poly(D,L-lactic acid), poly(D,L-lactic-co-glycolic acid), and poly(monomethoxypolyethylene glycol-co-D,L-lactide), polymers that offer different degrees of hydrophobicity while maintaining constant the particle size, demonstrated an increase in antigen internalization by dendritic cells for particles of larger hydrophobicity, along with an increase in the expression of certain surface receptors.[25] Finally, hydrophobic portions have been also related to an increase in adjuvant capabilities by the use of poly(g-glutamic acid) with different degrees of grafting with L-phenylalanine ethyl ester.[26] This method showed an increase in antibody generation (along side an increase in inflammatory cytokines) when the grafting degree of the particles was larger (more hydrophobic). Taken together, these results suggest the generality of

the phenomenon and demonstrate the significant potential of hydrophobic portions for modulating of the immune responses towards NPs.

Amino acids: It is a well-known fact that the immune system has evolved to be able to recognize molecular motifs of proteins from the bacteria wall as foreign to generate an attack, or from the body as self to induce tolerance. It is a well-known fact that this distinction involves the recognition of specific amino acid sequences of those proteins. Based on this knowledge, Mingyao Liu et al. reported that bone marrow dendritic cells were activated by NPs bearing different types of small peptides.[27] The report shows that the activity depends on the peptide sequence, and as a general trend, the presence of aromatic amino acids induced more response. However, it seems that peptide presentation is an important factor given the fact that in some cases the peptide can be recognized only when coated on the surface of a NP. For example, Puntes et al. found that bone marrow macrophages could only recognize peptides when they were attached to gold NPs, while neither the peptide alone nor the control NPs were recognized.[28] The macrophage activation and subsequent cytokine release was dependent on peptide sequence at the NP surface instead of peptide length and polarity. Another interesting approach to this phenomenon is the study of peptides that make NP able to scape the response of the immune system. This is of critical importance for the development of more efficient delivery vehicles. Following this idea, Discher et al. functionalized polystyrene nanobeads with a variety of small self-peptides derived from the CD47 glycoprotein, trying to make NPs that resemble a self-entity.[29] By the use of this approach, they were able to delay macrophage-mediated clearance and promote persistent circulation, revealing the great potential of this technique in the development of new nanomaterials.

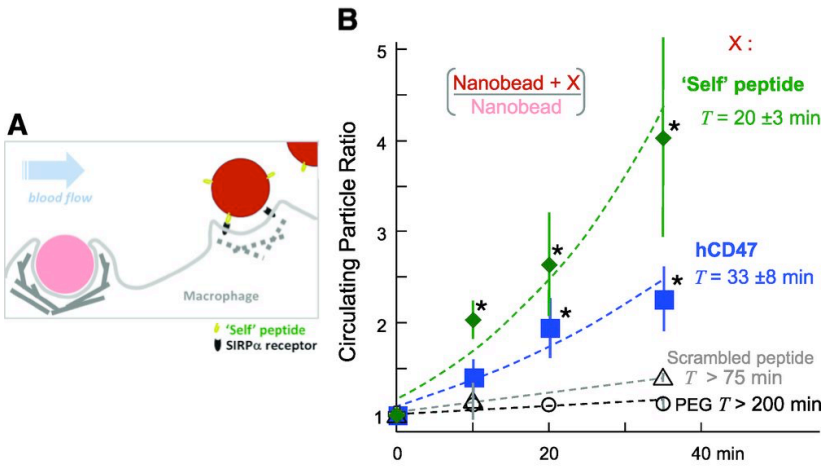

Figure 1.3. a) Schematic cartoon of the circulation of nanobeads with (recognized and released) and without (cleared) the self-peptide functionalization. c) Circulation profiles for the nanobeads functionalized with the self-peptide and different controls. Reproduced with permission from reference 29.

To achieve these activities, many different types of nanomaterials are being used, taking advantage of the great variety of nanomaterials available. However, to understand the underlying chemical phenomenon that is the interaction between NPs and the immune system, a uniform NP framework needs to be employed. The work described in this dissertation is based on the use of a gold nanoparticle system that has been developed in the Rotello lab for its optimal use in structure-activity correlation studies as described in the next section.[10]

1.3. Monolayer-protected gold nanoparticles

To ensure proper structure-activity correlations of the NP surface with biological activities, one must select an appropriate system that offers a means to vary one parameter at a time while maintaining other properties constant. Gold nanoparticles (AuNPs) offer a uniform system with properties that make them ideal for exploratory studies.[30] First, gold cores are intrinsically inert and they are non-toxic *per se*, allowing their integration in therapeutic applications.[31] Second, the

synthesis of highly monodisperse gold cores is relatively easy nowadays since the introduction of the Brust-Schiffrin methodology,[32] and the understanding of their properties is extensive and dating back to 1857 when Michael Faraday first described them (Faraday's gold).[33] Finally, an perhaps the most important characteristic, gold nanoparticles can be coated with a monolayer of ligands in a straightforward fashion taking advantage of the strong nature of the gold-thiol bond.[34] Using this methodology, many researches have functionalized AuNPs with small compounds and biologically relevant macromolecules, such as proteins and nucleic acids.[3] Once the core has been defined, the properties of the nanoparticle will rely principally in the chemical design of the surface ligand.

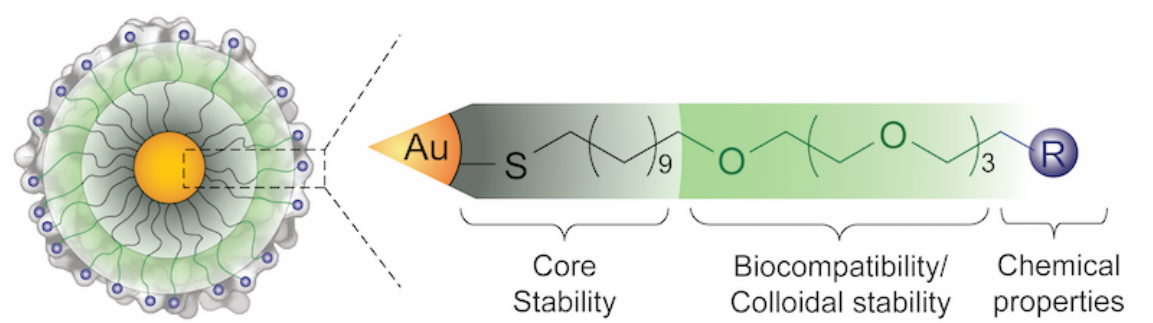

Figure 1.4. Chemical design of the nanoparticles used in this dissertation, specifically designed for structure-activity relationship studies with biological systems. To a gold core (~2nm), ligands are attached by the use of a thiol, followed by a hydrophobic section that inhibits core-core fusion. A tetra(ethylene glycol) spacer is then attached to confer stability in water, as well as to isolate the interior of the NP (eliminate interactions). The outer sphere of the NP (the surface) is composed of chemical groups that are modified at will to study their effects and to cause desired biological effects.

In order to achieve clear structure-property correlations when studying nanoparticles and biological systems, a uniform and non-interactive system is required to be used as a template in which the properties will be modified and studied. The development of the ideal non-interacting starting point (tabula rasa, i.e.,"blank slate") has been the work of various generations of chemists

in the Rotello group, and its creation (and constant evolution) has been reviewed elsewhere.[10] In general terms, and as depicted in Figure 1.4, after the thiol anchor that binds the NP with the ligand, a hydrophobic section is required for particle stability. An aliphatic section composed of 11 carbons has been utilized for this, as the use of shorter chains may induce core fusion, a phenomena that needs to be avoided. However, possible interactions arising from this hydrophobic chain need to be passivated, otherwise denaturation of the biological systems and other secondary effects may be seen if the hydrophobic section is not properly masked.[35] For this purpose, the next section of the ligand is composed of a tetra(ethylene glycol) spacer, that not only removes the mentioned background effects, but also promotes the solubility of the NPs in water, a requirement for their biological use.[36] The length of this spacer (4 ethylene glycols) has been optimized to minimize particle aggregation even in complex fluids.[37] Once the effects from the interior of the ligand have been removed, different functional groups can be attached to the ligand termini, to be displayed at the NP surface. After the different ligands have been attached to the NP core (achieved by a place-exchange reaction as explained in Section 2.4), we verify that all the other physiochemical properties are kept constant (e.g. size and surface charge), ensuring that the only change among the NPs is the chemical identity.[10] Using this methodology NPs can be functionalized with specific headgroups allowing us to ascertain the interactions of these functional groups with biosystems in a quantitative fashion.

1.4. Dissertation Overview

As described previously in this section, understanding the interaction of NPs with biological system is of significant importance for the appropriate use of these materials in nanomedicine. The research that I conducted during my graduate studies is based on this premise, and is divided in 2 sections: 1) understanding how chemical properties of the NP surface relate to

immunological properties, and 2) the development of new NP coatings to optimize the immunological outcomes.

In Chapter 2 we will see which chemical properties govern the immune recognition of NPs. Hydrophobicity rises as one of the most important factors, as a strong correlation between this property and immune responses is observed both *in vitro* and *in vivo*. However, we will also observe that due to the cationic nature of the NPs employed in these studies, protein adsorption limits the immunomodulatory control that can be achieved by our initial chemical design (Chapter 3). This challenge offered us the opportunity for the development of a new ligand to create NPs with the capability of displaying different degrees of hydrophobicity while reducing protein adsorption, which will be described in Chapter 4. Finally the evaluation of the immunomodulatory capabilities of these new systems in immunologically challenged systems is presented in Chapter 5.

1.5. References

1. a) Sperling, R. A.; Gil, P. R.; Zhang, F.; Zanella, M.; Parak, W. J. *Chem. Soc. Rev.* **2008**, *37*, 1896. b) Giljohann, D. A.; Seferos, D. S.; Daniel, W. L.; Massich, M. D.; Patel, P. C.; Mirkin, C. A. *Angew. Chem. Int. Ed.* **2010**, *49*, 3280.

2. a) Xia, X.-R.; Monteiro-Riviere, N. A.; Riviere, J. E. *Nat. Nanotechnol.* **2010**, *5*, 671. b) Leszczynski, J. *Nat. Nanotechnol.* **2010**, *5*, 633.

3. Niemeyer, C. M. *Angew. Chem. Int. Ed.* **2001**, *40*, 4128.

4. (a) Sharrna, P.; Brown, S.; Walter, G.; Santra, S.; Moudgil, B. *Adv. Colloid Interface Sci.* **2006**, *123*, 471. b) Lewin, M.; Carlesso, N.; Tung, C.-H.; Tang, X.-W.; Cory, D.; Scadden, D. T.; Weissleder, R. *Nat. Biotechnol.* **2000**, *18*, 410.

5. a) Ghosh, P.; Han, G.; De, M.; Kim, C. K.; Rotello, V. M. *Adv. Drug Deliver. Rev.* **2008**, *60*, 1307. b) Tonga, G. Y.; Moyano, D. F.; Kim, C. S.; Rotello, V. M. *Curr. Opin. Coll. Inter. Sci.* **2014**, *19*, 49.

6. a) Peng, G.; Hakim, M.; Broza, Y. Y.; Brillan, S.; Abdah-Bortnyak, R.; Kuten, A.; Tisch, U.; Haick, H. *Br. J. Cancer* **2010**, *103*, 542. b) Miranda, O. R.; Creran, B.; Rotello, V. M. *Curr. Opin. Chem. Biol.* **2010**, *14*, 728.

7. a) Grzelczak, M.; Pérez-Juste, J.; Mulvaney, P.; Liz-Marzán, L. M. *Chem. Soc. Rev.* **2008**, *37*, 1783. b) Tao, A. R.; Habas, S.; Yang, P. *Small* **2008**, *4*, 310.

8. a) Verma, A.; Stellacci, F. *Small* **2010**, *6*, 12. b) Nobs, L.; Buchegger, F.; Gurny, R.; Allémann, E. *J. Pharm. Sci.* **2004**, *93*, 1980.

9. Albanese, A.; Tang, P. S.; Chan, W. C. W. *Annu. Rev. Biomed. Eng.* **2012**, *14*, 1.

10. Moyano, D. F.; Rotello, V. M. *Langmuir* **2011**, *27*, 10376.

11. a) Li, W.; Szoka Jr., F. C. *Pharm. Res.* **2007**, *24*, 438. b) Ding, Y.; Jiang, Z.; Saha, K.; Kim, C. S.; Kim, S. T.; Landis, R. F.; Rotello, V. M. *Mol. Ther.* **2014**, *22*, 1075. c) Lai, W.-F.; Lin, M. C.-M. *J. Control. Release* **2009**, *134*, 158.

12. Saha, K.; Agasti, S. S.; Kim, C.; Li, X.; Rotello, V. M. *Chem. Rev.* **2012**, *112*, 2739.

13. a) Hubbell, J. A.; Thomas, S. N.; Swartz, M. A. *Nature* **2009**, *462*, 449. b) Lewis, J. S.; Roy, K.; Keselowsly, B. G. *MRS Bulletin* **2014**, *39*, 25. c) Dobrovolskaia, M. A.; McNeil, S. E. *Nat. Nanotechnol.* **2007**, *2*, 469. d) Smith, D. M.; Simon, J. K.; Baker Jr, J. R. *Nat. Rev. Immunol.* **2013**, *13*, 592-605.

14. a) Moon, J. J.; Huang, B.; Irvine, D. J. *Adv. Mater.* **2012**, *24*, 3724. b) Elsabahy, M.; Wooley, K. L. *Chem. Soc. Rev.* **2013**, *42*, 5552. c) Jiao, Q.; Li, L.; Mu, Q.; Zhang, Q. *Biomed. Res. Int.* **2014**, *2014*, 426028.

15. a) Ghosh, P.; Han, G.; De, M.; Kim, C. K.; Rotello, V. M. *Adv. Drug Deliver. Rev.* **2008**, *60*, 1307. b) Lonez, C.; Vandenbranden, M.; Ruysschaert, J.-M. *Adv. Drug Deliver. Rev.* **2012**, *64*, 1749.

16. Kedmi, R.; Ben-Ariea, N.; Peer, D. *Biomaterials* **2010**, *31*, 6867.

17. Patel, P. C.; Giljohann, D. A.; Daniel, W. L.; Zheng, D.; Prigodich, A. E.; Mirkin, C. A.; *Bioconjugate Chem.* **2010**, *21*, 2250.

18. Monopoli, M. P.; Walczyk, D.; Campbell, A.; Elia, G.; Lynch, I.; Bombelli, F. B.; Dawson, K. A. *J. Am. Chem. Soc.* **2011**, *133*, 2525.

19. Yang, W.; Liu, S.; Bai, T.; Keefe, A. J.; Zhang, L.; Ella-Menye, J.; Li, Y.; Jiang, S. *Nano Today* **2014**, *9*, 10.

20. Hamad, I.; Al-Hanbali, O.; Hunter, A. C.; Rutt, K. J.; Andresen, T. L.; Moghimi, S. M. *ACS Nano* **2010**, *4*, 6629.

21. Cho, W.; Cho, M.; Jeong, J.; Choi, M.; Cho, H.; Han, B.; Kim, S.; Kim, H.; Lim, Y.; Chung, B.; Jeong, J. *Toxicol. Appl. Pharm.* **2009**, *236*, 16.

22. Reddy, S.; Van Der Vlies, A. J.; Simeoni, E.; Angeli, V.; Randolph, G. J.; O'Neil, G. P.; Lee, L. K.; Swartz, M. A.; Hybbell, J. A. *Nat. Biotechnol.* **2007**, *25*, 1159.

23. Seong, S.-Y.; Matzinger, P. *Nat. Rev. Immunol.* **2004**, *4*, 469.

24. Shahbazi, M.-A.; Fernández, T. D.; Mäkilä, E. M.; Guével, X. L.; Mayorga, C.; Kaasalainen, M. H.; Salonen, J. J.; Hirvonen, J. T.; Santos, H. A. *Biomaterials* **2014**, *35*, 9224.

25. Liu, Y.; Yin, Y.; Wang, L.; Zhang, W.; Chen, X.; Yang, X.; Xu, J.; Ma, G. *J. Mater. Chem. B* **2013**, *1*, 3888.

26. Shima, F.; Akagi, T.; Uto, T.; Akashi, M. *Biomaterials* **2013**, *34*, 9709.

27. Yang, H.; Zhou, Y.; Fung, S.; Wu, L.; Tsai, K.; Tan, R.; Turvey, S. E.; Machuca, T.; De Perrot, M.; Waddell, T. K.; Liu, M. *Part. Syst. Charact.* **2013**, *30*, 1039.

28. Bastós, N. G.; Sanchez-Tillo, E.; Pujals, S.; Farrera, C.; López, C.; Giralt, E.; Celada, A.; LIoberas, J.; Puntes, V. *ACS Nano* **2009**, *3*, 1335.

29. Rodriguez, P. L.; Harada, T.; Christian, D. A.; Pantano, D. A.; Tsai, R. K.; Discher, D. E. *Science* **2013**, *339*, 971.

30. a) Weintraub, K. *Nature* **2013**, *495*, S14. b) Daniel, M.-C.; Astruc, D. *Chem. Rev.* **2004**, *104*, 293.

31. Connor, E. E.; Mwamuka, J.; Gole, A.; Murphy, C. J.; Wyatt, M. D. *Small* **2005**, *1*, 325.

32. Brust, M.; Walker, M.; Bethell, D.; Schiffrin, D. J.; Whyman, R. *J. Chem. Soc., Chem. Commun.* **1994**, 801.

33. Faraday, M. *Phil. Trans. R. Soc. Lond.* **1857**, *147*, 145.

34. Gronbeck, H.; Curioni, A.; Andreoni, W. *J. Am. Chem. Soc.* **2000**, *122*, 3839.

35. Hong, R.; Fischer, N. O.; Verma, A.; Goodman, C. M.; Emrick, T. S.; Rotello, V. M. *J. Am. Chem. Soc.* **2004**, *126*, 739.

36. Jordan, B. J.; Hong, R.; Han, G.; Rana, S.; Rotello, V. M. *Nanotechnology* **2009**, *20*, 43004.

37. You, C.-C.; De, M.; Rotello, V. M. *Org. Lett.* **2005**, *7*, 5685.

CHAPTER 2

NANOPARTICLE SURFACE HYDROPHIBICITY DICTATES IMMUNE RESPONSES

"Strictly speaking, we do not make decisions, decisions make us."
- Jose Saramago, *Todos os Nomes*

2.1. Introduction

Navigating the response of the immune system is a major issue in the design of nanomaterials for *in vivo* applications. For example, avoiding immune system detection is an important consideration in gene and drug delivery,[1] whereas in the case of adjuvants for vaccine therapies, immune activation is desired.[2] Therefore, a deeper understanding of how nanomaterials elicit immune responses is essential for the optimization of these systems for biomedical applications.[3]

A key issue in understanding immune system activation by macromolecular probes is determining interactions of these materials with the innate immune system, the first line of defense of the body and the gatekeeper to full immunoresponse.[4] Innate immune activation is associated with the recognition of conserved molecular motifs related with pathogens (pathogen-associated molecular patterns)[5] as well as nonspecific danger-associated molecular patterns (DAMPs).[6] Hydrophobicity per se has been considered to be a DAMP.[7] Under healthy conditions, hydrophobic cellular materials ("hyppos") are hidden from the external environment. During necrotic cell disruption or protein denaturation, however, these hyppos become exposed, and by interaction with membranes and specific surface receptors, an innate immune response is generated. This response has been hypothesized to be the origin of the need for oil-based adjuvants in vaccine treatments.[8] In addition, it has also been observed that the NP surface

hydrophobicity plays a central role in the interaction of NPs with biomacromolecules, allowing its use in the development of sensors (Appendix 1 and 2).

Quantifying the relationship between hydrophobicity and immune response is experimentally challenging. In aqueous environments, structural changes and aggregation accompany variations in the hydrophobic content of synthetic[9] and biomolecular agents (e.g., proteins and lipids).[10] As a result, immune response to the hydrophobicity of these materials is also influenced by structural differences in the probe, complicating the structure−activity correlation of these systems.[11] As described in the previous section, we have developed a family of AuNPs (Figure 2.1) designed to explore structure-activity relationships at biological interfaces.[12] This chapter illustrates the use of this AuNP model to explore which molecular motifs play a significant role in immune activation, both *in vitro* and *in vivo*.

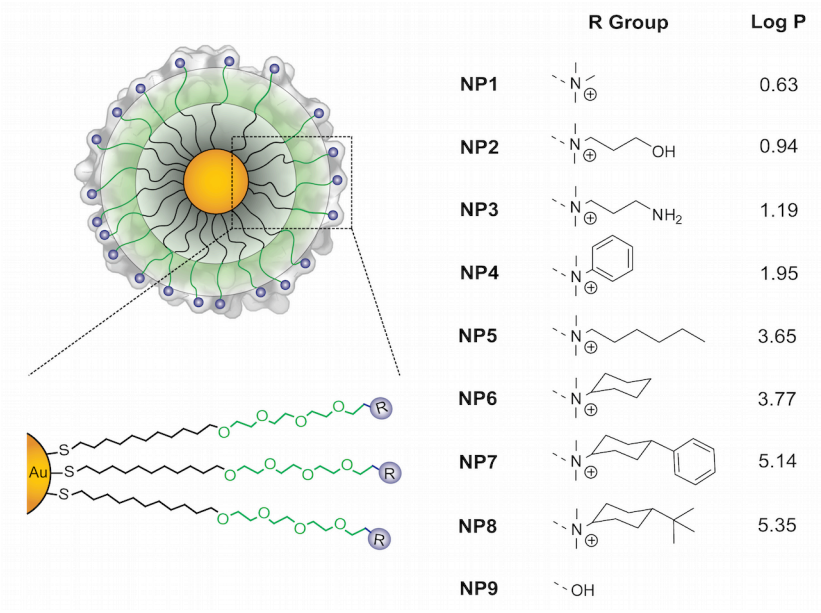

Figure 2.1. Chemical structure of the monolayer-protected 2-nm core diameter gold nanoparticles. To generate the profiles for structure-activity relationship studies, functionalities (blue) are tuned at the ligand termini to control surface hydrophobicity, as well as introducing functional groups with h-bond (donor/acceptor) and aromatic motifs. Log P represents the calculated hydrophobic values of the headgroups.

2.2. Results and discussion

Structure-activity relationship studies at the nanomaterial level provide an efficient tool in the analysis of nanoparticles properties.[13] When other structural parameters are controlled, nanoparticle properties can be described and established on the basis of descriptors of their surfaces.[14] Given that NP1−8 differ only in their surface functionality (Figure 2.1) and their physicochemical properties are similar (both at room temperature and at 37 °C, please refer to supporting information in section 2.6), we used the computationally predicted n-octanol/water partition coefficient[15] of the ligand headgroup (R groups, Figure 2.1) as the quantitative descriptor of relative nanoparticle surface hydrophobicity. Besides changes in hydrophobicity, we also included other chemical moieties such as hydroxyl groups, amino groups and aromatic moieties, to observe if these functionalities affect immunological responses.

In our initial studies we explored the immune response of NP1-8 with splenocytes, profiling cytokine mRNA levels to provide a direct assessment of immune response.[16] This measurement can be done since protein expression follows gene expression for the cytokines under study.[17] Splenocytes were selected as the experimental model of study as they are the reservoir of immune cells packed in the largest lymphoid organ in the body. These cells are comprised mostly of lymphocytes, but also include T cells and monocytes.[18] Taken together, these jointly represent both the innate and the adaptive arms of the immune system.[19]

As shown in Figure 2.2a, the plot of cytokine expression against log P reveals an essentially linear correlation between hydrophobicity and immune response, with the exception of NP1. This trend was observed for each of the cytokines under study, with variations only observed in the relative level of expression (Figure 2.3), indicating a selective type of immune response.[20] The distinct behavior of NP1 can be explained by its highly exposed charge, capable of inducing alternate responses through electrostatic interactions or by contact with specific amino acids.[21] Interestingly, no other chemical moiety seems to affect the immunological

response. For example, the presence of hydroxyl (NP2) and amino groups (NP3) does not trigger a higher response than that expected for hydrophilic NPs. Similarly, the addition of aromatic rings does not vary the response comparative with NPs of similar hydrophobicity (e. g. NP7 and NP8).

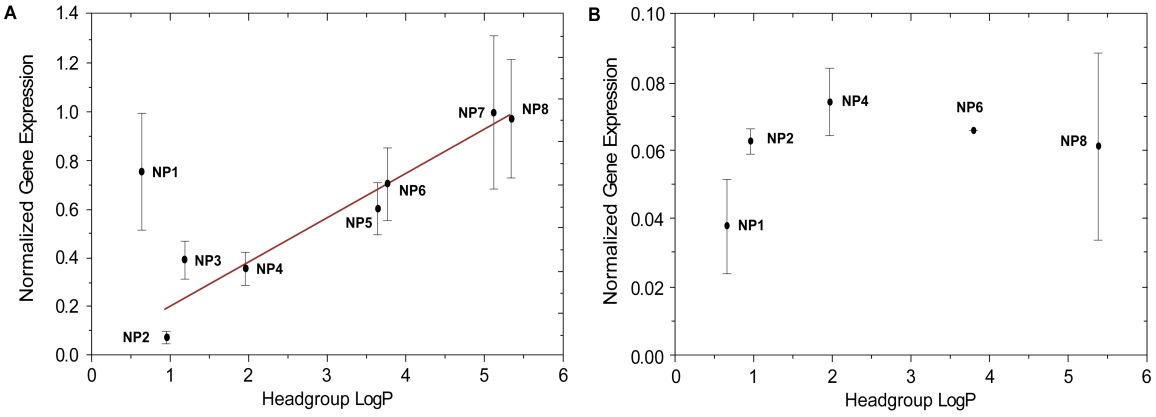

Figure 2.2. Cytokine gene expression as a function of nanoparticle headgroup log P. (A) TNFα (a representative pro-inflammatory cytokine) *in vitro* gene expression and (B) IL-10 (a representative anti-inflammatory cytokine) *in vivo* gene expression as a function of the calculated AuNP headgroup log P. The gene expression values are normalized by dividing the observed response against the values of a positive control under the same experimental set. NPs were used at a concentration of 10 μM for *in vitro* and 5 mg/kg for *in vivo* studies. Data were taken 2 h (*in vitro*) and 1.5h (*in vivo*) after exposure to AuNPs. *In vivo* correlation is lost at 6h (Figure 2.4).

In vivo response to nanomaterials is much more complex than *in vitro* systems.[22] We probed immune response to NP1-8 using mouse models. Figure 2.2b presents the tendency of cytokine expression against log P *in vivo*. At lower log P values, increasing hydrophobicity elicits increased immune response. However, with high degrees of hydrophobicity the dependence is less evident, and a maximum in immune response is observed. This leveling off can be explained by the expected changes in biodistribution for hydrophobic nanoparticles, in particular the poor biodistribution expected for highly hydrophobic particles.[23] Nonetheless, it is clear that, upon availability of hydrophobic portions in the system, immune response is generated (Figure 2.4, correlation is lost at 6 h time).[20]

2.3. Conclusions

In summary, we have demonstrated a direct, quantitative correlation between hydrophobicity and immune system activation, as per our initial hypothesis. This correlation provides a promising starting point for determining the specific molecular mechanisms of immune cell activation,[24] an issue of importance for understanding the evolution of the innate immune system.[25] Moreover, these probes present both a tool for harnessing the immune system and a probe for quantifying the role of hydrophobicity in immune response.[26]

2.4. Experimental section

Nanoparticle synthesis and characterization: 2nm diameter gold cores stabilized with a monolayer of 1-pentanethiol were synthetized by the Brust-Schiffrin two-phase methodology.[27] These clusters were purified with successive extractions with ethanol and acetone, according to our own protocol to certify that the phase-transfer catalyst do no interfere in the biological tests.[28] A Murray place-exchange reaction[29] was carried out by mixing the gold cores with each ligand, stirring the solution for 3 days at room temperature (5:1 w/w ratio of ligand/gold cores, ligands synthetized according to the reported procedure).[12,30] CH_2Cl_2 was evaporated in vacuum without heating and the dark oily residue (monolayer-protected nanoparticles now functionalized with the ligands of interest) was redispersed in water. The excesses of ligand and pentanethiol were removed by dialysis using a 10,000 MWCO snake-skin membrane for 5 days. The final concentration was measured by UV spectroscopy on a Molecular Devices SpectraMax M2 at 506nm according to the reported methodology.[31] To assess quality and ensure similar properties for the different nanoparticles, characterization by Dynamic Light Scaterring (DLS, for both

hydrodynamic size and zeta potential) on a Malvern Nano Zetasizer, and Transmission Electron Microscopy on a JEOL100S electron microscope were carried out.

Hydrophobicity descriptor: LogP values were estimated using MacroModel (Maestro 8.0). The calculations were performed at 298 K using the Merck Molecular Force Field (MMFF94).

In vitro and in vivo studies: Splenocytes harvested from mice were exposed to each nanoparticle (10μM) under *in vitro* conditions. After 2h, the cells were washed and lysed. Quantitative RT-PCR was employed to quantify the mRNA expression level associated with each one of the cytokines; primers for IL-2, IL-6, IL-10, TNFα, IFNγ, and the interferon responsive genes OAS1, STAT1, and IFNβ were used to preferably amplify them from the cDNA library and normalized against housekeeping genes HPRT1 and GAPDH.20. For the *in vivo* studies, mice (12 weeks old) were injected intravenously (100 μL) via the tail vein. Each group of mice (n = 6 mice per group) received a single dose of a specific nanoparticle at 5 mg/kg. At 1.5 and 6 h post-IV administration, the mice were sacrificed and splenocytes harvested and treated as before to assess cytokine mRNA expression levels.

2.5. Supporting information

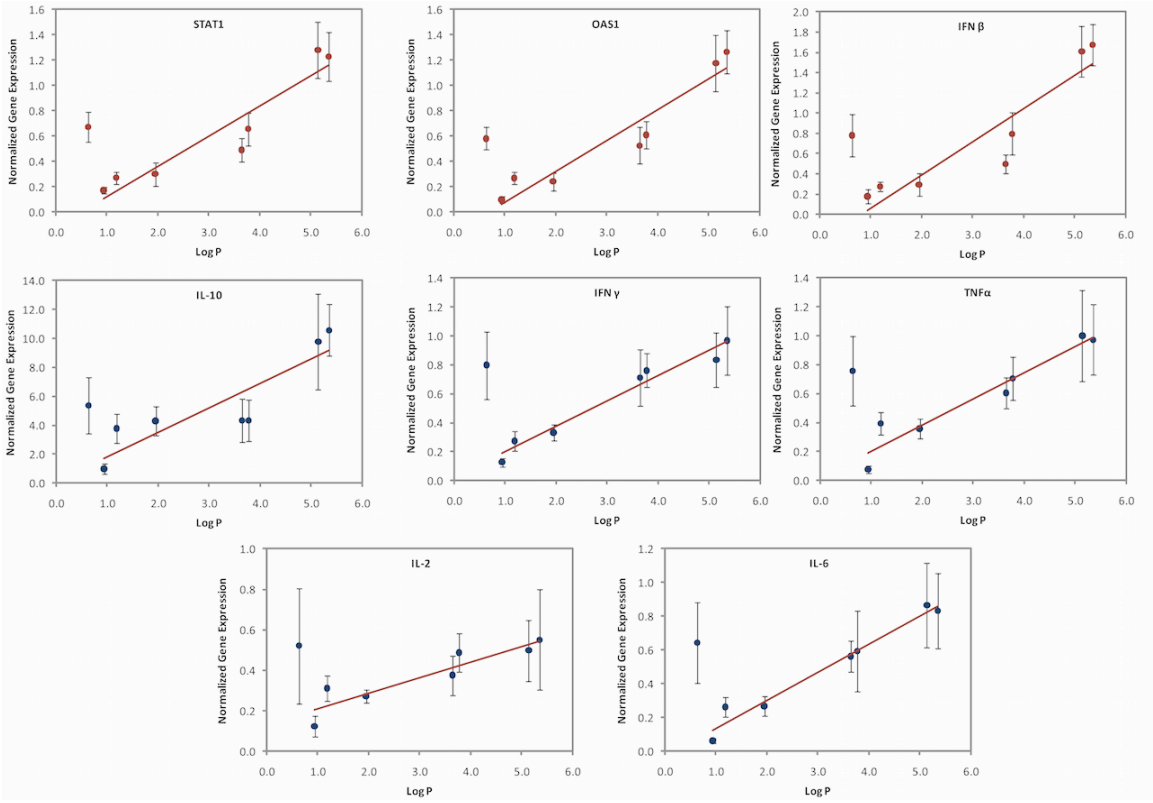

Figure 2.3. Gene expression for IRGs STAT1, OAS1 and IFNβ, and cytokines IFNγ, IL-2, IL-6, IL-10, and TNFα for the *in vitro* studies 2h after exposing the splenocytes to the NPs. Values normalized against a positive control (Poly I:C for IRGs and LPS for cytokines) for comparison, and housekeeping genes (HPRT1 and GADPH) in the PCR.

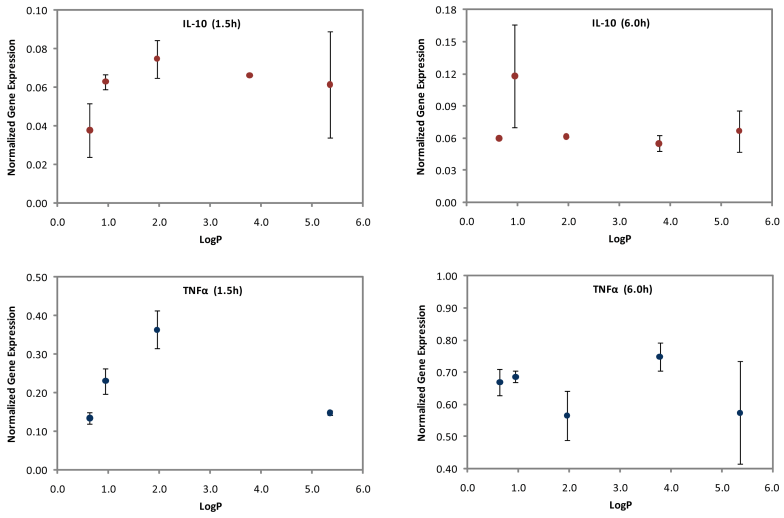

Figure 2.4. Gene expression for IL-10 and TNFα for the *in vivo* studies at 1.5h and 6h after the AuNPs IV injection. Values normalized against positive control (Poly I:C for IRGs and LPS for cytokines) for comparison.

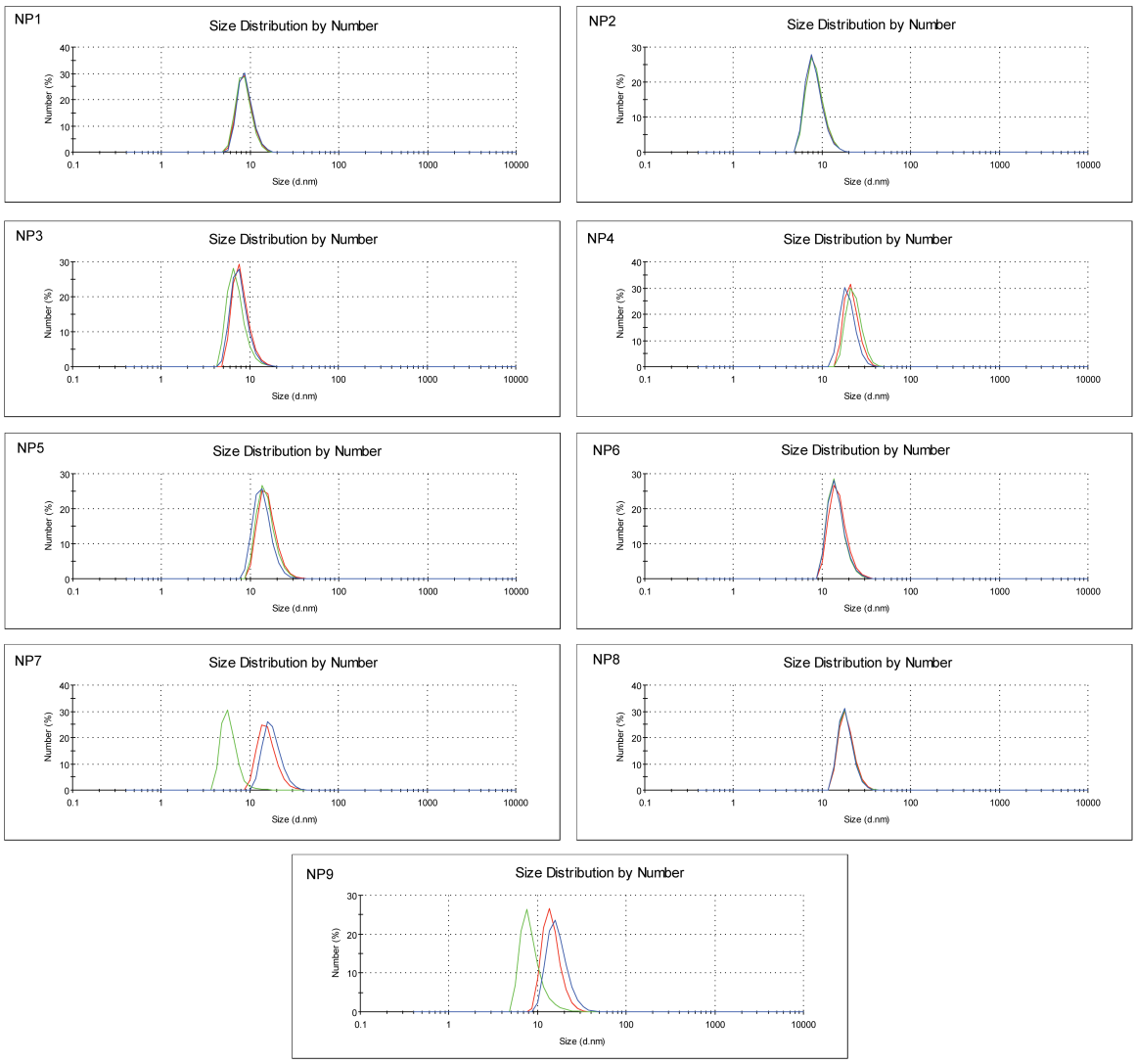

Figure 2.5. DLS measurements of nanoparticle hydrodynamic size at room temperature (1uM of AuNPs in PB 5mM, pH 7.4).

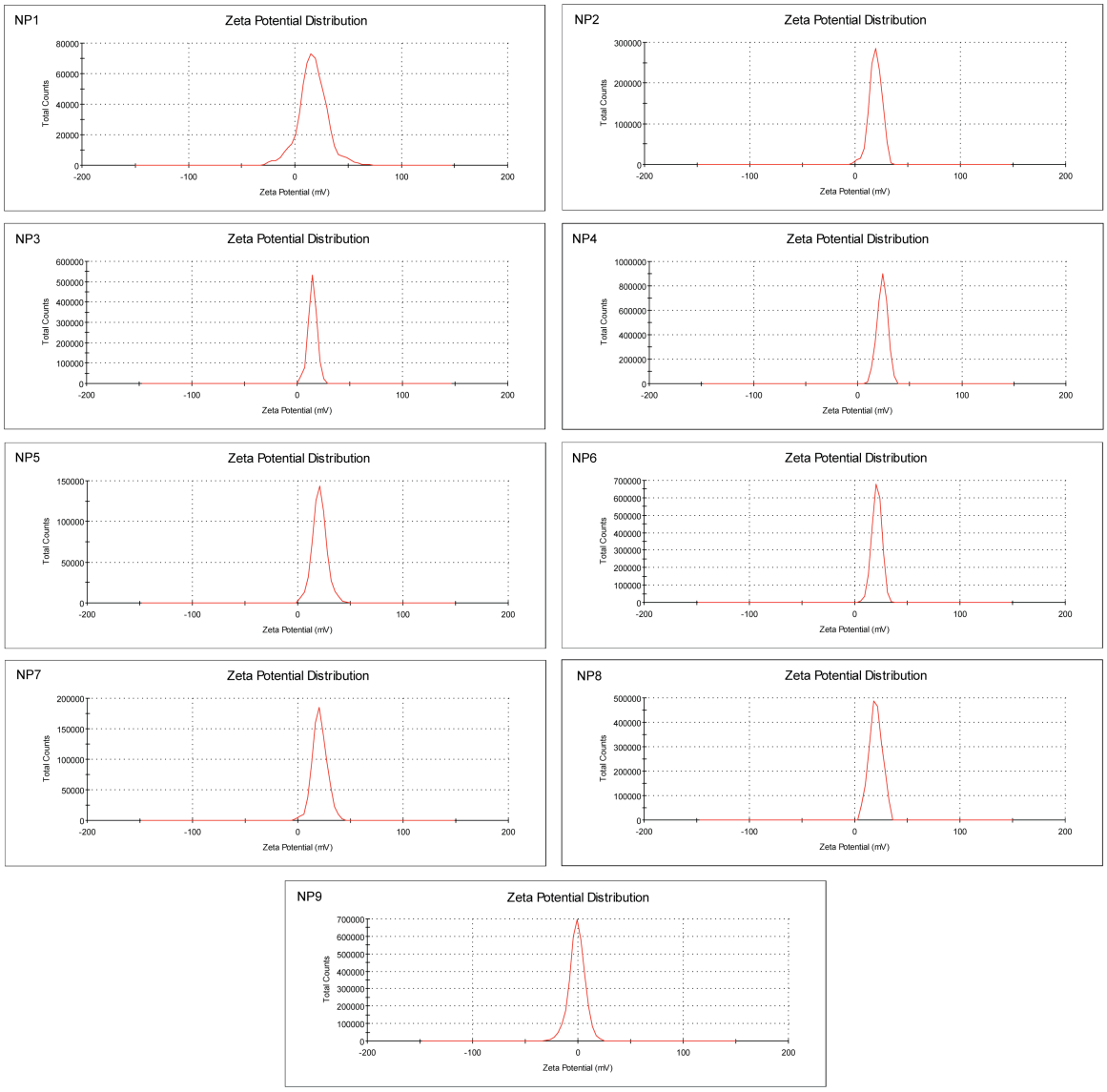

Figure 2.6. Zeta potential values of the functionalized gold nanoparticles (1uM of AuNPs in PB 5mM, pH 7.4).

2.6. References

1. (a) LaVan, D. A.; McGuire, T.; Langer, R. *Biotechnology* **2003**, *21*, 1184. (b) Kumar, M. N. V. R. *J. Pharm. Pharm. Sci.* **2000**, *3*, 234.

2. (a) Akagi, T.; Wang, X.; Uto, T.; Baba, M.; Akashi, M. *Biomaterials* **2007**, *28*, 3427. (b) Maltzahn, G. V.; Park, J.-H.; Lin, K. Y.; Singh, N.; Schwoppe, C.; Mesters, R.; Berdel, W. E.; Ruoslahti, E.; Sailor, M. J.; Bhatia, S. N. *Nat. Mater.* **2011**, *10*, 545.

3. (a) Mizrahy, S.; Raz, S. B.; Hasgaard, M.; Liu, H.; Soffer-Tsur, N.;Cohen, K.; Dvash, R.; Landsman-Milo, D.; Bremer, M. G. E. G.; Moghimi, S. M.; Peer, D. J. *Controlled Release* **2011**, *156*, 231. (b) Massich, M. D.; Giljohann, D. A.; Seferos, D. S.; Ludlow, L. E.; Horvath, C. M.; Mirkin, C. A. *Mol. Pharm*. **2009**, *6*, 1934.

4. (a) Janeway, C. A. Jr.; Medzhitov, R. Annu. Rev. *Immunol.* **2002**, *20*, 197. (b) Gallucci, S.; Lolkema, M.; Matzinger, P. *Nat. Med*. **1999**, *5*, 1249.

5. Janeway, C. A. Jr. *Cold Spring Harb. Symp. Quant. Biol*. **1989**, *54*, 1.

6. Matzinger, P. Annu. *Rev. Immunol*. **1994**, *12*, 991.

7. Seong, S.-Y.; Matzinger, P. *Nat. Rev. Immunol*. **2004**, *4*, 469.

8. Wang, Z.; Jiang, J.; Li, Z.; Zhang, J.; Wang, H.; Qin, Z. J. *Immunother*. **2010**, *33*, 167.

9. Pike, J. K.; Ho, T.; Wynne, K. J. *Chem. Mater.* **1996**, *8*, 856.

10. (a) Rose, G. D.; Wolfenden, R. *Annu. Rev. Biopharm. Biomed*. **1993**, *22*, 381. (b) Chen, Z.; Ward, R.; Tian, Y.; Baldelli, S.; Opdahl, A.; Shen, Y.-R.; Somorjai, G. A. *J. Am. Chem. Soc*. **2000**, *122*, 10615.

11. Lonez, C.; Vandenbranden, M.; Ruysschaert, J.-M. *Prog. Lip. Res*. **2008**, *47*, 340.

12. (a) Moyano, D. F.; Rotello, V. M. *Langmuir* **2011**, *27*, 10376. (b) Miranda, O. R.; Chen, H.-T.; You, C.-C.; Mortenson, D. E.; Yang, X.-C.; Bunz, U. H. F.; Rotello, V. M. *J. Am. Chem. Soc*. **2010**, *132*, 5285.

13. (a) Puzyn, T.; Rasulev, B.; Gajewicz, A.; Hu, X.; Dasari, T. P.; Michalkova, A.; Hwang, H.-M.; Toropov, A.; Leszczynska, D.; Leszczynski, J. *Nat. Nanotechnol.* **2011**, *6*, 175. (b) Xia, X.-R.; Monteiro-Riviere, N. A.; Riviere, J. E. *Nat. Nanotechnol*. **2011**, *5*, 671.

14. (a) Fourches, D.; Pu, D.; Tassa, C.; Weissleder, R.; Shaw, S. Y.; Mumper, R. J.; Tropsha, A. *ACS Nano* **2010**, *4*, 5703. (b) Puzyn, T.; Leszczynska, D.; Leszczynski, J. *Small* **2009**, *5*, 2494.

15. Toropov, A. A.; Leszczynska, D.; Leszczynski, J. *Comput. Biol.Chem.* **2007**, *31*, 127.

16. Peer, D.; Park, E. J.; Morishita, Y.; Carman, C. V.; Shimaoka, M. *Science* **2008**, *319*, 627.

17. Shebl, F. M.; Pinto, L. A.; García-Piñeres, A.; Lempicki, R.; Williams, M.; Harro, C.; Hildesheim, A. *Cancer Epidem. Biomar*. **2010**, *19*, 978.

18. Fong, A. M.; Premont, R. T.; Richardson, R. M.; Yu, Y.-R. A.; Lefkowitz, R. J.; Patel, D. D. *Proc. Natl. Acad. Sci. U.S.A.* **2002**, *99*, 7478.

19. Iwasaki, A.; Medzhitov, R. *Science* **2010**, *327*, 292.

20. Matzinger, P.; Kamala, T. *Nat. Rev. Immunol*. **2011**, *11*, 221.

21. (a) Ma, Z.; Li, J.; He, F.; Wilson, A.; Pitt, B.; Li, S. *Biochem. Biophys. Res. Commun*. **2005**, 3*30*, 755. (b) Kedmi, R.; Ben-Arie,N.; Peer, D. *Biomaterials* **2010**, *31*, 6867.

22. (a) Cho, E. C.; Xie, J.; Wurm, P. A.; Xia, Y. *Nano Lett*. **2009**, *9*, 1080. (b) Arvizo, R. R.; Miranda, O. R.; Moyano, D. F.; Walden, C. A.; Giri, K.; Bhattacharya, R.; Robertson, J. D.; Rotello, V. M.; Reid, J. M.; Mukherjee, P. *PLoS One* **2011**, *6*, e24374.

23. (a) Zhu, Z.-J.; Carboni, R.; Quercio, M. J. Jr.; Yan, B.; Miranda, O. R.; Anderton, D. L.; Arcaro, K. F.; Rotello, V. M.; Vachet, R. W. *Small* **2010**, *6*, 2261. (b) Leeson, P. D.; Springthorpe, B. Nat. *Rev. Drug Discovery* **2007**, *6*, 881.

24. Akira, S.; Takeda, K. *Nat. Rev. Immunol*. **2004**, *4*, 499.

25. Kimbrell, D. A.; Beutler, B. *Nat. Rev. Genet.* **2001**, *2*, 256.

26. Kono, H.; Rock, K. L. *Nat. Rev. Immunol*. **2004**, *8*, 279.

27. Brust, M.; Walker, M.; Bethell, D.; Schiffrin, D. J.; Whyman, R. *J. Chem. Soc., Chem. Commun.* **1994**, 801.

28. Moyano, D. F.; Duncan, B.; Rotello, V. M. *Method. Mol. Biol.* **2013**, *1025*, 3.

29. Templeton, A. C.; Wuelfing, W. P.; Murray, R. W. *Accounts Chem. Res.* **2000**, *33*, 27.

30. De, M.; Rana, S.; Akpinar, H.; Miranda, O. R.; Arvizo, R. R.; Bunz, U. H. F.; Rotello, V. M. *Nat. Chem.* **2009**, *1*, 461.

31. Liu, X.; Atwater, M.; Wang, J.; Huo, Q. *Colloid. Surface. B* **2007**, *58*, 3.

CHAPTER 3

PROTEIN ADSORPTION SUPPRESSES THE HEMOLYTIC ACTIVITY OF NANOPARTICLES: THE PROTEIN CORONA

"I accept chaos, I'm not sure whether it accepts me"
- Bob Dylan

3.1. Introduction

Before nanomaterials can be used in therapeutic applications, safety needs to be ensured. One of the principal problems that limit applications of nanomedicine is the intravascular rupture of red blood cells (RBCs) by NPs, that can elevate the plasma level of cell-free hemoglobin leading to endothelial cell dysfunction and vascular thrombosis.[1] This acute hemolysis can further cause hemolytic anemia that results in multiple organ failure[2] and death.[3] Several reports have recently demonstrated the hemolytic activities of therapeutic NPs both *in vitro*[4] and *in vivo*,[5] indicating potential adverse side-effects of NPs. However, a lack of parametric study *in vitro* of NP hemolytic behavior makes their interaction profile difficult to predict *in vivo*.

As discussed previously, the surface functionality of NPs is central to their effective use in therapeutic applications, imparting functional properties[6] and dictating their circulation profile in the blood stream.[7] However, in contrast to small molecule therapeutics the formation of a protein corona on the NP surface during blood circulation[8] alters the surface chemical behavior of NPs and defines the physiological responses.[9] This interplay between the NP surface functionality and the protein corona formed *in situ* would be expected to dictate the overall interaction of NPs with RBCs, regulating the hemolytic behavior of NPs. To date, however, there is no clear understanding of how changes on the NP surfaces coupled with the formation of a protein corona control the hemolytic properties of NPs.[10]

Based on our preliminary results of immune responses (Chapter 3), and thinking ahead on possible immunomodulatory applications, we wanted to observe if hydrophobic nanoparticles can be used safely, and if the adsorption of proteins modify their biological behavior. As such, in this section we evaluate the role of NP surface functionality on hemolytic activity in the presence and absence of plasma proteins.

3.2. Results and discussion

To understand the role of NP surface hydrophobicity in blood compatibility (our property of interest after the results described in Chapter 2), a family of nine cationic NPs was synthesized systematically changing the degree of surface hydrophobicity by the use of specific chemical groups (Figure 3.1).[11] Using this system, the NP properties can be translated into numerical descriptors (Log P), as discussed in the Chapter 2.[12] As such, the log P values of the headgroups (R groups, Figure 3.1) were employed to describe the relative hydrophobic nature of the NP surfaces.

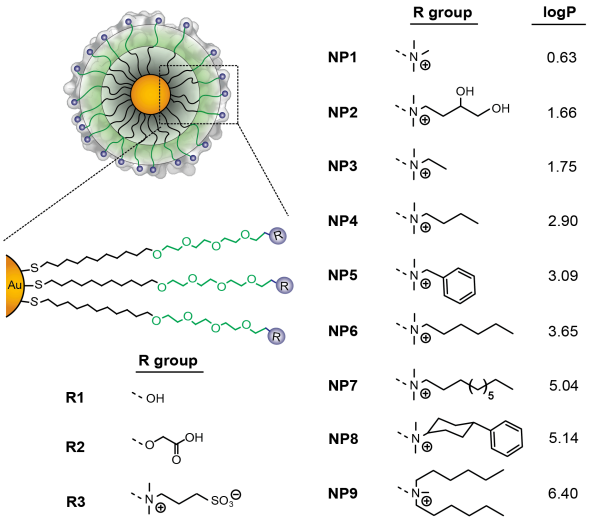

Figure 3.1. The structure of the NPs used in the current study. Log P denotes the calculated n-octanol/water partition coefficients of the R groups.

The role of NP surface hydrophobicity on hemolytic behavior was established by incubating NP1–NP9 (500 nM each) with RBCs as mentioned above. A direct increase in hemolytic activity was observed for NP1–NP9 with an increase of the hydrophobicity (Figure 3.2a,b), demonstrating the role of the NP surface hydrophobicity on the hemolysis. Significantly, NPs with similar headgroup logP values but different chemical functionalities, e.g.NP2 and NP3, demonstrated different degrees of hemolysis (~4.5% and 13.5%, respectively), providing evidence for the role of specific functional groups in the observed hemolytic behavior.

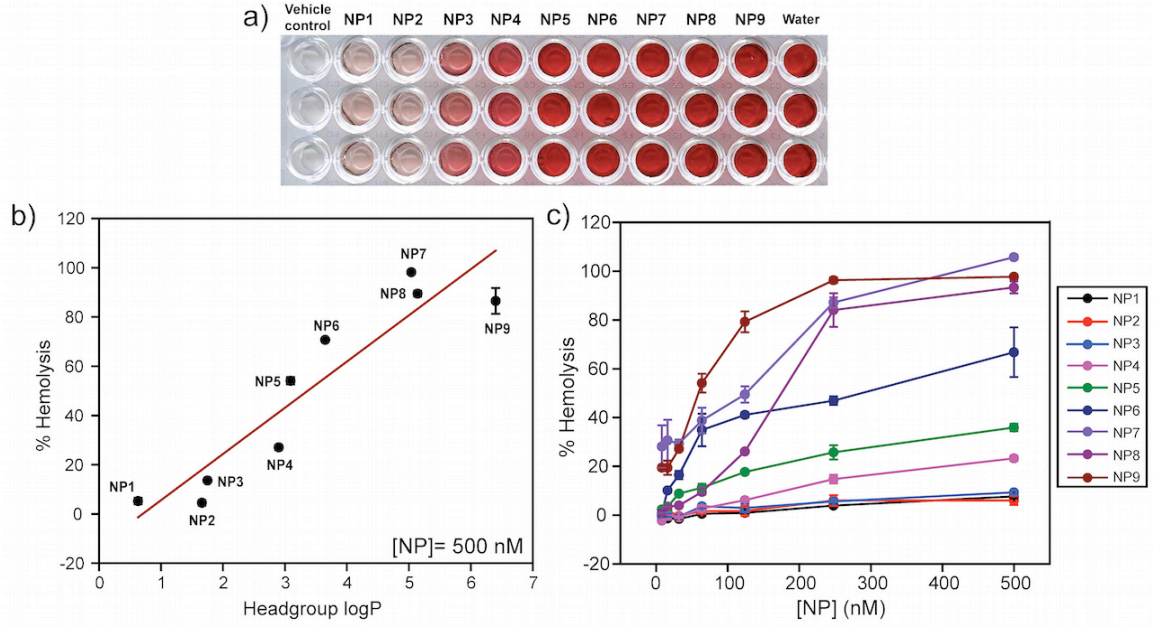

Figure 3.2. (a,b) Hemolytic activities of NP1–NP9 (500 nM each) in the absence of plasma proteins. RBCs were incubated with NPs for 30 min in PBS at 37 °C and the mixture was centrifuged to detect the cell-free hemoglobin in the supernatant. % hemolysis was calculated using water as the positive control. Error bars represent standard deviations (n = 3). (c) Dose-dependent hemolytic activity of NP1–NP9 in the absence of plasma proteins. % Hemolysis was calculated using water as the positive control. Error bars represent standard deviations (n = 3).

The dose-dependent hemolytic behavior of these NPs was investigated by exposing RBCs to a range of concentrations of NPs from 8 nM to 500 nM. As shown in Figure 3.2c, a dose-

dependent increase of hemolysis was observed for all NPs. NP1–NP3 did not show significant hemolysis at the highest concentration tested (500 nM), demonstrating biocompatibility of these particles with RBCs. Significantly, a sigmoidal dose–response curve was observed for more hydrophobic NPs (see section 3.5), demonstrating the co-operative nature of the hemolytic process for these NPs.[13] This result demonstrated that the subtle changes on NP surfaces can modulate the interaction profile with RBCs, leading to different hemolytic profiles.

The binding of plasma proteins on a NP can mask the chemical nature of the NP surface, altering its activity *in vivo*.[14] The hemolytic activities of NP1–NP9 were further studied in the presence of 55% plasma protein, a condition NPs will meet when administered in the blood stream. NPs were pre-incubated with 55% plasma in PBS for 30 min and then added to the RBCs. The pre-incubation time was chosen to ensure protein absorption, although protein coronas form within minutes after NP exposure.[15] Following incubation with RBCs, the absorbance of the supernatant was measured at 570 nm to monitor the extent of hemolysis. In presence of plasma, little to no hemolysis was observed for NP1–NP6 (Figure 3.3). Significantly, NP6, which showed ~70% hemolysis in the absence of plasma protein, demonstrated no hemolytic activity in the presence of plasma even after 24 h, a striking example of the effect of protein corona formation on the NP surface. Likewise, NP7–NP9 demonstrated a significant decrease in hemolytic activity (more than 20-fold) in the presence of plasma within 30 minutes. However, NP7–NP9 still showed ~5% hemolysis within 30 min, demonstrating the hemolytic potential of these NPs even in the presence of plasma proteins. This behavior was more pronounced after 24 h where NP7 and NP9 showed severe hemolysis (Figure 3.3). Significantly, NP7 and NP8 showed different hemolytic activities after 24 h in the presence of plasma proteins, despite their similar headgroup hydrophobicity, suggesting that surface topology plays a role in hemolysis propensity. Nonetheless, this study signifies the interplay of the chemical functionalities on the NP surface and the protein corona formed *in situ*, making NPs 'silent' towards hemolytic consequences.

However, NPs with a high degree of surface hydrophobicity (headgroup log P > 4) demonstrated severe hemolysis, providing a limit to the NP surface hydrophobicities tested in this study.

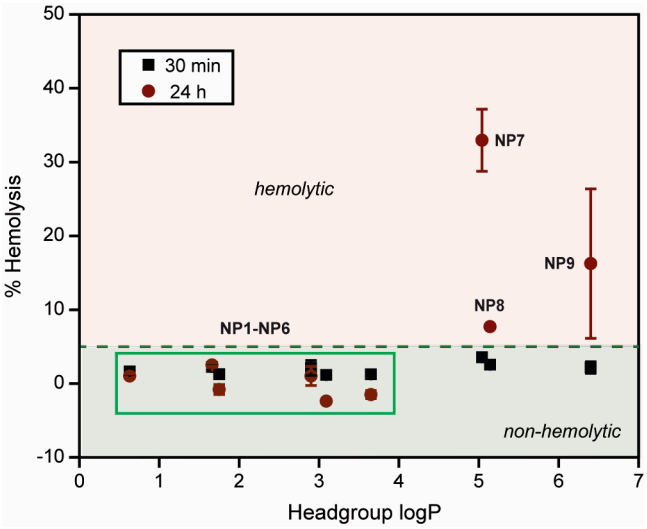

Figure 3.3. Hemolytic activities of NP1–NP9 (500 nM each) in the presence of plasma proteins. NPs were pre-incubated with 55% plasma in PBS following incubation with RBCs for 30 min and 24h at 37°C. The mixture was centrifuged to detect the cell-free hemoglobin in the supernatant. % Hemolysis was calculated using water as a positive control. Error bars represent standard deviations (n = 3).

3.3. Conclusions

In summary, we have demonstrated the important synergy between the NP surface chemical functionalities and the protein corona, leading to dramatically attenuated hemolytic behaviour of NPs. In the absence of plasma proteins, a linear hemolytic profile was observed with increasing NP surface hydrophobicity. Significantly, the presence of plasma protein passivated both hydrophilic and hydrophobic NP surfaces leading to no hemolysis within 30 min. NPs with the highest degrees of hydrophobicity (headgroup log P > 4), however, maintained their hemolytic properties (for 24 h), potentially due to aggregation in the presence of plasma proteins.

This study demonstrates the protective role of the protein corona for improved blood compatibility and provides extended design parameters for therapeutic nanomaterials without toxic consequences. However, these results also illustrates that protein corona needs to be avoided if subtle modulation of biological activities is required, as in the case of immunomodulation.

3.4. Experimental section

Nanoparticle synthesis: All the nanoparticles were synthesized and characterized as described in Section 2.4.

Hemolysis assay in the absence of plasma proteins: Citrate-stabilized human whole blood (pooled, mixed gender) was purchased from Bioreclamation LLC, NY and processed as soon as received. 10 mL of phosphate buffered saline (PBS) was added to the blood and centrifuged at 5000 r.pm. for 5 minutes. The supernant was carefully discarded and the red blood cells (RBCs) were dispersed in 10 mL of PBS. This step was repeated at least five times. The purified RBCs were diluted in 10 mL of PBS and kept on ice during the sample preparation. 0.1 mL of RBC solution was added to 0.4 mL of nanoparticle (NP) solution in PBS in 1.5 mL centrifuge tube (Fisher) and mixed gently by pipetting. RBCs incubated with PBS and water were used as negative and positive control respectively. All NP samples as well as controls were prepared in triplicate. The mixture was incubated at 37 ˚C for 30 minutes while shaking at 150 r.p.m. After incubation period, the solution was centrifuged at 4000 r.p.m. for 5 minutes and 100 μL of supernatant was transferred to a 96-well plate. The absorbance value of the supernatant was measured at 570 nm using a microplate reader (SpectraMax M2, Molecular devices) with absorbance at 655 nm as a reference. The percent hemolysis was calculated using the following formula:

% Hemolysis = ((sample absorbance-negative control absorbance)) / ((positive control absorbance-negative control absorbance)) × 100.

Hemolysis assay in the presence of plasma proteins: Human plasma (pooled, mixed gender) were purchased from Biochemed Pharmaceuticals, VA and kept at -20˚C for further use. NPs were pre-incubated in 55% of plasma solution in PBS (v/v) for 30 minutes at 37˚C. After the pre-incubation period, 0.1 mL of washed RBCs were added to the solution and further incubated for 30 minutes or 24 hours. The same procedure was followed to determine the hemolysis in the presence of plasma (vide supra).

3.5. Supporting information

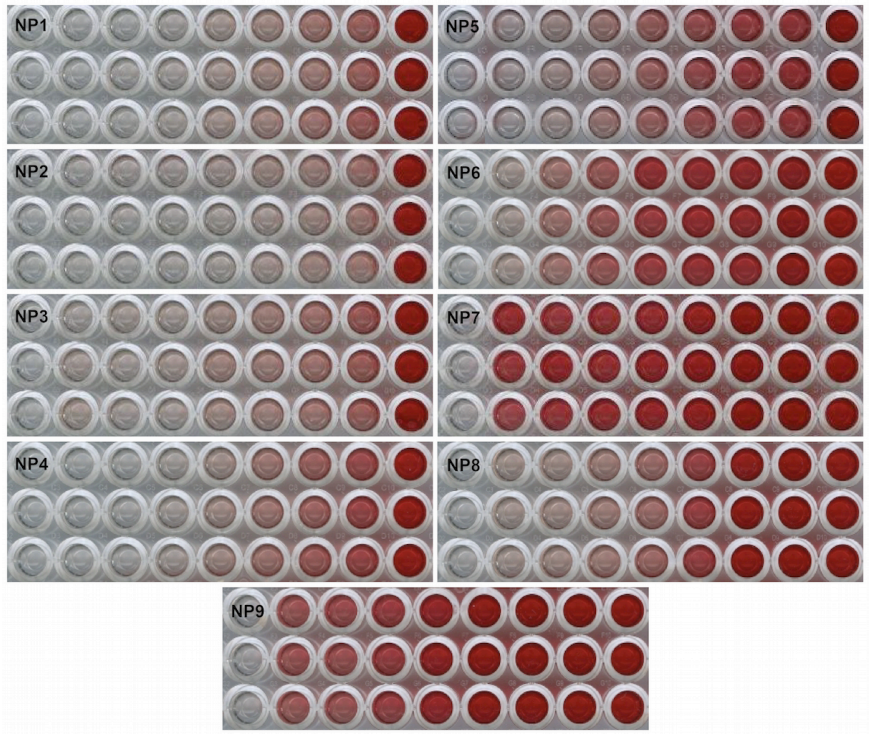

Figure 3.4. Dose dependence study for nanoparticles NP1-NP9. Experiments were performed by triplicate using concentrations of 8, 16, 32, 64, 125, 250, 500nM. Extreme left and right values are negative control (no nanoparticles) and positive control (water).

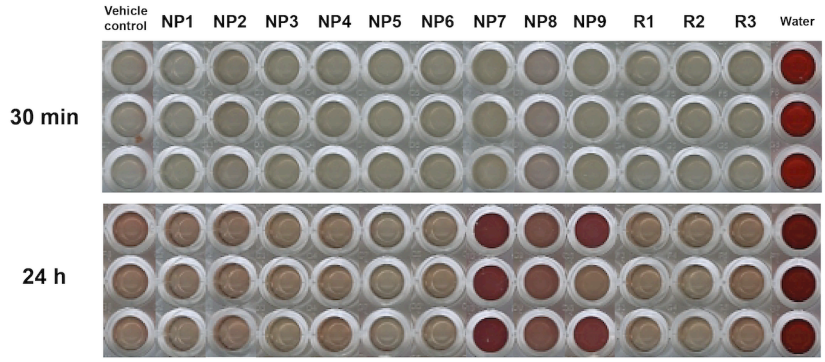

Figure 3.5. Hemolysis in the presence of plasma for NP1-NP9 at 30 min and 24 h. Extreme left and right values are negative control (no nanoparticles) and positive control (water).

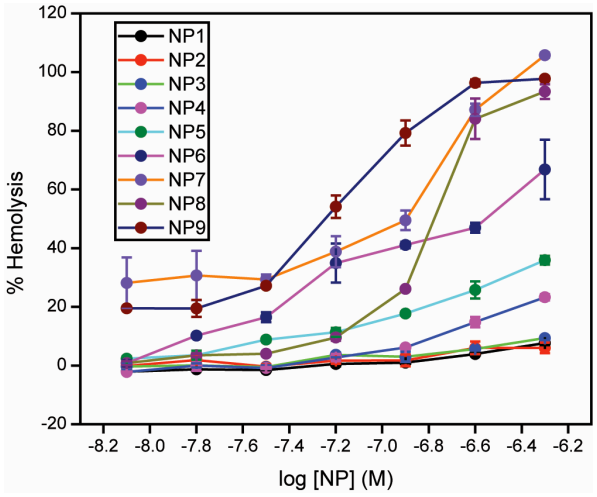

Figure 3.6. Dose-dependent hemolysis in log scale demonstrating the co-operative nature of the hemolytic process for more hydrophobic NPs.

3.6. References

1. Rother, R. P.; Bell, L.; Hillmen, P.; Gladwin, M. T. *JAMA, J.Am. Med. Assoc.* **2005**, *293*, 1653.

2. (a) Stroncek, D.; Procter, J. L.; Johnson, J. *Am. J. Hematol.* **2000**, *64*, 67. (b) Saitoh, D.; Kadota, T.; Senoh, A.; Takahara, T.; Okada, Y.; Mimura, K.; Yamashita, H.; Ohno, H.; Inoue, M. *Am. J. Emerg. Med.* **1993**, *11*, 355. (c) Scharte, M.; Fink, M. P. *Crit. Care Med*. **2003**, *31*, S651.

3. (a) Perkins, J.; *Asian J. Transfus. Sci.* **2008**, *2*, 20. (b) Yuerek, S.; Riess, H.; Kreher, S.; Doerken, B.; Salama A. *Transfus. Med*. **2010**, *20*, 265.

4. (a) Love, S. A.; Thompson, J. W.; Haynes, C. L. *Nanomedicine* **2012**, *7*, 1355. (b) Choi, J.; Reipa, V.; Hitchins, V. M.; Goering, P. L.; Malinauskas, R. A. *Toxicol. Sci*. **2011**, *123*, 133. (c) Zhao, Y. N.; Sun, X. X.; Zhang, G. N.; Trewyn, B. G., Slowing, I. I.; Lin, V. S. Y. *ACS Nano* **2011**, *5*, 1366.

5. (a) Lu, S. L.; Duffin, R.; Poland, C.; Daly, P.; Murphy, F.; Drost, E.; MacNee, W.; Stone, V.; Donaldson, K. *Environ. Health Perspect.* **2009**, *117*, 241. (b) Li, Y. T.; Liu, J.; Zhong, Y. J.; Zhang, J.; Wang, Z. Y.; Wang, L.; An, Y. L.; Lin, M.; Gao, Z. Q.; Zhang, D. S. *Int. J. Nanomed.* **2011**, *6*, 2805.

6. (a) Saha, K.; Bajaj, A.; Duncan, B.; Rotello, V. M. *Small* **2011**, *7*, 1903. (b) Mout, R.; Moyano, D. F.; Rana, S.; Rotello, V. M. *Chem. Soc. Rev*. **2012**, *41*, 2539.

7. Yoo, J. W.; Chambers, E.; Mitragotri, S. *Curr. Pharm. Des*. **2010**, *16*, 2298.

8. (a) Walkey, C. D.; Chan, W. C. W. *Chem. Soc. Rev*. **2012**, *41*, 2780. (b) Monopoli, M. P.; Aberg, C., Salvati, A; Dawson, K. A. *Nat. Nanotechnol*. **2012**, *7*, 779. (c) Arvizo, R. R.; Giri, K.; Moyano, D.; Miranda, O. R.; Madden, B.; McCormick, D. J.; Bhattacharya, R.; Rotello, V. M.; Kocher, J. P.; Mukherjee, P. *PLoS One*, **2012**, *7*, e33650.

9. (a) Salvador-Morales, C.; Flahaut, E.; Sim, E.; Sloan, J.; Green, M. L. H.; Sim, R. B. *Mol. Immunol*. **2006**, *43*, 193. (b) Owens, D. E.; Peppas, N. A. *Int. J. Pharm*. **2006**, *307*, 93.

10. (a) Joglekar, M.; Roggers, R. A.; Zhao, Y. N.; Trewyn, B. G. *RSC Adv*. **2013**, *3*, 2454. (b) Kwon, T.; Woo, H. J.; Kim, Y. H.; Lee, H. J.; Park, K. H.; Park, S.; Youn, B. *J. Nanosci. Nanotechnol*. **2012**, *12*, 6168.

11. Moyano, D. F.; Rotello, V. M. *Langmuir* **2011**, *27*, 10376.

12. Rana, S.; Yu, X.; Patra, D.; Moyano, D. F.; Miranda, O. R.; Hussain, I.; Rotello, V. M. *Langmuir* **2012**, *28*, 2023.

13. Andreeva, Z. I.; Nesterenko, V. F.; Fomkina, M. G.; Ternovsky, V. I.; Suzina, N. E.; Bakulina, A. Y.; Solonin, A. S.; Sineva, E. V. *Biochim. Biophys. Acta* **2007**, *1768*, 253.

14. (a) Lynch, I.; Dawson, K. A. *Nano Today* **2008**, *3*, 40. (b) Mahmoudi, M.; Lynch, I.; Ejtehadi, M. R.; Monopoli, M. P.; Bombelli, F. B.; Laurent, S. *Chem. Rev.* **2011**, *111*, 5610.

15. (a) Dell'Orco, D.; Lundqvist, M.; Oslakovic, C.; Cedervall, T.; Linse, S. *PLoS One* **2010**, *5*, e10949. (b) Barran-Berdon, A. L.; Pozzi, D.; Caracciolo, G.; Capriotti, A. L.; Caruso, G.; Cavaliere, C.; Riccioli, A.; Palchetti, S.; Lagana, A. *Langmuir* **2013**, *29*, 6485.

CHAPTER 4

REMOVING THE PROTEIN CORONA: FABRICATION OF ZWITTERIONIC NANOPARTICLES WITH TUNABLE HYDROPHOBICITY

"I know nothing of that directly; I only know what I have been told by other young ones who couldn't have known directly either. I want to find out the truth about them and the wanting has grown until there is more of curiosity in me than fear"
- Isaac Asimov, *The Gods Themselves*

4.1 Introduction

As discussed previously, surface functionalization of NPs is an essential tool to modulate the behavior of these materials both *in vitro* and *in vivo*.[1,2] However, when NPs are exposed to biofluids, such as plasma or serum, proteins and other biomolecules adsorb on the surface of these materials (Figure 4.1a).[3,4,5] This in situ formation of a "protein corona"[6,7] masks the engineered functionalities on the nanoparticle surfaces, dramatically changing the nature of their interaction with biosystems.[8,9,10] For example, in the previous section we observed that the hemolytic properties of NPs are drastically modified when proteins are adsorbed over the NP surface. In addition, other authors have also seen that the targeting efficacy of antibody-functionalized NPs are compromised due to the high levels of opsonization.[11,12]

Many approaches have been investigated to prevent the formation of the protein corona to provide NPs with non-fouling properties. One classical approach is the use of a non-charged poly(ethylene glycol) (PEG) polymer that prevents the NP from adsorbing proteins.[13,14] However, it has been observed that PEG-functionalized NPs do indeed interact with certain plasma proteins, inducing the activation of different immune responses.[15] Moreover, systematic changes in the surface properties of PEG-functionalized NPs are difficult to achieve as the absence of charge

allows the internalization of pendant hydrophobic functionalities, reducing exposure.[16] An alternative to the use of PEG is the incorporation of zwitterion functionalities onto the NP surface, including amino acids[17] and polybetaines.[18] The strong electrostatic binding of water with zwitterions (as opposed to water hydrogen bonding with PEG) has been postulated as the rationale behind the high degree of stability and non-fouling properties observed with zwitterionic systems.[19] However, pH dependence of carboxy-based systems[20] and the difficulty of systematic functionalization[21,22] limit the ability to control surface properties while maintaining biocompatibility and corona-free character.

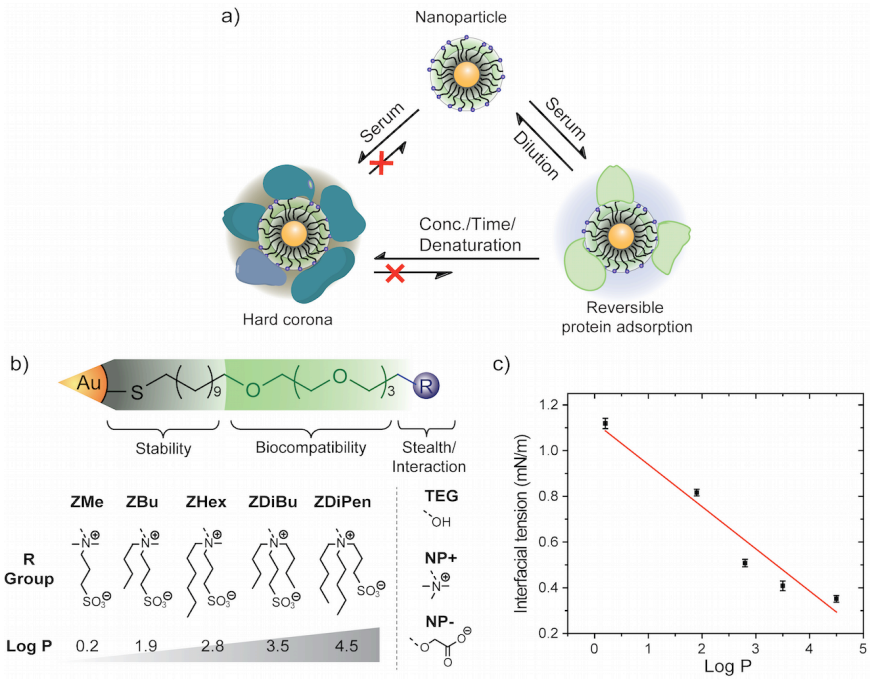

Figure 4.1. (a) Reversible adsorption of proteins and formation of irreversible hard corona over the NP surface. (b) Structures of the non-fouling NPs, along with TEG, NP+, and NP- controls. The ligand structure consists of a hydrophobic interior that confers stability to the NP core, an oligo(ethylene glycol) chain used as a first layer for biocompatibility, and the zwitterionic headgroups to confer ultra-fouling properties. The zwitterionic headgroups (the NP surface) differ only in their hydrophobicity, whose relative values can be estimated by the calculated log P of the terminal functionality. (c) Correlation of the calculated log P (ligand headgroups) with toluene/water interfacial tension of the NPs.

In this section, the synthesis and use of a new family of NP surface coverages that exhibit tunable hydrophobicity while preventing the formation of a protein corona is described. This nanoparticle ligand design maintains corona-free behavior at moderate protein levels and prevents the irreversible formation of "hard" corona at physiological serum concentrations, while allowing properties such as hydrophobicity to be varied. These "naked" particles allow a systematic molecular structure-based assessment of the effects caused directly by the NP surface, including cellular uptake and hemolytic activity.

4.2 Results and discussion

The chemical design of the NP ligand is based on a combination of a short oligo(ethylene glycol) spacer with sulfobetaine termini (Figure 4.1.b). This combination has been shown to provide better stealth properties to NPs compared to the ethylene glycol chains alone.[23] Hydrophobicity was chosen as the chemical variable due to the significant role played by this parameter at the nano-bio interface as described previously, including biomacromolecule-NP interaction,[24] and immune system recognition (Chapter 2). For this case, the degree of surface hydrophobicity was controlled with these ligands by systematically engineering the quaternary ammonium nitrogen (Figure 4.1b). As with the previous studies (and as described in section 1.3), all particles were fabricated from a 2 nm gold core, a factor that contributes to the observed corona-free character, given the reduced protein adsorption[3] and the increased plasma stability of small nanoparticles.[25]

Similar to the case of NPs in Chapter 2 and 3, a numerical descriptor is required to represent the property that is being tested (hydrophobicity). Computational calculation of the n-octanol/water partition coefficient of the NP headgroups (log P of R groups, Figure 4.1b) provides a readily accessible means to describe the relative hydrophobicity of NPs.[26] These

calculated values were correlated with water/toluene interfacial tension (IFT) measurements, a technique that has been used to describe the effective surface hydrophobicity of NPs independent of the material of origin.[27] As can be observed in Figure 4.1c, the calculated log P values and the experimental IFT results are essentially linearly correlated, indicating that the hydrophobicity of the NPs is predicted by the log P descriptor. The very low threshold of values of the IFT of these NPs evidenced their high degree of amphiphilicity, a characteristic that is on favor of their colloidal stability despite the overall neutral zeta-potential. ZDiPen represents the limit in terms of hydrophobicity: if the log P of the headgroup is above 4.5 (IFT < 0), or if the length of the straight chain substituents is larger than six carbons, the NPs were insoluble in water.

To determine the preliminary interactions of the synthesized NPs with proteins,[20,28] dynamic light scattering (DLS) measurements were recorded in the presence of 1% serum, the highest concentration that did not overwhelm the NP signal (Figure 4.10; experiment also performed in 1% plasma, Figure 4.12). The principal change in the DLS profile of serum after the addition of NP+ (cationic), NP- (anionic), and TEG (neutral oligo(ethylene glycol)-capped particles) was the shift of the ~9 nm hydrodynamic diameter peak to ~20 nm, evidencing the formation of discrete protein/NP complexes, namely, the protein corona (Figure 4.2a,b). For NP+, the formation of a peak above 1000 nm was also observed, indicating the presence of extended protein-NP aggregates (Figure 4.10). In contrast, only the peak at ~9 nm was observed with the zwitterionic NPs ZMe to ZDiPen (Figure 4.2a,b). These results can easily be contrasted by comparing the predicted histogram in the case where no corona is formed (the addition of the individual serum and NP histograms) with the experimental DLS distribution after mixing the NPs with serum (Figure 4.2c). As observed in Figure 4.2d, the subtraction of the experimental histograms from the predicted additive histograms shows that while NP+ presents residuals at the ~20 and ~1000 nm zones indicative of both aggregation and corona formation, ZMe has minimal

residual, indicating the absence of corona at these protein levels (additional NPs in Figures 4.11 and 4.13).

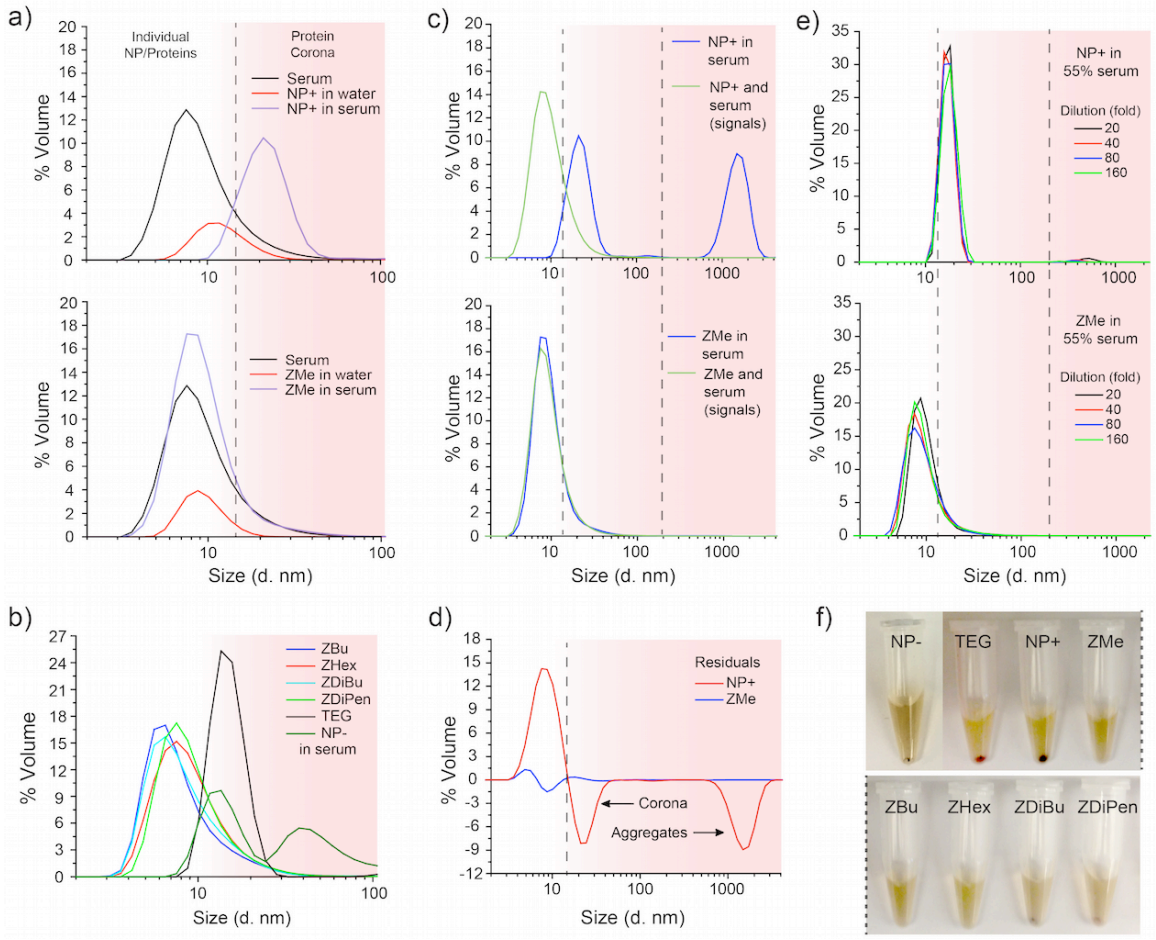

Figure 4.2. (a) Particle size distribution for cationic NP+ and zwitterionic particle ZMe in the presence and absence of serum proteins (1% serum, background) evidencing the formation of NP/protein complexes (~20 nm) with NP+ but not with ZMe (complete spectra and additional analysis in plasma in the Supporting Information section). (b) Lack of corona formation for zwitterionic particles in serum and corona formation for TEG (lacking zwitterionic headgroup) and anionic NP-. (c) Comparison between the experimental DLS profiles of each NP in serum with the additive histogram of the combination of the individual serum and NP. (d) Residuals of the spectra in serum after removing the individual NP and serum histograms, evidencing corona and aggregate formation for NP+ with minimal residual observed for ZMe (additional NPs in Figure 4.11). (e) Dilution studies showing lack of hard corona formation for ZMe after incubation in 55% human serum, with contrasting behavior by the cationic NP+. (f) Sedimentation experiments for the series of NPs in 55% plasma showing that zwitterionic NPs ZMe to ZDiPen did not aggregate, in contrast to NP+, NP-, and TEG that formed pellets.

Corona formation involves both reversible and irreversible (hard corona) adsorption of proteins on the NP surface (Figure 4.1a).[29,30,31] While we were unable to verify the lack of reversible protein adsorption at physiological serum concentrations, we were able to verify the absence of hard corona formation on zwitterionic NPs through incubation and dilution. For this purpose, we incubated the set of NPs with 55% human serum at 37ºC for 30 min, diluted the solutions, and recorded DLS measurements to observe if irreversible protein-NP interactions had occurred for the controls and if crowding effects may alter the absence of corona for the zwitterionic NPs. As observed in Figure 4.2e, although the peak of the NP-protein conjugates (>1000 nm) for NP+ decreased when the sample was diluted, the peak at ~20 nm that describes discrete NP-protein complexes remained present after dilution, indicating a strong irreversible protein binding (hard corona). Similar results were obtained for NP- and TEG, suggesting that the larger protein-NP conjugates dissociated and only the discrete ones remained after dilution (Figure 4.14). In contrast, for NPs ZMe-ZDiPen (Figures 4.2e and 4.14), the ~9 nm peak was the only one observed, indicating the absence of an irreversible protein layer (hard corona).

Further studies using electrophoresis established that zwitterionic particles ZMe-ZDiPen are non-interacting in plasma (55% in PBS, v/v), a more complex matrix. As expected, the mobilities of cationic NP+ and anionic NP- were affected by the presence of proteins due to the corona formation. In contrast, similar mobilities were observed for the zwitterionic NPs in the presence and absence of plasma proteins (Figure 4.15). Likewise, TEG presented a minimal difference between the two conditions, and the subtle band movement in the presence of protein presumably occurs due to NP aggregation. Despite these results, gel electrophoresis does not provide a definitive result on the absence of corona formation due to the poor mobility of all of the NPs in the agarose matrix. To further corroborate our hypothesis, sedimentation experiments were performed in the presence of 10%, 55%, and undiluted plasma, mimicking *in vitro* and *in vivo* conditions.[42] As expected, while NP+ formed a pellet, NPs ZMe to ZDiPen presented

minimal or no aggregates even at physiological plasma levels (Figure 4.2f and Figure 4.16a, with no pellets formed even under ultracentrifuge conditions). These qualitative observations were validated by UV measurements of the supernatants before and after the sedimentation process (Figure 4.16b). NP- presented a pellet of smaller size than NP+, a result that correlates with the observations by DLS and gel electrophoresis. Significantly, TEG presented sedimentation similar to the one observed for NP+. This outcome mirrors the results from DLS experiments and is consistent with previous findings that postulate the recognition of PEG functionalities by proteins of the bloodstream.[15]

We wanted to observe if we were able to obtain pellets for the zwitterionic NPs using other variants of the sedimentation experiments and also confirm that the sedimentation of NP+ was due to the formation of corona and no simple NP precipitation. To this end, we repeated the sedimentation experiments using different sucrose gradients, a technique that has been used to separate NP/protein complexes from NPs alone.[10] Under these conditions, we obtained similar results as with the direct sedimentation experiments, with a thick pellet only observed for NP+ (Figure 4.17a). We further ran a SDS-PAGE gel treating all the samples as if precipitation was observed, and from the results, it can be observed that NP+ did adsorb proteins over the surface while ZMe-ZDiPen behave as the negative control (composed of serum alone, no NPs added, Figure 4.17b). This further confirms the absence of irreversible protein adsorption over the surface of zwitterionic NPs at physiological protein levels. It is important to note that we did observe a very faint precipitation for the more hydrophobic NPs; however, this precipitate was redissolved in the washing steps with PBS (intended to remove loosely bound proteins). This result indicates that even if NP-protein interactions are observed at large values of hydrophobicity, these interactions are reversible and no hard corona is formed.

Once the absence of corona was established, we investigated the effects of NP hydrophobicity on cellular uptake,[32] a phenomenon critically affected by the NP surface and the protein corona.[33,34] For this purpose, uptake studies were performed in serum containing and

serum-free media, conditions that critically affect the trend of uptake of NPs of varying hydrophobicity.[35] As seen in Figure 4.3a, there was an increase in cellular uptake with increasing surface hydrophobicity for both cases. In previous studies, when NPs were exposed to the cells in serum-free conditions, increasing hydrophobicity increased cell uptake, similar to the results that we obtained.[35] However, when the studies were performed in media with serum, increasing the hydrophobicity of NPs led to greater protein adsorption over the NP surface,[36] which in turn reduced the cellular uptake.[37,38] In contrast to these prior systems, we obtained similar cellular uptake trends for NPs ZMe-ZDiPen both in the presence and in the absence of serum. This result indicates that direct correlations between the NP surface chemistry and biological responses can be assessed with these NPs, providing further proof of the absence of proteins on the NP surfaces and the direct presentation of the chemical motifs to the cellular environment. As expected, overall uptake was low[39] and there was a marked difference in the absolute amount of NP uptake in the presence and absence of serum (~2-fold higher uptake without serum). This latter phenomenon has been observed previously for other particles independent of their charge,[40,41] possibly due to nonspecific binding of proteins and NPs to the cell membrane, a competitive process that slows the uptake of NPs when proteins are present.[41,42] This phenomenon may be the rationale behind the fact that the trend of cellular uptake with NP hydrophobicity in serum was more evident at 24 h (Figure 4.18). Finally, it is important to note that at the conditions of the study the nanoparticles were non-cytotoxic (Figure 4.19).

Due to the corona-free character, these NPs have the potential for long blood circulation times,[43] increasing the possibility of hemolytic activity (and as discussed in Chapter 3). As such, hemolytic assays were performed as a means to probe the compatibility of the NPs with red blood cells (RBCs), following the same procedure described in section 3.4.[44,45] NPs ZMe to ZDiPen were incubated with RBCs isolated from commercially purchased human whole blood. The experiments were performed both in the presence and in the absence of blood plasma.[46] The

results (Figure 4.3b) provide evidence that no significant cell lysis was elicited by the zwitterionic NPs either in the presence or in the absence of plasma. Hemolytic activity was only observed for the more hydrophobic NP (ZDiPen) at 24 h without plasma proteins, consistent with a critical change in the behavior of NPs at extreme values of hydrophobicity. However, it is important to note that during the half-life that is expected for these particles (~6 h),[23] no significant hemolytic response was observed in the presence of plasma proteins for the zwitterionic NPs.

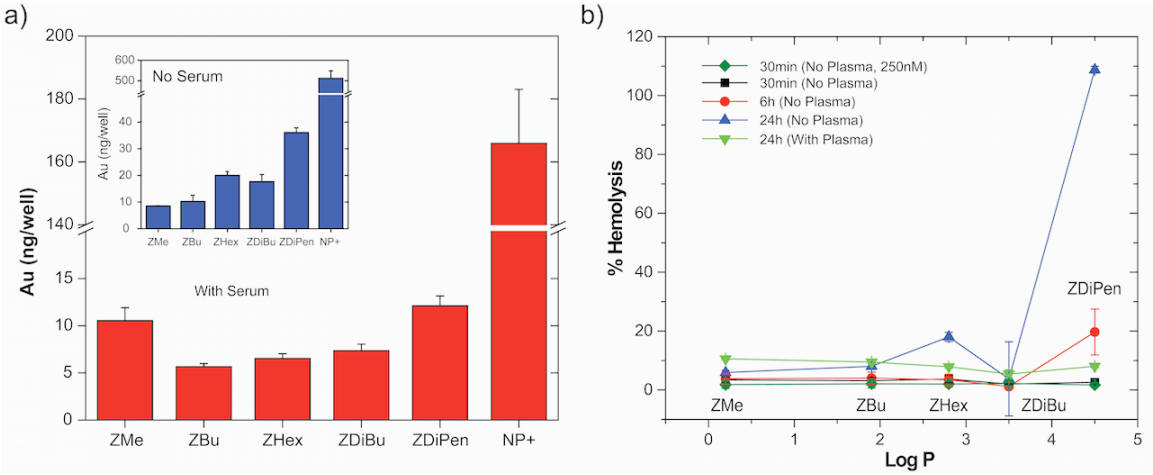

Figure 4.3. (a) Cellular uptake (MCF7 cells, 3 h) of zwitterionic NPs ZMe to ZDiPen and NP+ in presence and absence (inset) of serum, showing similar uptake trends for both experimental conditions (24 h result in Figure 4.18). (b) Hemolytic activity of the NPs at different time points and in the presence and absence of plasma (NPs at a concentration of 500 nM unless otherwise stated)

4.3 Conclusions

In summary, we have demonstrated that sulfobetaine headgroups can be engineered to provide particles with controlled hydrophobicity. These particles do not adsorb proteins at moderate serum protein concentrations nor do they form a hard corona at physiological serum conditions. The ligand design provides the potential to directly control the interaction of the

nanomaterials with biosystems without interference from protein binding. As such, these coverages provide promising scaffolds for delivery vehicles and self-therapeutic systems. They also open new avenues for probing the fundamental nature of the nano-bio interface through direct interfacing of synthetic and biological components without intermediary complications arising from the protein corona.

4.4. Experimental section

Nanoparticle synthesis: The synthetic route used in the development of the nanoparticles is depicted in Figure 4.4. Briefly, compounds 1 to 4 were synthesized according to the reported procedure.[47] Compound 5 (tertiary amine derivatives) was synthesized by adding a library of amines (2eq.) to a solution of compound 4 (~2g) under nitrogen in dry CH_2Cl_2 (20ml). The reaction mixture was then left to stir at 40°C for 48 h and monitored using TLC (10% MeOH in CH_2Cl_2, ninhydrin dip). Upon completion, CH_2Cl_2 was evaporated under vacuum and the crude product was purified by column chromatography over silica gel (flash running) using MeOH/DCM (0.5:9.5 and 1.5:8.5 v/v) as an eluent. Solvent was evaporated under vacuum to obtain compound 5 as a yellow oil. Compound 5 was then dissolved in ethyl acetate, and 1,3-propanesultone (1.2 eq) was added under nitrogen to obtain Compound 6 (zwitterion derivatives). The reaction mixture was stirred at 40°C for 72hrs and monitored using TLC (10% MeOH in CH_2Cl_2, ninhydrin dip). Upon completion, the solvent was evaporated under vacuum and the crude product was purified by column chromatography over silica gel using MeOH/CH_2Cl_2 (0.5:9.5 and 2:8 v/v) as an eluent. Solvent was evaporated under vacuum to obtain compound 6 as yellow oil. Compound 7 (final ligands) was obtained by adding an excess of trifluoroaceticacid (20eq.) to a solution of compound 6 (dry CH_2Cl_2, 5mL), while stirring under inert atmosphere for 10 min. As a second step, triispropylsilane (1.2eq.) was added slowly while maintaining stirring, and the reaction was left to completion for 5h. The solvent was then evaporated and the crude

product was washed several times with hexanes to obtain the final product. The nanoparticles were then coated with the ligands by the methodology described in section 2.4.

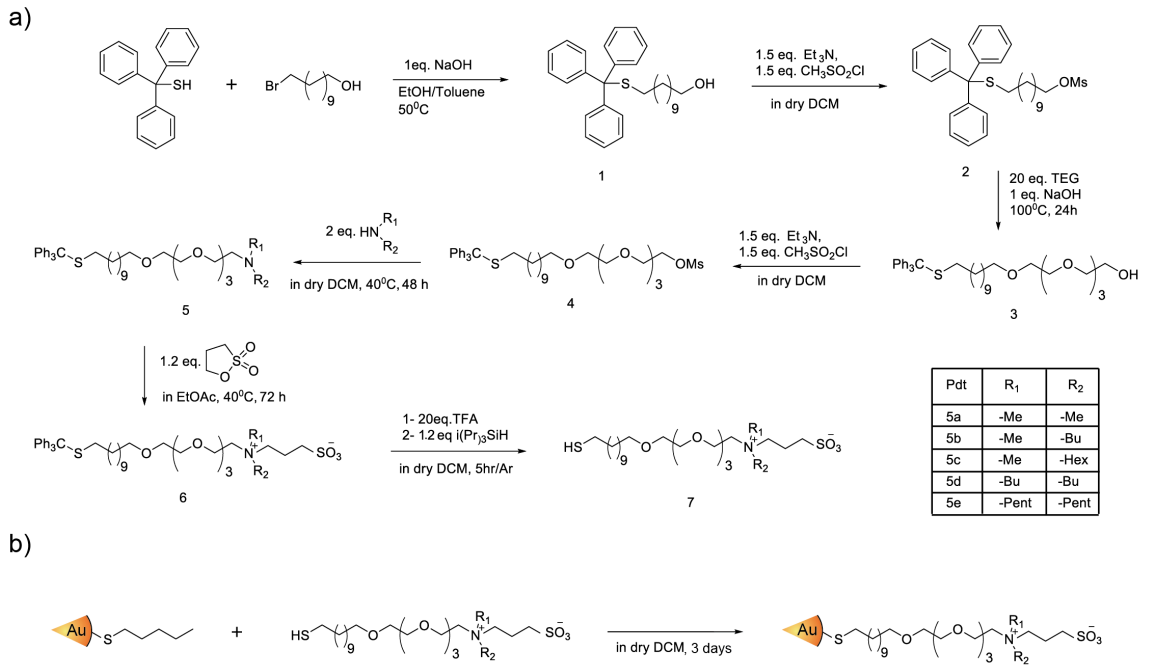

Figure 4.4. Synthetic scheme of the (a) zwitterionic ligands and (b) the corresponding functionalized nanoparticles.

Nanoparticle characterization: The functionalized gold nanoparticles were characterized by ^{1}HNMR (Bruker Avance 400 MHz, 600 scans, [NP]=20µM), MALDI-MS (Bruker Autoflex III MALDI-TOF MS, 200 shots-20 off-laser 55%, suppress up to 400Da), DLS and ZP (Malvern NanoZeta Sizer, [NP]=1 µM) to observe the chemical composition of the monolayer, the hydrodynamic size, and the surface zeta potential, and the results are depicted in the supporting information section (section 4.5). The log P values of the ligand headgroups (R groups of Figure 4.1) were estimated using ChemDraw Ultra 12.0. For immunological experiments (Chapter 5), limulus amebocyte lysate (LAL) gel cloth test was performed to determine that the NPs are free of endotoxins, using a Pyrosate® Kit from Associates of Cape Cod, Inc. with a limit of detection

of 0.03EU/mL. No visible clots were observed after incubating the lysate with NPs at a concentration of 100nM during 50min at 37ºC.

Interfacial Tension: The dynamic interfacial tension of the NPs at the toluene-water interface was measured by the pendant drop method using an OCA20 measuring instrument (Dataphysics, Stuttgart). A syringe filled with an aqueous solution of NPs (1 μM) connected to a blunt needle was fixed vertically with the needle immersed in the toluene phase. A small amount of solution was injected from the syringe to form a drop. The variation of drop shape with time until equilibrium (interfacial tension) and drop fall was captured by automated camera. The measurements were performed in triplicate.

Dynamic Light Scattering: DLS profiles were recorded in 1% human serum (~16 μM protein concentration) diluted in phosphate buffered saline (PBS, pH 7.4) at 37°C with NPs at a concentration of 1 μM using a Malvern Zetasizer Nano ZS. For the dilution profiles, NPs at a concentration of 50 μM were incubated for 30 min at 37ºC in 55% human serum, then diluted accordingly. The subtraction of the individual NP and serum spectra from the "NP in serum" results was done point by point using normalized data to take into account the concentration of each species (spectra of individual NPs and serum reported as normalized). The results are reported as % number when individual NPs are analyzed (characterization) and as % volume for the NP/protein mixtures due to the dependence on the different refractive index of each entity.

Sedimentation: To a solution of 10 and 55% plasma (in PBS) and undiluted plasma, NPs were added to achieve a final concentration of 500 nM (500 μL total volume). The solutions were incubated for 5 min, and the tubes were subjected to centrifugation for 30 min at 14 000 rpm. After centrifugation, 200 μL of the supernatant was transferred to a 96-well plate alongside 200 μL of the same mixture before the centrifugation. The absorbance values were measured at 506 nm, which is the wavelength at which NP concentration is determined. The absorbance generated by the proteins was subtracted using a blank protein sample with no particles. UV differences

were significant only at 10% plasma, as the proteins have much more interference at 55% plasma. All NPs and blank samples were prepared in triplicate. For the sucrose gradients, NP samples in undiluted serum/plasma were centrifuged at 14,000 rpm for 30 min using a sequential gradient of 24, 12, and 6% sucrose and a sharp gradient of 24% for the gel. Ultracentrifugation experiments were run at 60 000 rpm for 1 h.

Agarose Gel Electrophoresis: Agarose gels were prepared in PBS at a 0.5% final agarose concentration. NPs at a concentration of 1 μM were incubated with or without 55% plasma in PBS for 15 min, and 2 μL of 50% glycerol was added to the solution to ensure proper gel loading. The mixture was loaded in each well, and the gels were run at a constant voltage of 100 V for 30 min.

Protein Isolation from NPs and SDS-Polyacrylamide Gel Electrophoresis: NP+ and NPs ZMe-ZDiPen (0.5 μM) were incubated in undiluted human serum for 24 h at 37 C. After incubation, serum-NP mixtures were loaded onto a sucrose cushion (24%) to rapidly separate NP-protein complexes from serum by centrifugation at 14,000 rpm for 30 min.[10] The supernatant was carefully removed, and the residues were washed with 1 mL of PBS three times. Proteins were eluted from the nanoparticles by adding 4 Laemmli sample buffer (Biorad 161-0747) with 2-mercaptoethanol to the pellet and subsequent incubation at 95ºC for 5 min. For 1D gel electrophoresis, 20 μL of recovered proteins in sample buffer was separated on a 12% SDS-PAGE gel. Gels were run at the constant voltage of 150 V for 1 h, and silver staining was performed to visualize the bands according to the previously published protocol.[48] A 0.1% human serum sample was also run for comparison.

Cellular Uptake: MCF7 cells (breast adenocarcinoma) were cultured at 37ºC under a humidified atmosphere of 5% CO2. The cells were grown in low glucose Dulbecco's modified Eagle's medium (DMEM, 1.0 g/L glucose) containing 10% fetal bovine serum and 1% antibiotics (100 U/mL penicillin and 100 μg/mL streptomycin). For the uptake experiment, 20 000 cells/well were plated in a 48-well plate prior to the experiment. On the following day, cells were washed

one time with PBS followed by NP treatment (25 nM/well) and further incubated with or without 10% serum for 3 h (or 24 h). Following incubation, cells were lysed and the intracellular gold amount was measured using inductively coupled plasma mass spectrometry (Elan 6100, PerkinElmer, Shelton, CT, USA). Each cell uptake experiment was done in triplicate, and each replicate was measured five times by ICP-MS. ICP-MS operating conditions are as below: rf power 1600 W; plasma Ar Flow rate, 15 mL/min, nebulizer Ar flow rate, 0.98 mL/min and dwell time, 45 ms.

Hemolysis: Hemolytic activity was measured as described in section 3.4

Cell Viability: The cell viability was determined by alamar blue assay according to manufacturer protocol (Life Technologies, DAL1100). MCF7 cells (15 000 cells/well) were seeded in a 96- well plate 24 h prior to the experiment. On the following day, the old medium was aspirated and the cells were washed with PBS one time. NPs ZMeZDiPen (25 nM each) were then incubated with the cells in 10% serum containing media for 24 h at 37 C. After the incubation period, the cells were washed three times with PBS and 220 µL of 10% alamar blue solution in serum-containing media was added to each well and cells were further incubated at 37ºC for 3 h. After 3 h, 200 µL of solution from each well were taken out and loaded in a 96-well black microplate. Red fluorescence, resulting from the reduction of the alamar blue solution by viable cells, was measured (ex: 560 nm, em: 590 nm) on a SpectroMax M2 microplate reader (Molecular Device). Viability (%) of NP-treated cells was calculated taking untreated cells as 100% viable. All experiments were performed using at least four parallel replicates.

4.5. Supporting information

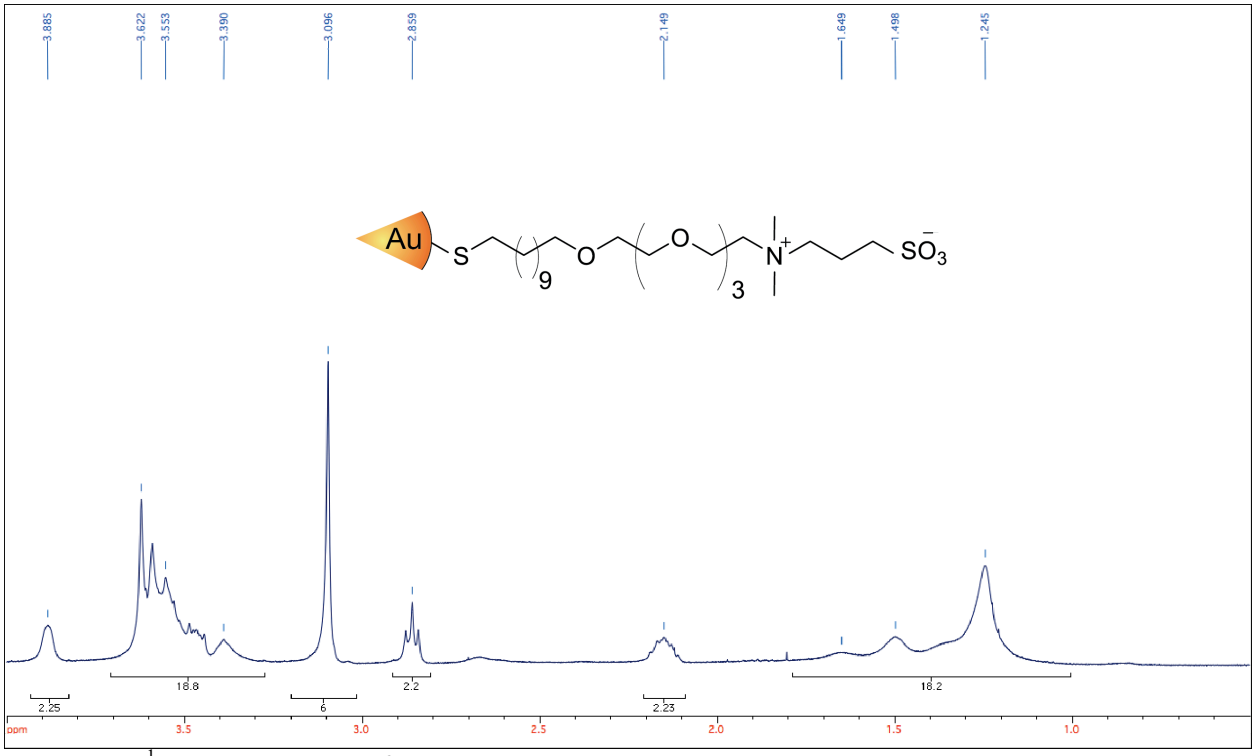

Figure 4.5. ^{1}HNMR spectrum of ZMe.

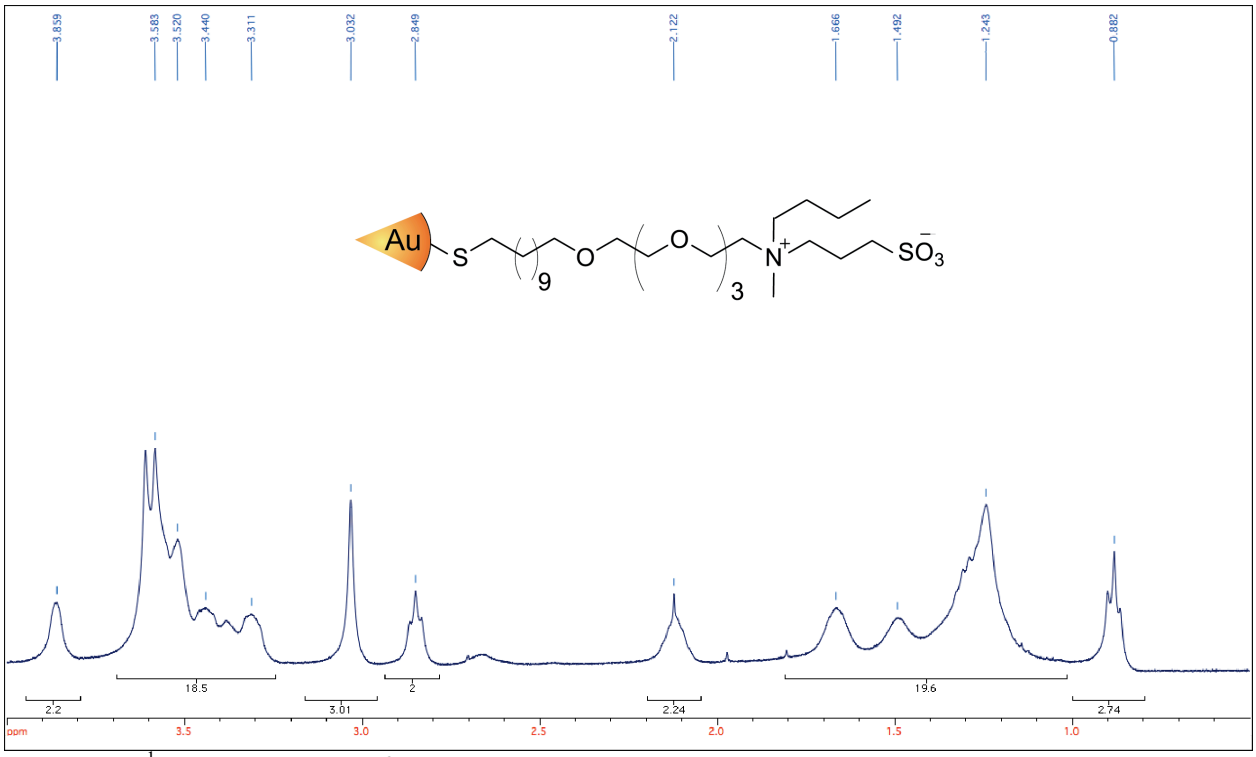

Figure 4.6. ^{1}HNMR spectrum of ZBu.

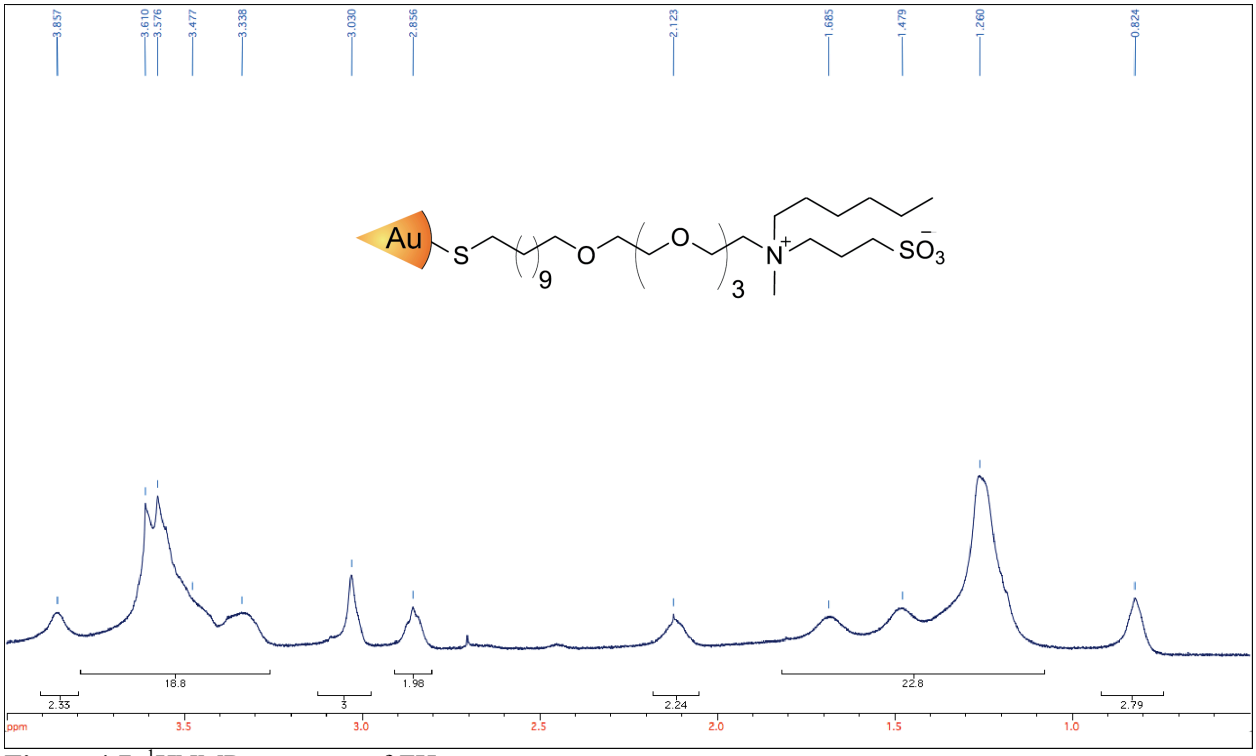

Figure 4.7. ^{1}HNMR spectrum of ZHex.

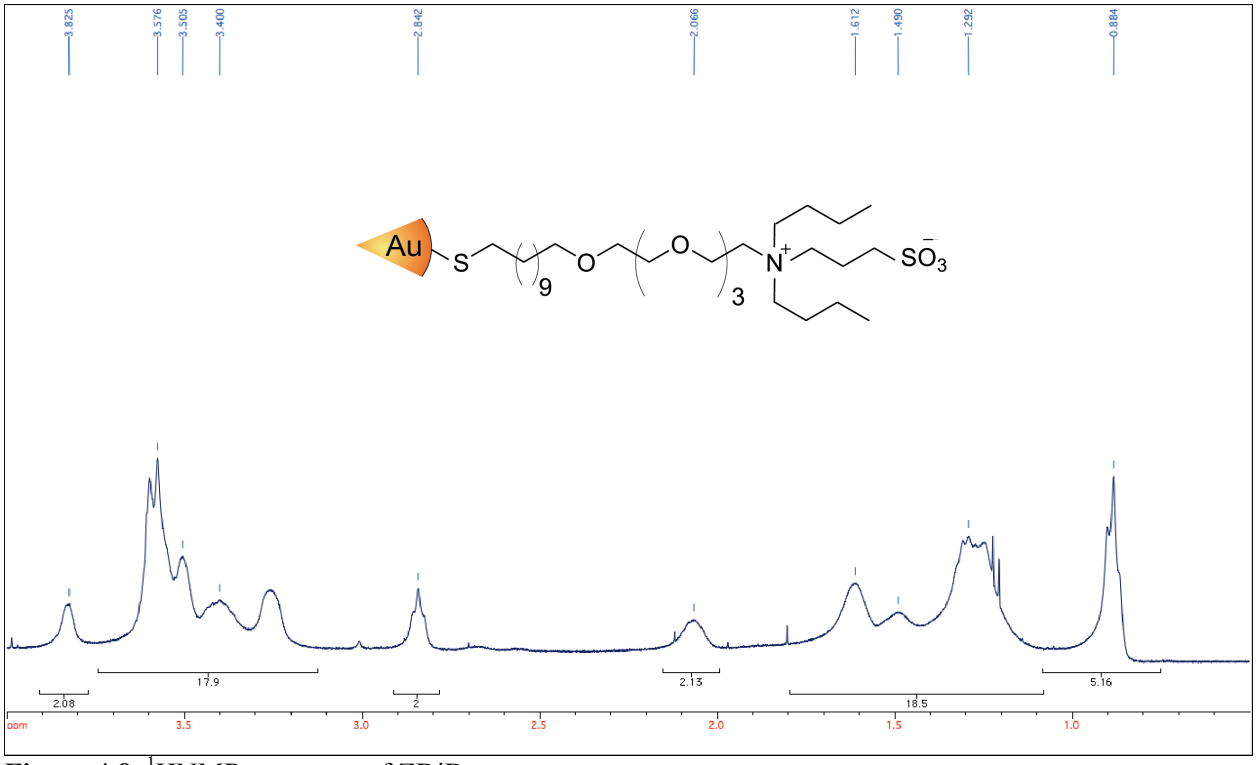

Figure 4.8. ^{1}HNMR spectrum of ZDiBu.

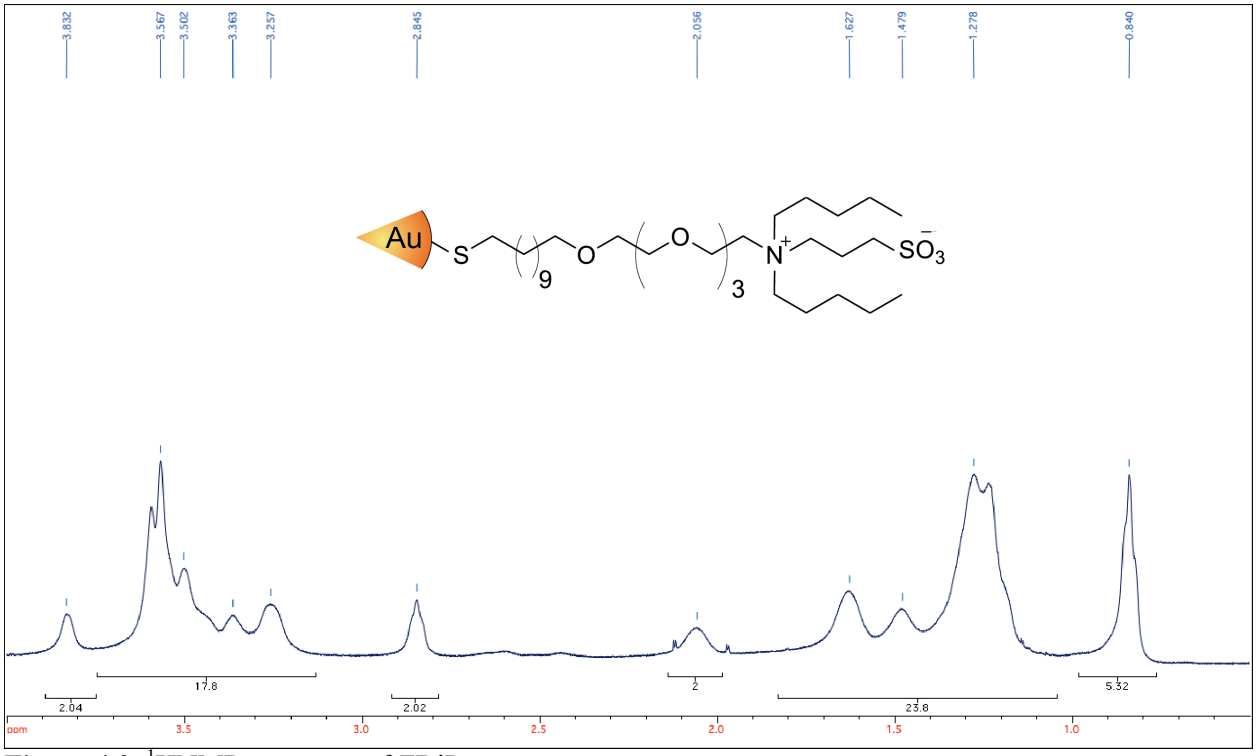

Figure 4.9. ^{1}HNMR spectrum of ZDiPen.

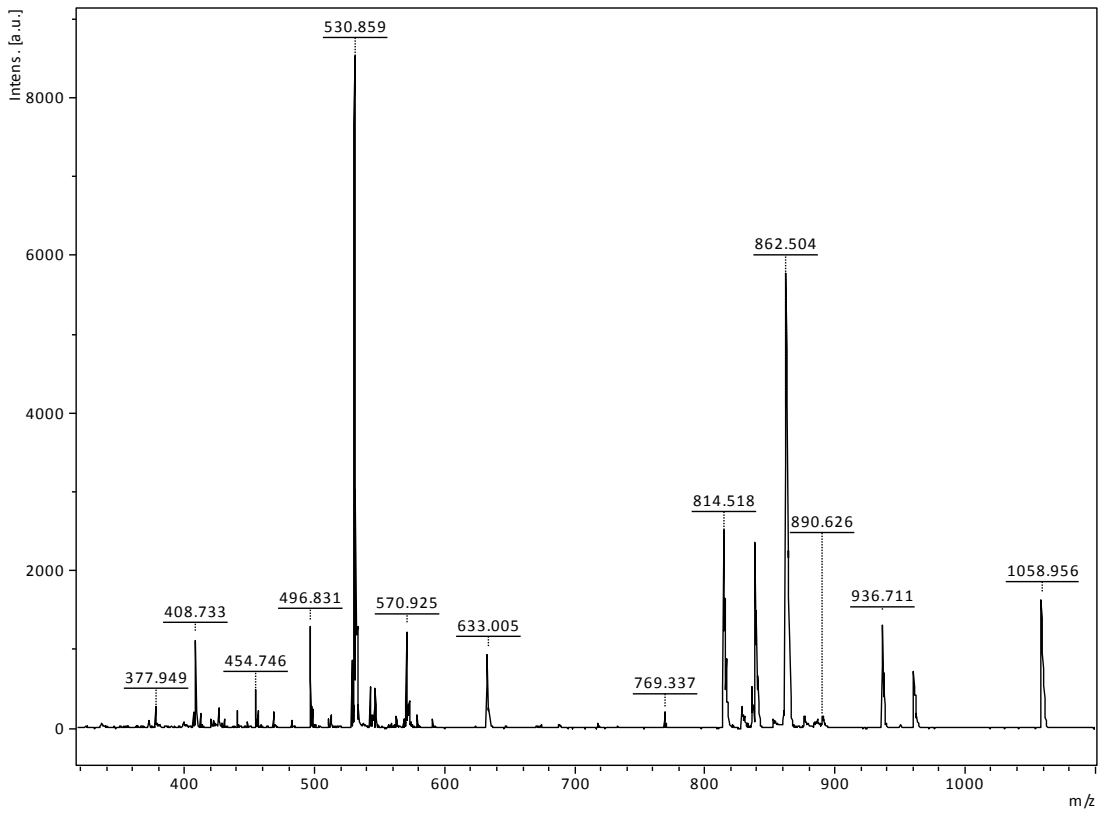

Figure 4.10. Mass spectrum of ZMe (MW=529.31/mol).

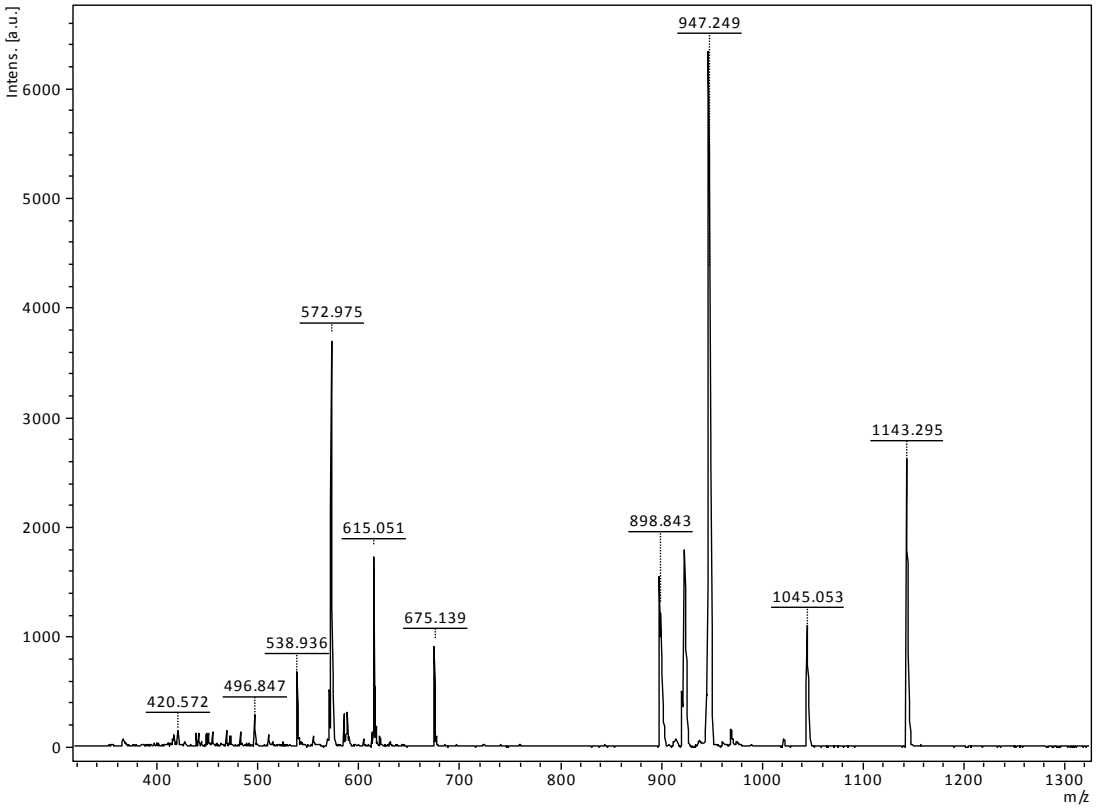

Figure 4.11. Mass spectrum of ZBu (MW=571.36/mol).

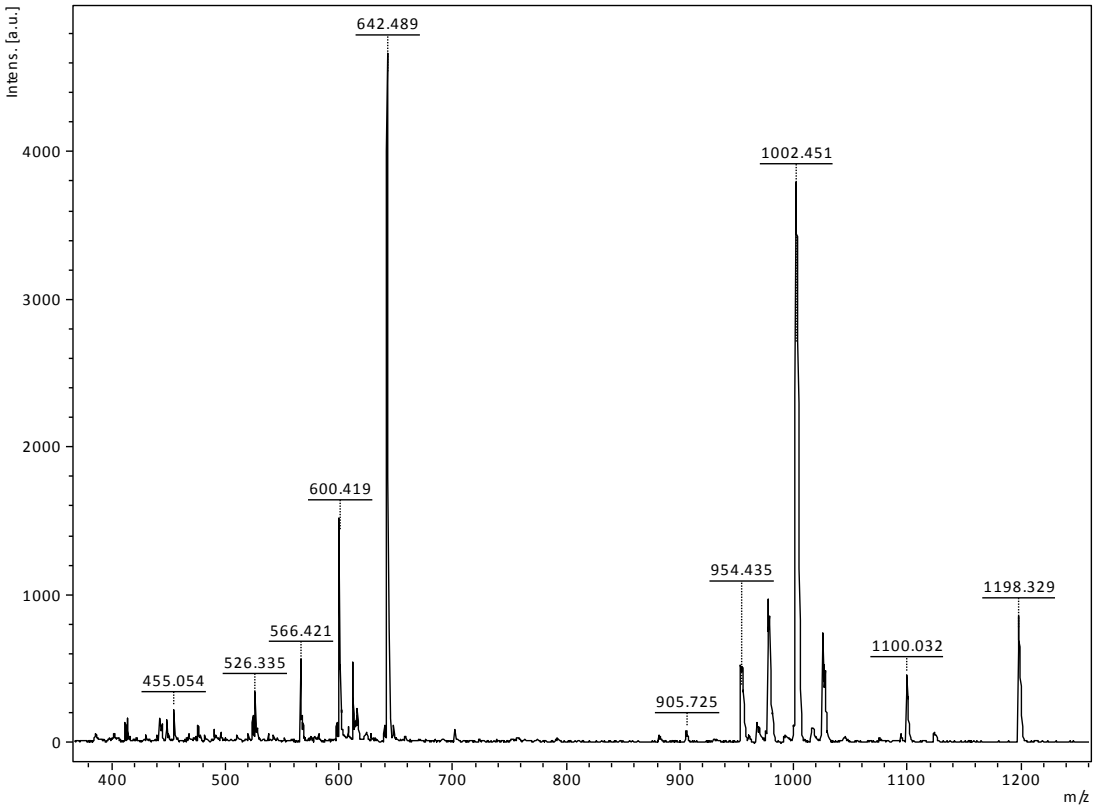

Figure 4.12. Mass spectrum of ZHex (MW=599.39/mol).

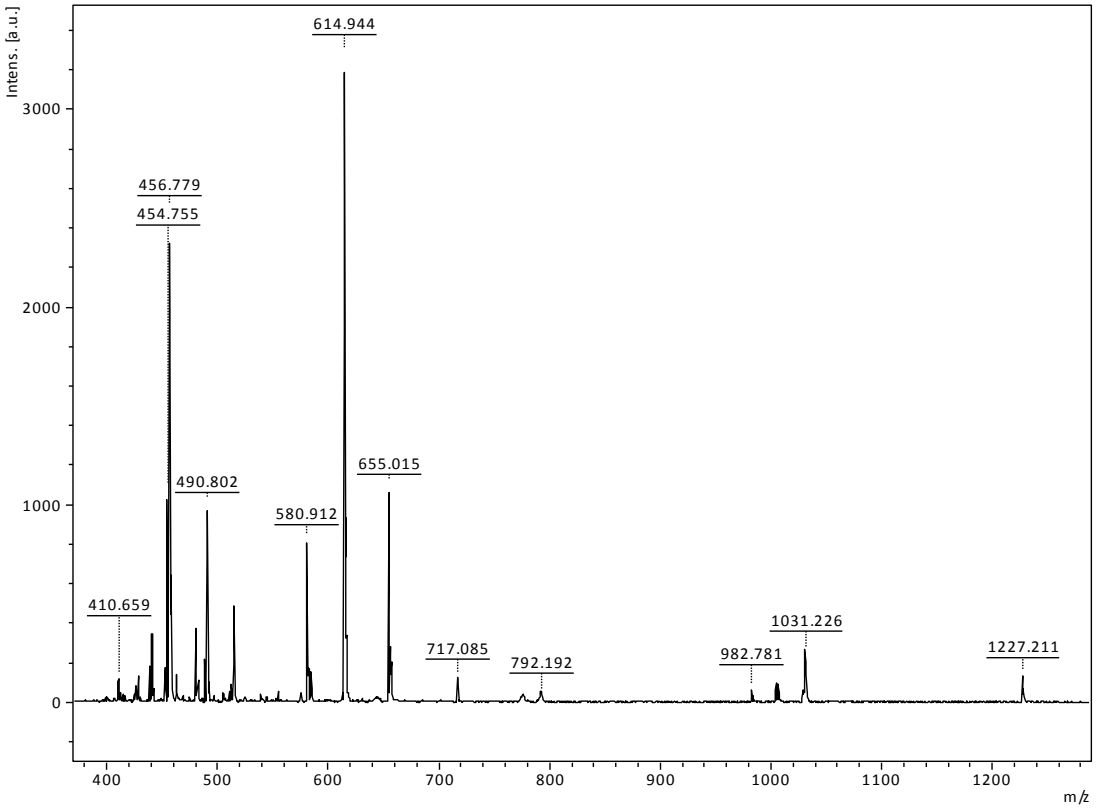

Figure 4.13. Mass spectrum of ZDiBu (MW=613.40/mol).

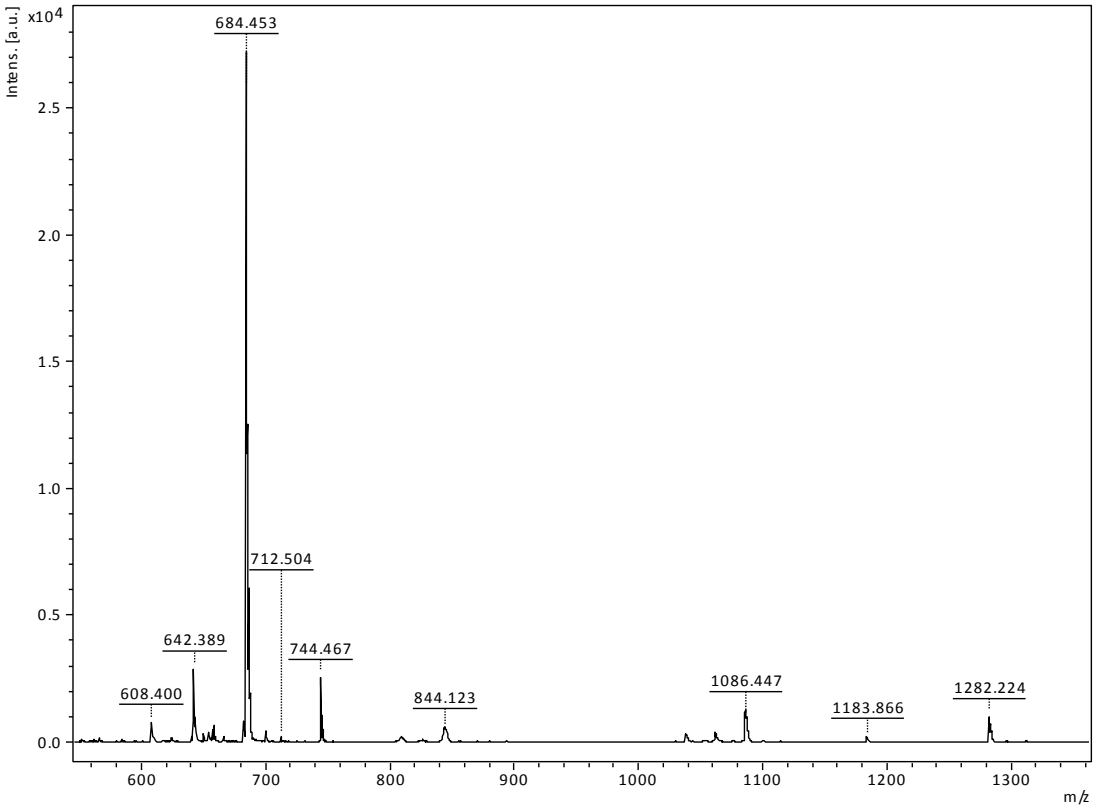

Figure 4.14. Mass spectrum of ZDiPen (MW=641.44/mol).

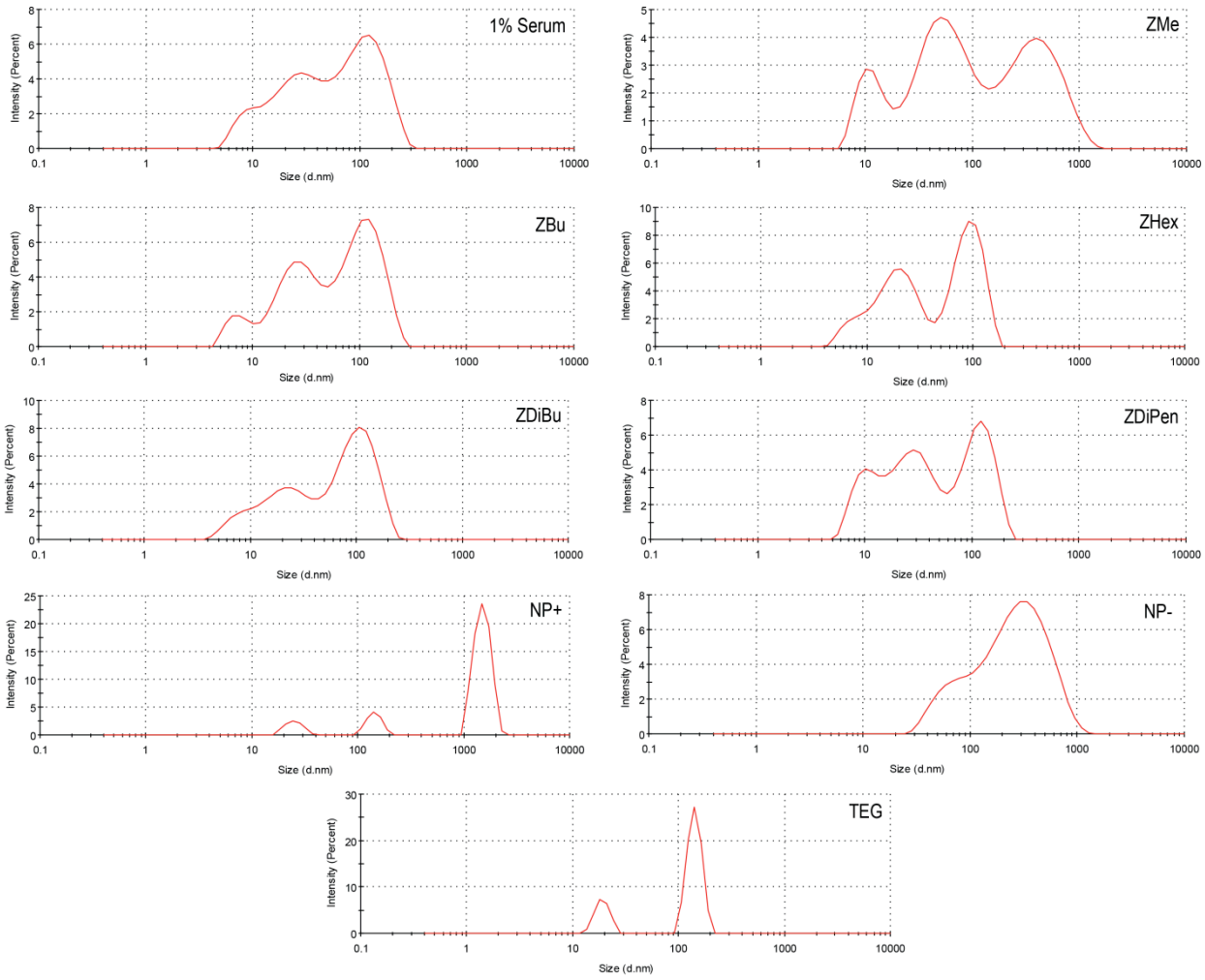

Figure 4.15. Representative DLS profiles (% Intensity) of the series of zwitterionic NPs and controls after incubation in 1% human serum.

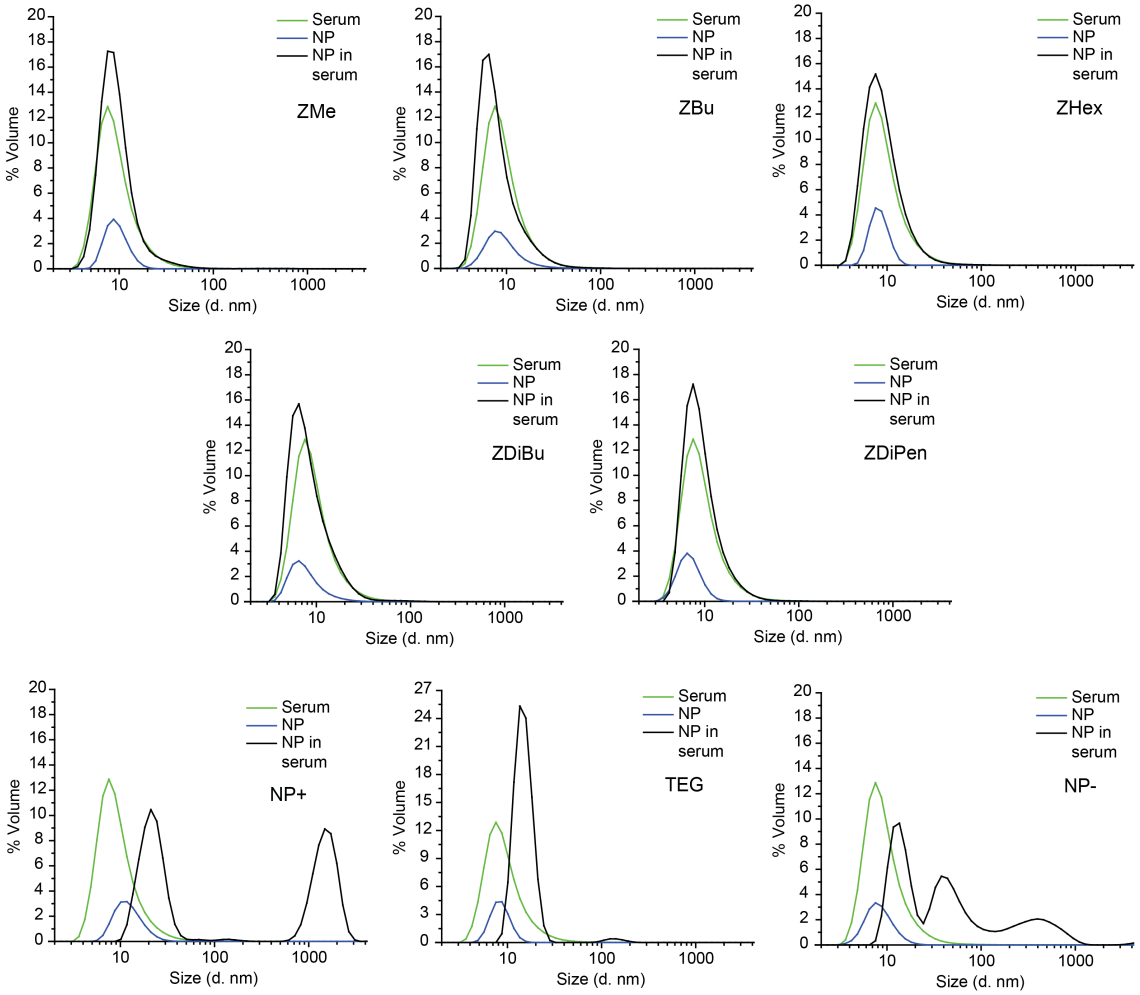

Figure 4.16. DLS profiles (%Volume) for the different NPs in the presence and absence of serum proteins (1% serum background, spectrums of the NPs and serum reported as normalized according to the concentration of each species).

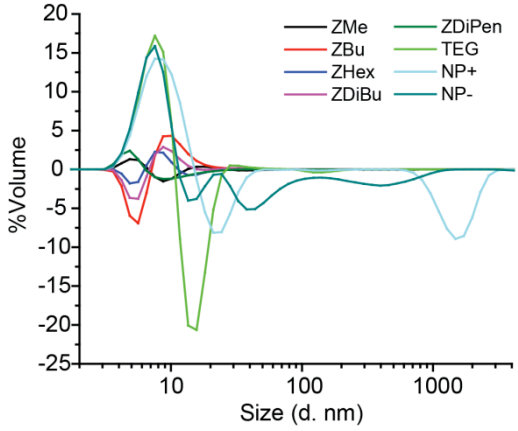

Figure 4.17. Residuals of the DLS profiles in serum after removing the individual NP and serum spectrums for each NP.

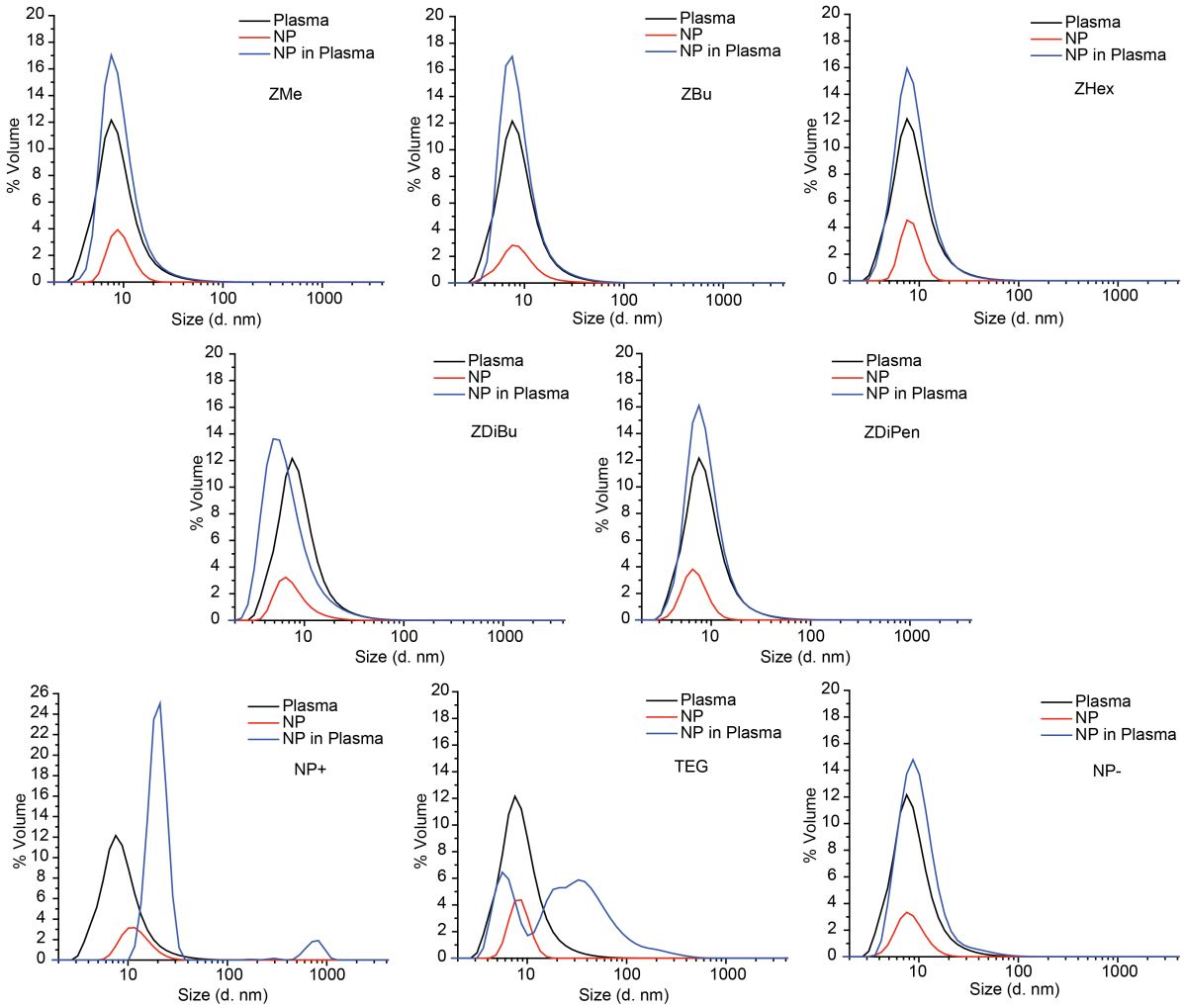

Figure 4.18. DLS profiles (%Volume) for the different NPs in the presence and absence of plasma (1% plasma background, spectrums of the NPs and serum reported as normalized according to the concentration of each species).

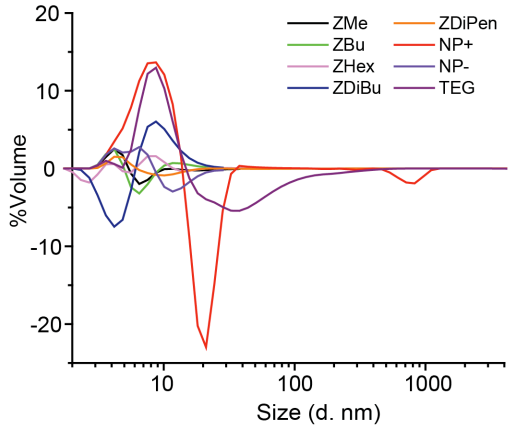

Figure 4.19. Residuals of the DLS profiles in plasma after removing the individual NP and plasma spectrums for each NP.

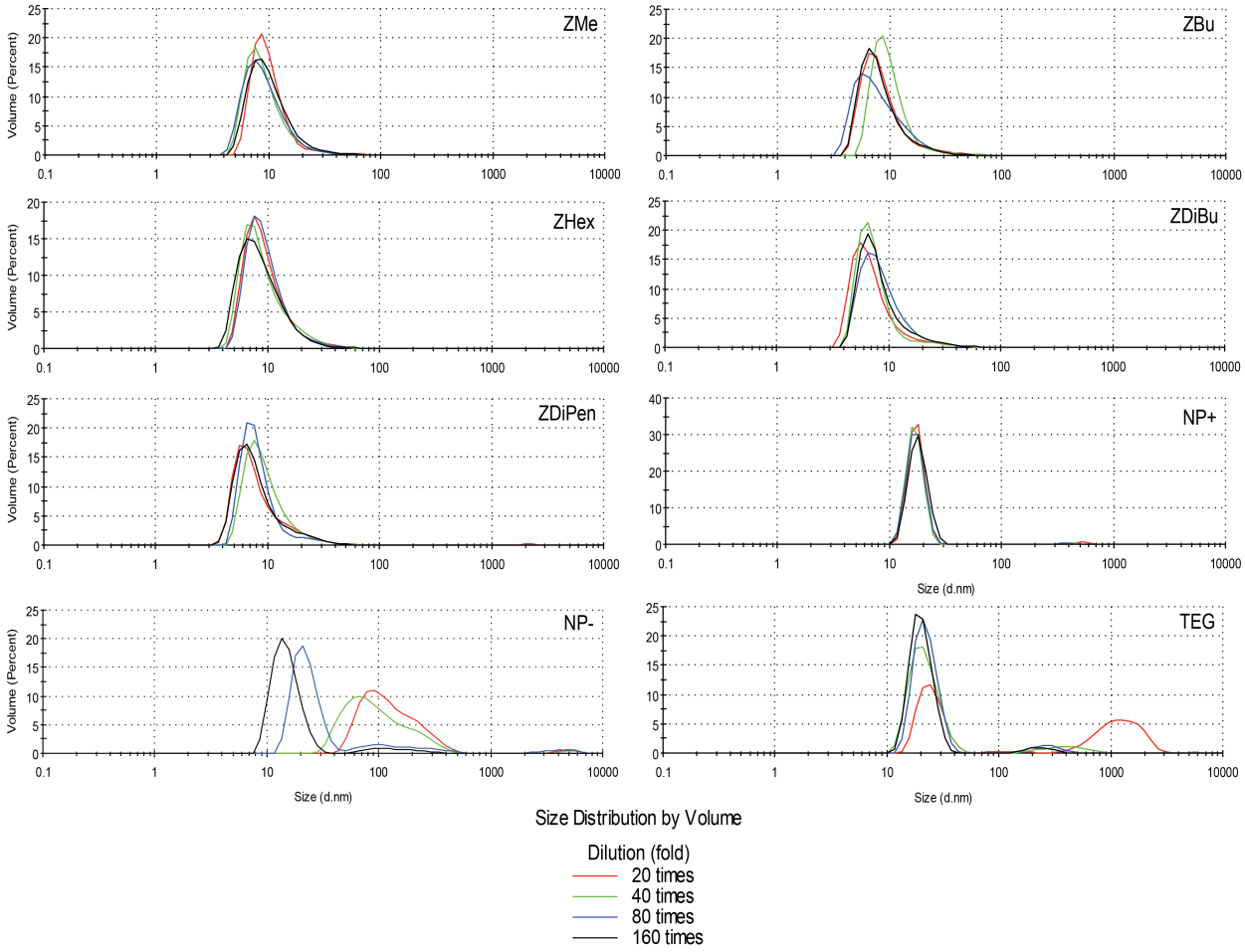

Figure 4.20. DLS profiles (% Volume) of the series of NPs after incubation in 55% human serum and successive dilutions, evidencing the absence of protein corona for ZMe-ZDiPen while NP+, NP- and TEG present NP/protein complexes.

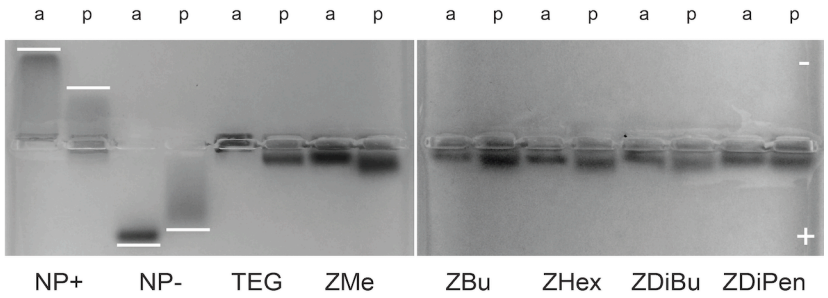

Figure 4.21. Agarose gel electrophoresis showing similar mobilities for NPs ZMe-ZDiPen in the presence and absence of plasma, while NP+ and NP- present a retarded band due to conjugation with proteins (a = NPs alone, p = mixture of plasma and NPs). NP concentration is 1 μM.

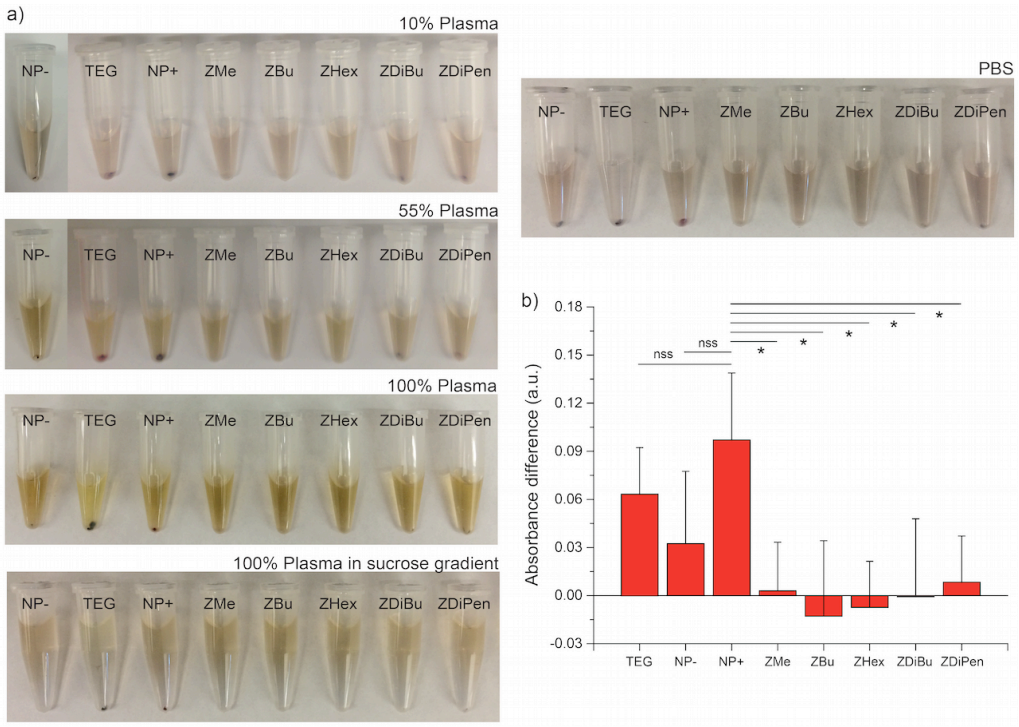

Figure 4.22. (a) Sedimentation experiments at 10% and 55% plasma concentration. (b) UV differences (λ=506nm) of the supernatants before and after centrifugation in 10% serum evidencing the significant difference in sedimentation between TEG, NP+, NP- and ZMe to ZDiPen (*p*-values < 0.05). The sediment observed in the case of ZDiBu and ZDiPen were removed after washing with PBS 1-2 times indicating a reversible binding, while the positive control retained the pellet.

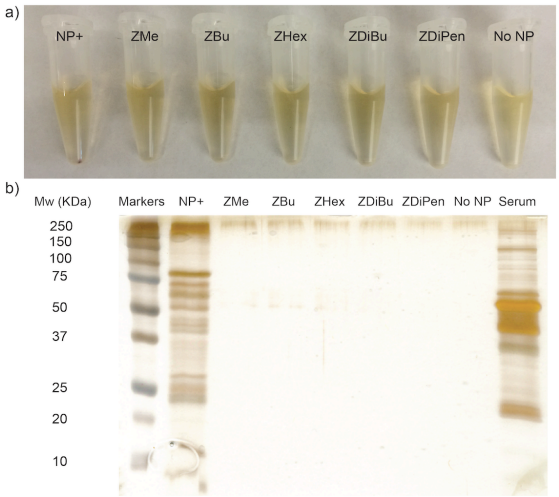

Figure 4.23. (a) Sedimentation assay using a sucrose cushion of 24%. (b) Gel electrophoresis of the samples obtained by the 24% sucrose sedimentation, evidencing very low level of proteins in the samples of the zwitterionic NPs (ZMe – ZDiPen, similar to control with no NP), while NP+ presented protein bands indicating corona formation. Serum lane indicates a sample with 0.1% serum directly loaded into the gel.

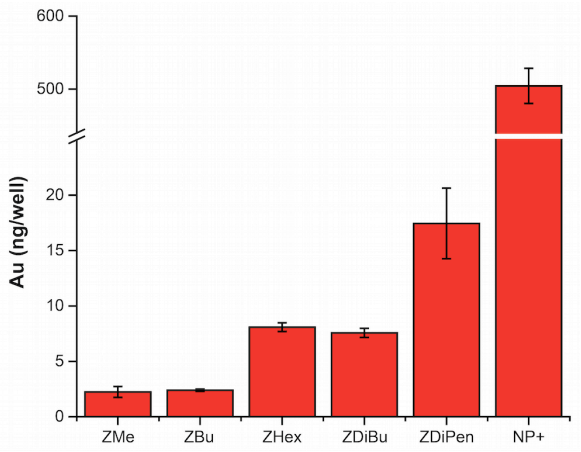

Figure 4.24. Cellular uptake (MCF-7 cells) at 24h of incubation with NPs in the presence of serum.

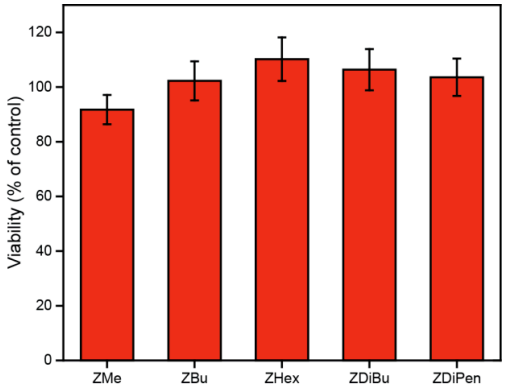

Figure 4.25. Viability of MCF7 cells at 24h for the different NPs.

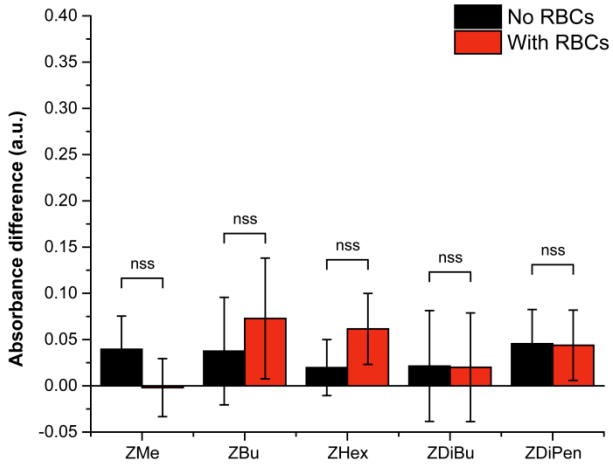

Figure 4.26. Differences in the absorbance for the sedimentation experiments between the presence and absence of RBCs. 'nns' denotates *p*-values > 0.05 (no statistical significance).

4.6. References

1. Sapsford, K. E.; Algar, W. R.; Berti, L.; Gemmill, K. B.; Casey, B. J.; Oh, E.; Stewart, M. H.; Medintz, I. L. *Chem. Rev*. **2013**, *113*, 1904.

2. Mout, R.; Moyano, D. F.; Rana, S.; Rotello, V. M. *Chem. Soc. Rev*. **2012**, *41*, 2539.

3. Walkey, C. D.; Chan, W. C. W. *Chem. Soc. Rev.* **2012**, *41*, 2780.

4. Monopoli, M. P.; Aberg, C.; Salvati, A.; Dawson, K. A. *Nat. Nanotechnol*. **2012**, *7*, 779.

5. Del Pino, P.; Pelaz, B.; Zhang, Q.; Maffre, P.; Nienhausbc, G. U.; Parak, W. J. *Mater. Horiz.* **2014**, *1*, 301.

6. Pelaz, B.; Charron, G.; Pfeiffer, C.; Zhao, Y.; de la Fuente, J. M.; Liang, X.-J.; Parak, W. J.; Del Pino, P. *Small* **2013**, *9*, 1573.

7. Mahmoudi, M.; Lynch, I.; Ejtehadi, M. R.; Monopoli, M. P.; Bombelli, F. B.; Laurent, S. *Chem. Rev.* **2011**, *111*, 5610.

8. Lundqvist, M.; Stigler, J.; Elia, G.; Lynch, I.; Cedervall, T.; Dawson, K. A. *Proc. Natl. Acad. Sci. U.S.A.* **2008**, *105*, 14265.

9. Aggarwal, P.; Hall, J. B.; McLeland, C. B.; Dobrovolskaia, M. A.; McNeil, S. E. *Adv. Drug Delivery Rev.* **2009**, *61*, 428.

10. Tenzer, S.; Docter, D.; Kuharev, J.; Musyanovych, A.; Fetz, V.; Hecht, R.; Schlenk, F.; Fischer, D.; Kiouptsi, K.; Reinhardt, C.; Landfester, K.; Schild, H.; Maskos, M.; Knauer, S. K.; Stauber, R. H. *Nat. Nanotechnol*. **2013**, *8*, 772.

11. Mirshafiee, V.; Mahmoudi, M.; Lou, K. Y.; Cheng, J. J.; Kraft, M. L. *Chem. Commun.* **2013**, *49*, 2557.

12. Salvati, A.; Pitek, A. S.; Monopoli, M. P.; Prapainop, K.; Bombelli, F. B.; Hristov, D. R.; Kelly, P. M.; Aberg, C.; Mahon, E.; Dawson, K. A. *Nat. Nanotechnol*. **2013**, *8*, 137.

13. Jokerst, J. V.; Lobovkina, T.; Zare, R. N.; Gambhir, S. S. *Nanomedicine* **2011**, *6,* 715.

14. Karakoti, A. S.; Das, S.; Thevuthasan, S.; Seal, S. Angew. Chem., Int. Ed. **2011,** 50, 1980.

15. Hamad, I.; Al-Hanbali, O.; Hunter, A. C.; Rutt, K. J.; Andresen, T. L.; Moghimi, S. M. *ACS Nano* **2010**, *4*, 6629.

16. Sekiguchi, S.; Niikura, K.; Matsuo, Y.; Ijiro, K. *Langmuir* **2012**, *28*, 5503.

17. Rosen, J. E.; Gu, F. X *Langmuir* **2011**, *27*, 10507.

18. Yang, W.; Zhang, L.; Wang, S.; White, A. D.; Jiang, S. Y. *Biomaterials* **2009**, *30*, 5617.

19. Cao, Z. Q.; Jiang, S. Y. *Nano Today* **2012**, *7*, 404.

20. Murthy, A. K.; Stover, R. J.; Hardin, W. G.; Schramm, R.; Nie, G. D.; Gourisankar, S.; Truskett, T. M.; Sokolov, K. V.; Johnston, K. P. *J. Am. Chem. Soc.* **2013**, *135*, 7799.

21. McCormick, C. L.; Lowe, A. B. *Acc. Chem. Res.* **2004**, *37*, 312.

22. Matyjaszewski, K. *Macromolecules* **2012**, *45*, 4015.

23. Arvizo, R. R.; Miranda, O. R.; Moyano, D. F.; Walden, C. A.; Giri, K.; Bhattacharya, R.; Robertson, J. D.; Rotello, V. M.; Reid, J. M.; Mukherjee, P. *PLoS One* **2011**, *6*, e24374.

24. a) Moyano, D. F.; Rana, S.; Bunz, U. H. F.; Rotello, V. M. *Faraday Discuss.* **2011**, *152*, 33. b) Elci, S. G.; Moyano, D. F.; Rana, S.; Tonga, G. Y.; Philips, R. L.; Bunz, U. H. F.; Rotello, V. M. *Chem. Sci.* **2013**, *4*, 2076.

25. Zhang, G.; Yang, Z.; Lu, W.; Zhang, R.; Huang, Q.; Tian, M.; Li, L.; Liang, D.; Li, C. *Biomaterials* **2009**, *30*, 1928.

26. Rana, S.; Yu, X.; Patra, D.; Moyano, D. F.; Miranda, O. R.; Hussain, I.; Rotello, V. M. *Langmuir* **2012**, *28*, 2023.

27. Xiao, Y.; Wiesner, M. R. *J. Hazard. Mater*. **2012**, *215*, 146.

28. Zhang, C.; Macfarlane, R. J.; Young, K. L.; Choi, C. H. J.; Hao, L.; Auyeung, E.; Liu, G.; Zhou, X.; Mirkin, C. A. *Nat. Mater*. **2013**, *12*, 741.

29. Milani, S.; Bombelli, F. B.; Pitek, A. S.; Dawson, K. A.; Rädler, J. *ACS Nano* **2012**, *6*, 2532.

30. Casals, E.; Puntes, V. F. *Nanomedicine* **2012**, *7*, 1917.

31. Monopoli, M. P.; Pitek, A. S.; Lynch, I.; Dawson, K. A. *Methods Mol. Biol*. **2013**, *1025*, 137.

32. Zhu, Z.-J.; Ghosh, P.; Miranda, O. R.; Vachet, R. W.; Rotello, V. M. *J. Am. Chem. Soc.* **2008**, *130*, 14139.

33. Mortimer, G. M.; Butcher, N. J.; Musumeci, A. W.; Deng, Z. J.; Martin, D. J.; Minchin, R. F. *ACS Nano* **2014**, *8*, 3357.

34. Walkey, C. D.; Olsen, J. B.; Guo, H.; Emili, A.; Chan, W. C. *J. Am. Chem. Soc.* **2012**, *134*, 2139.

35. Zhu, Z. J.; Posati, T.; Moyano, D. F.; Tang, R.; Yan, B.; Vachet, R. W.; Rotello, V. M. *Small* **2012**, *8*, 2659.

36. Gessner, A.; Waicz, R.; Lieske, A.; Paulke, B. R.; Mader, K.; Muller, R. H *Int. J. Pharm.* **2000**, *196*, 245.

37. Baier, G.; Costa, C.; Zeller, A.; Baumann, D.; Sayer, C.; Araujo, P. H. H.; Mailander, V.; Musyanovych, A.; Landfester, K. *Macromol. Biosci.* **2011**, *11*, 628.

38. Patil, S.; Sandberg, A.; Heckert, E.; Self, W.; Seal, S. *Biomaterials* **2007**, *28*, 4600.

39. Kim, C. K.; Ghosh, P.; Pagliuca, C.; Zhu, Z.-J.; Menichetti, S.; Rotello, V. M. *J. Am. Chem. Soc.* **2009**, *131*, 1360.

40. Hühn, D.; Kantner, K.; Geidel, C.; Brandholt, S.; Cock, I. D.; Soenen, S. J. H.; Rivera_Gil, P.;Montenegro, J.-M.; Braeckmans, K.; Müllen, K.; Nienhaus, G. U.; Klapper, M.; Parak, W. J. *ACS Nano* **2013**, *7*, 3253.

41. Fleischer, C. C.; Kumar, U.; Payne, C. K. *Biomater. Sci.* **2013**, *1*, 975.

42. Lesniak, A.; Fenaroli, F.; Monopoli, M. R.; Aberg, C.; Dawson, K. A.; Salvati, A. *ACS Nano* **2012**, *6*, 5845.

43. Xiao, W. C.; Lin, J.; Li, M. L.; Ma, Y. J.; Chen, Y. X.; Zhang, C. F.; Li, D.; Gu, H. C. *Contrast Media Mol. Imaging* **2012,** *7*, 320.

44. Lin, Y. S.; Haynes, C. L. *J. Am. Chem. Soc.* **2010**, *132*, 4834.

45. Lin, Y. S.; Haynes, C. L. *Chem. Mater.* **2009**, *21*, 3979.

46. Saha, K.; Moyano, D. F.; Rotello, V. M. *Mater. Horiz.* **2014**, *1*, 102.

47. You, C. C.; De, M.; Miranda, O. R.; Gider, B.; Ghosh, S. P.; Kim, I.; Erdogan, B.; Krovi, S. A.; Bunz, U. H. F.; Rotello, V. M. *Nat. Nanotechnol.* **2007**, *2*, 318.

48. Chevallet, M.; Luche, S.; Rabilloud, T. *Nat. Protoc*. **2006**, *1*, 1852.

CHAPTER 5

CONTROLLING INFLAMMATORY RESPONSES IN CHALLENGED SYSTEMS BY THE USE OF NANOPARTICLES

"For the moment, the jazz is playing;
there is no melody, just notes, a myriad of tiny tremors.
The notes know no rest, an inflexible order gives birth to them then destroys them,
without ever leaving them the chance to recuperate and exist for themselves....
I would like to hold them back, but I know that, if I succeeded in stooping one,
there would only remain in may hand a corrupt and languishing sound."
- Jean Paul Sartre, *La Nausée*

5.1. Introduction

The ability to control immune responses by tailoring the NP surface chemical identity has opened new avenues for the use of these materials as therapeutics.[1] For example, new vaccine formulations have been developed by the use of specific immunogenic peptides, or by using different NP properties to boost the response.[2] These applications rely on the capability of enhancing immune responses (adjuvancy) by either delivering the antigen of interest or by enhancing antigen presentation.[3] By the use of this *prophylactic* approach, vaccines against cancer, hepatitis B, and other diseases have been developed.[4] However, much less understood is the potential for NPs to behave positively or adversely in challenged systems, for example when an inflammatory event is already present (*remedial* approach, Figure 5.1a). This is a promising area to explore since immunomodulation, most specifically inflammatory profiles, plays a significant role in the development of many diseases such as arthritis and fibromyalgia, and current non-prophylactic approaches offer very limited efficacy.[5]

So far we have observed that the hydrophobicity of NPs dictates immunological outcomes both *in vitro* and *in vivo*, and that the protein corona needs to be eliminated to avoid interferences caused by adsorbed proteins. Similarly, we engineered a NP system that can control the

presentation of hydrophobicity without the interference of the protein corona. Now we seek to test the immunomodulatory capabilities of these NPs, and systems with an immunological challenge (i. e. inflammation) offer us the opportunity to explore both the immunological properties of these materials and also their therapeutic capabilities. As such, in this section we report the use of the zwitterionic gold NPs to probe immunological responses when an inflammatory challenge is presented, a key event in infectious, autoimmune and inflammation induced tissue degenerative diseases.

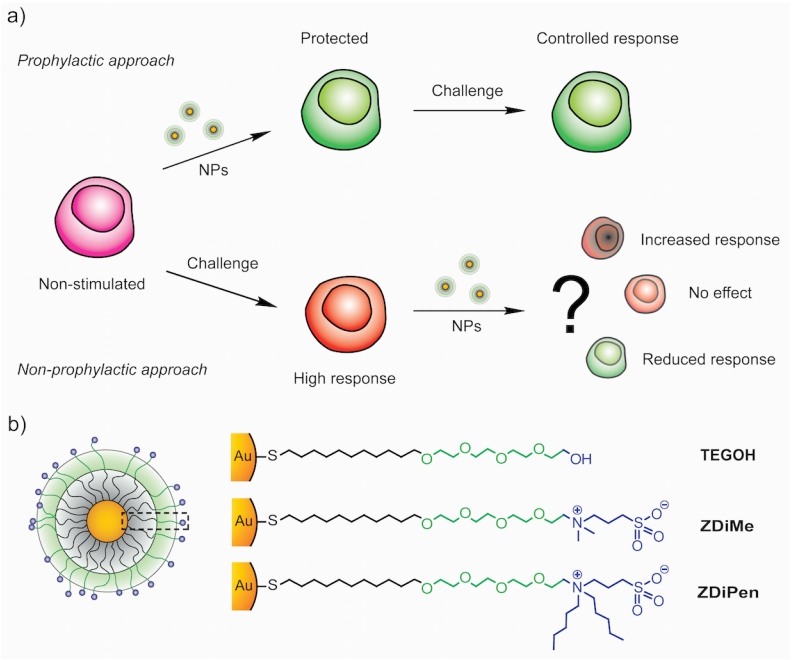

Figure 5.1. a) Differences between a prophylactic and a remedial (non-prophylactic) therapeutic approach. For our non-prophylactic studies, the challenge is comprised of a stimulation with LPS, which induces a strong inflammatory response. b) Chemical structure of the NPs bearing different chemical groups while maintaining a net neutral charge.

5.2. Results and discussions

Inflammation was selected as the immunological read out given its significant role in the development of diseases such as arthritis, atherosclerosis, and fibromyalgia. In our experiments, inflammation was induced by lipopolysaccharide (LPS), a bacterial agent that is known to trigger strong inflammatory responses.[6] As the readout we measured the expression of TNFα, a cytokine characteristic of pro-inflammatory cellular profiles.[7] Since this cytokine is directly associated with the level of inflammatory responses in the system, a decrease or increase in TNFα levels suggest the reduction or boosting of inflammation respectively. For the nanoparticle system, three different types of surface chemical functionalities were selected based on their known interactions with the immune system (Figure 5.1b). TEGOH is structurally based on poly(ethylene glycol) coatings that are commonly used in nanomaterials, a functionality that can be recognized by different components of the immune system *in vivo* such as the complement system.[8] Likewise, hydrophobic NPs (ZDiPen) are capable of triggering various types of innate immune responses as described in Chapter 2, and have been used in the development of vaccines.[9] We engineered these NPs to bear a neutral charge that decreases non-specific adsorption of proteins, thus reducing interference and allowing the study of immune responses intrinsic to the chemical functionalities (as described in Chapter 4).

We first tried *in vitro* studies by the use of J774.2 cells, as monocytes are known to interact strongly with nanomaterials in addition to being highly sensitive to LPS stimulation.[10] As observed in Figure 2a, ZDiMe did not affect the expression of TNFα comparative to the control without NPs. This result suggests that NPs coated with this functionality have minimal interaction with the cells, an observation that is in agreement with the low cellular uptake of these NPs (Figure 5.2c). On the other hand, both TEGOH and ZDiPen decreased the expression of TNFα, indicating detrimental effect on the inflammatory response. Similarly, the cellular uptake of these two NPs was higher than ZDiMe, demonstrating its greater interaction with the monocytes. This

result is in agreement with previous reports depicting the greater cellular uptake of hydrophobic NPs, possibly due to a stronger interaction with the hydrophobic portions of the cell membrane. However, TEG NPs were not uptaken as much as ZDiPen despite the fact that a reduction in TNFα expression was also observed for these particles. This observation suggests that the phenomenon does not merely depend on cellular uptake generated by the NP surface functionality. These studies were also repeated in fully differentiated macrophages (RAW 264.7 cells), and similar results were obtained as presented in Figure 5.6, indicating that the phenomenon is not exclusive to J774.2.

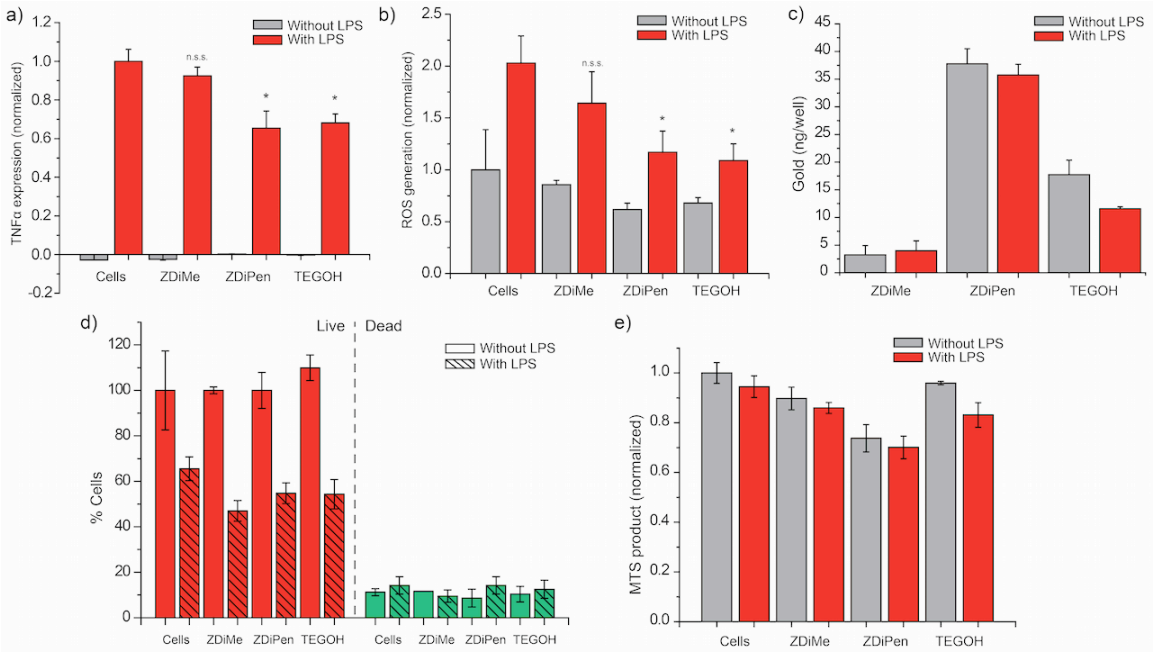

Figure 5.2. a) TNFα expression of J774.2 cells in the presence of the different NPs, with and without LPS stimulation after 3h incubation. Values were normalized against the positive control (Cell + LPS). b) ROS generation of J774.2 cells under the same experimental conditions (LPS challenge, 24h). Values normalized against the normal cell response. c) Cellular uptake of the different NPs for both LPS challenged and unchallenged conditions. d) Cell viability (live/dead cells) of J774.2 after 24h incubation with the different NPs and LPS measured by trypan blue. e) MTS assay indicating the metabolism of cells after 24h exposure with NPs and LPS. Values normalized against the responses of untreated cells.

We wanted to examine whether other cellular responses were also hampered by the NPs. To this end, we measured the generation of Reactive Oxygen Species (ROS, an indicative of cell activation) by J774.2 cells after exposure to NPs and LPS, which shows the oxidative stress that the cells are generating. As observed in Figure 2b, both ZDiPen and TEG reduced the response of the cells significantly comparative to the baseline (cells alone). These results mimic our TNFα findings and indicate a decrease in the inflammatory activation of the cells. To observe that the change in these responses was indeed a reduction of activity and not simply a decrease in the viability of cells, we quantify live/dead cells after 24h of incubation using trypan blue. As observed in Figure 2d, J774.2 cells were viable for all the NPs under the conditions of the study, and both alive and dead cells were comparable to the controls, indicating no toxic effects of the particles. We further analyzed if the metabolism of cells was altered by the presence of the NPs by the use of (3-(4,5-dimethylthiazol-2-yl)-5-(3-carboxymethoxyphenyl)-2(4-sulfophenyl)-2H tetrazolium). This test measures the reaction of the substrate with dehydrogenase enzymes, present in cells that are metabolically active. Interestingly, while ZDiMe and TEG did not affect the metabolism of cells, ZDiPen decreased the metabolic activity both in the presence and the absence of LPS as shown in Figure 2e. This result depicts the differential effects of TEG and ZDiPen, and suggests that these two NPs might be achieving the desired reduction of activity through different biological mechanisms.

After our *in vitro* experiments, we then proceeded to examine the physiological relevance of these results by using LPS-challenged mice. Based on our *in vitro* leads, we wanted to observe if TEGOH and ZDiPen maintained their capability to reduce inflammation, and see if ZDiMe still did not cause a response. We first established a baseline of the response by measuring TNFα blood levels (overall expression) when C57BL/6 mice were challenged with different concentrations of LPS. Mice were sacrificed after 2h of the treatment and blood was extracted and processed as described in section 5.4. A concentration of LPS of 200ng/mice was chosen since this concentration was the lowest that induced a significant and robust TNFα readout

(Figure 5.8). We then injected (intraperitoneal, IP) mice with LPS, followed by an injection with the TEGOH, ZDiMe and ZDiPen (IP, injection scheme in Figure 5.8). In this case in addition to TNFα levels, we also measured the concentration of gold in the different organs by mass spectrometry, to observe how different functionalities affect the biodistribution of these NPs. As observed in Figure 3a, no change in the inflammatory response was observed with ZDiMe, mirroring the results *in vitro*. Although *in vivo* an inflammatory response was observed when ZDiMe NPs were injected alone, no boosting or decrease of inflammatory response was evident. Based on these results, it seems that hydrophilic zwitterionic structures avoid interaction with the immune system and do not trigger a significant response, an important property that should be taken into account for the design of delivery vehicles that require extended blood circulation times.

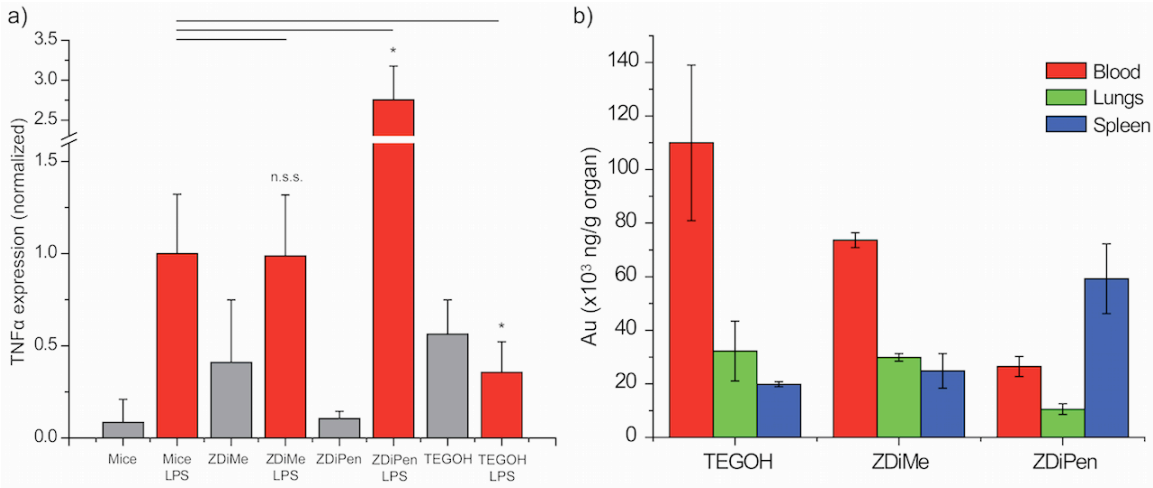

Figure 5.3. a) *In vivo* TNFα expression 2h after ZDiMe, ZDiPen and TEGOH were injected in mice with and without the presence of LPS. b) Nanoparticle distribution in the blood, lung and spleen of mice evidencing the fast elimination of ZDiPen comparative to the other two NPs.

More interesting, however, were the results obtained for TEGOH and ZDiPen. ZDiPen responded very differently *in vivo* than our in our *in vitro* studies, and a strong boost of

inflammatory response was observed when this NP was administered to mice. This result is particularly intriguing since hydrophobic NPs reduced inflammatory responses with macrophages in our *in vitro* studies. Our *in vivo* results suggest involvement of other immune cells to orchestrate the NP induced inflammatory responses. However, it is important to observe that the biodistribution profile was very distinct than that for ZDiMe (Figure 3b). Despite the fact that both NPs have the same surface charge and size, the presence of a hydrophobic tail decreased strongly the concentration of NPs in the blood and increased it in the spleen, demonstrating its fast elimination. This result coupled with the strong interaction with cells observed in the cellular uptake studies suggest that that the changes in the *in vitro*/*in vivo* behavior possibly arises from differences in the interaction with different components of the immune system. The strong synergistic response obtained by the combination of LPS and ZDiPen, a level that cannot be achieved by either LPS or ZDiPen alone, is interesting and suggests that these type of functionalities maybe employed in the future for adjuvant therapies (without the need of covalent conjugation between then antigen and the NP). On the other hand, TEGOH did decrease the expression of TNFα *in vivo*, mimicking the results observed *in vitro*. Interestingly, while TEGOH triggered an inflammatory response on its own, its biodistribution behavior was similar to that of the ZDiMe. PEG functionalities have been shown to interact with the complement system and some reports show that even antibodies are generated towards these functionalities. However, the fact that there is a decrease in inflammatory response, provide evidence for the potential that these NPs have to be used in anti-inflammatory therapies.

5.3. Conclusions

In summary, we have determined the immune response that NPs with different surface chemistry generate in the presence of an inflammatory challenge. We were able to observe that hydrophilic zwitterionic structure may be the ideal functionality when avoiding immune response

is a requirement, as these NPs did not generate a significant change in the observed activities. Likewise, the study of PEG-like structures let us foresee the possible use of these NPs in anti-inflammatory therapy. In the absence of an inflammatory challenge these NPs create a weak response on their own but combined with a challenge they have inhibit inflammation. Finally, the study of hydrophobic structures offered us important clues for the use of these functionalities in adjuvant therapy since a strong synergistic response was observed when LPS was present. These results strongly suggest the significant impact of the NP surface functionalities on the modulation of induced immune responses, more specifically inflammation. These findings offer us important 'lead structures' for the use of NPs in non-prophylactic applications, an important step towards the development of a new generation of immunotherapy methods.

5.4. Experimental section

Nanoparticle synthesis and characterization: Section 4.4 offers a detailed description of the synthesis and characterization of these particles, including LAL gel cloth assay to analyze the endotoxin-free conditions.

Cell culture: J774.2 mouse monocytes and RAW 264.7 macrophage cells were purchased from Sigma-Aldrich. Cells were grown in Roswell Park Memorial Institute media (RPMI 1640) supplemented with 10% fetal bovine serum, 1% antibiotics (100 µg/ml penicillin and 100 µg/ml streptomycin) and sodium pyruvate, and incubated at 37C under a humidified atmosphere of 5% CO2. Under the above culture conditions, the cells were subcultured once every four days.

Nanoparticle and LPS treatment: J774.2 and RAW 264.7 cells were seeded at 106 cells/well in a 24-well plate for 5h (overnight for RAW 264.7) and then incubated with the nanoparticles at a concentration of 50nM, with or without 1µl of LPS (1mg/mL, Enzo Life Sciences). The cells were incubated during 3h and 24h at 37C under a humidified atmosphere and 5% CO2. After the incubation time, the plate was centrifuged at 2,000 rpm and the media was collected for TNFα measurements. Experiments were done in triplicate.

Cell viability: After removing the supernatant media, 1mL of PBS buffer was added to each well (of the 24 well/plate) and cells were redispersed carefully. 10µL of the solution of cells was added to 90µL of a solution of trypan blue (0.1µM), and live/dead cells were counted with a hemocytometer.

TNFα expression: TNFα secretion was measured by Enzyme-Linked Immunosorbent Assay (ELISA) at 3h and 24h using TNFα kits (BD Biosciences, CA, USA) according to the manufacturer's instructions. Briefly, maxisorb 96 well plates (Krackeler) were coated with a solution of purified hamster anti-mouse TNF (0.5µg/mL in bicarbonate buffer pH=9.5, 100µL per well) overnight. The solution was then discarded and the plate was washed 3 times with a solution of 0.05% Tween 20 in PBS. 200µL of blocking buffer (1% BSA in PBS) was then added to each well and the plate was maintained at room temperature for 3h. The plate was washed again and 100µL of the media samples were added to each well and kept overnight at 4°C. The plate was then washed 3 times and 100µL of a solution of biotin human anti-mouse TNF (0.5µg/mL in assay diluent of 10%FBS in PBS) were added to each well and maintained at room temperature for 2h. The solution was discarded and the plate washed 3 more times, followed by the addition of a solution of Streptavidin HRP in assay diluent and kept 2h at room temperature. Finally the plate was washed 3 times and 100µL of a solution of TMB substrate (prepared according to the protocol of the manufacturer, BD OptEIA) was added, followed by the addition of 50µL of 1M sulfuric acid when the blue color developed. The adsorption at 450nm was recorded and compared to standards added and treated as described in the same plate. When required, samples were diluted in RPMI 1640 media.

Cellular uptake: After the cells were incubated with the gold nanoparticles and the supernatant media was removed, the remaining cells were carefully washed 3 times with PBS to remove NPs that were not uptaken. 250µl of lysis buffer was then added to each well and the plate was maintained at -20ºC for further treatment. The quantitative cellular uptake of gold nanoparticle was determined by ICP-MS. Briefly, the cells in one well were totally transferred to

metal ion-free tube, and gold was dissolved by freshly prepared Aqua Regia solution (HCl: HNO3= 1:3) for 15 min. Then, ultrapure water was added until 10mL, and the content of gold in the samples was analyzed by ICP-MS.

Reactive Oxygen species generation: ROS were determined by the use of 2',7'-dichlorodihydrofluorescein diacetate. Briefly, J774.2 cells were plated into a 96-well plate (105 cells/well) using similar conditions and time points as before. After the incubation period, cells were wash with PBS 3 times and were subsequently treated with the fluorescein dye (150 µL/well, 10µM). After incubating for 30 min, the cells were washed with PBS (3 times) and 150 µL of lysis buffer was added to each well. The solution was then transferred to a 96 black well plate and the fluorescence intensity, resulting from the oxidation of dye, was recorded (excitation/emission: 488 nm/520 nm).

Cell metabolism test (MTS): Cell Titer 96R Aqueous One Solution Cell proliferation Assay kit (Promega, USA) was used according to the manufacturer protocol. Briefly, J774.2 cells were plated in a 96 well plate using the same conditions as ROS. After washing the cells 3 times with PBS, 100uL of cell culture media with no serum and 20uL of the MTS solution were added to each well. The samples were then incubated for 1h at 37°C in a humidified atmosphere containing 5% of CO2. After the incubation time, the absorbance of the samples was recorded (490 nm).

Animal model: C57BL/6 mice were purchased from The Jackson Laboratory (Bar Harbor, ME) and were allowed to rest at least one week in the animal facilities before any procedure was performed. All the animal procedures were performed according to protocol IACUC 2014-0060 at the animal facilities of the University of Massachusetts Amherst.

LPS dose study: To assess sensitivity to lipopolysaccharide, solutions of different concentration of LPS in sterile PBS were injected via the peritoneum (IP), and 500µL of blood were extracted by heart puncture after the animals were sacrificed (CO2 chamber followed by cervical dislocation), 2h after the injection. Blood was allowed to clot for 1h at 37°C and then

overnight at 4°C. Blood was then centrifuged to separate the clots and the supernatant serum was carefully removed and stored at -20°C, until TNFα expression measurements were performed following the ELISA procedure described previously (vide supra). 3 mice per LPS concentration were used. Figure S5a depicts the TNFα expression for different concentrations of LPS. Upon these results, 200ng/mice was the selected dose for the studies.

In vivo nanoparticle and LPS treatment: Following the animal procedures described before, 100µL of NPs (5µM) were injected via the peritoneum, followed by an IP injection of 200µL of a solution of LPS (1ng/µL). As controls, untreated mice were sacrificed directly (negative), a group was injected only with LPS (positive), and 3 more groups were inject with NPs only (one group per nanoparticle, 3 mice per group) Figure S5b depicts the procedure for each group. After 2h, mice were sacrificed and blood was extracted and treated as described before. In addition, mice were dissected and the heart, lungs, pancreas, kidneys, spleen, intestine and brain were removed for biodistribution studies.

Organs treatment (biodistribution): the extracted organs were weighed and transferred to metal ion-free tubes, and the organs were dissolved by a solution of 1:3 H_2O_2 to HNO_3 overnight. The samples were then treated with Aqua Regia and diluted in ultrapure water as before, for further analysis of gold content by ICP-MS (Figure S6).

5.5. Supporting information

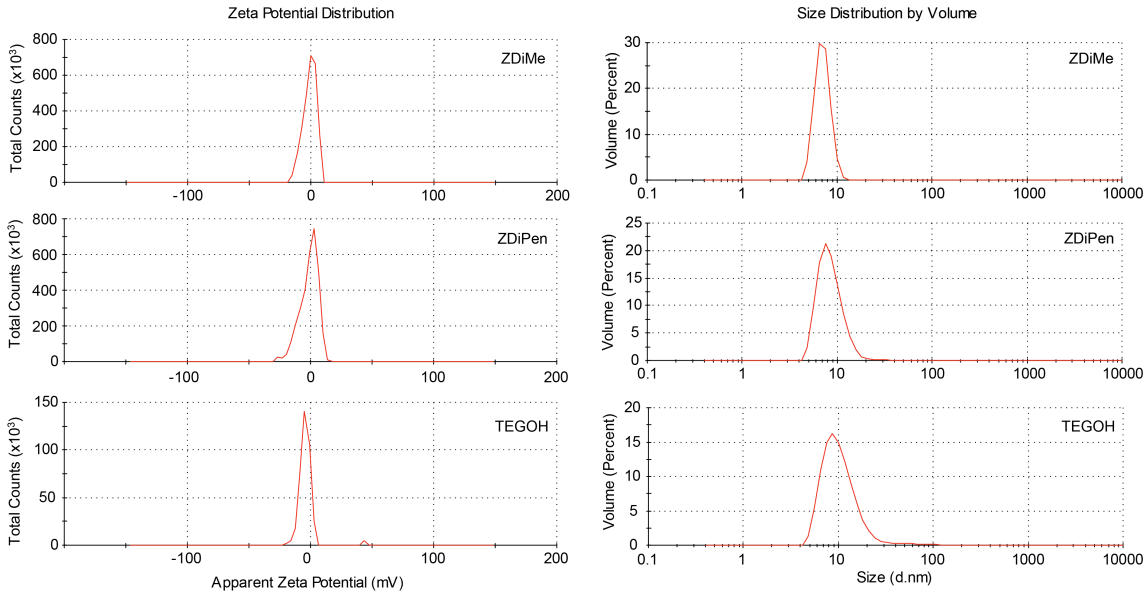

Figure 5.4. Hydrodynamic size and zeta potential of the NPs.

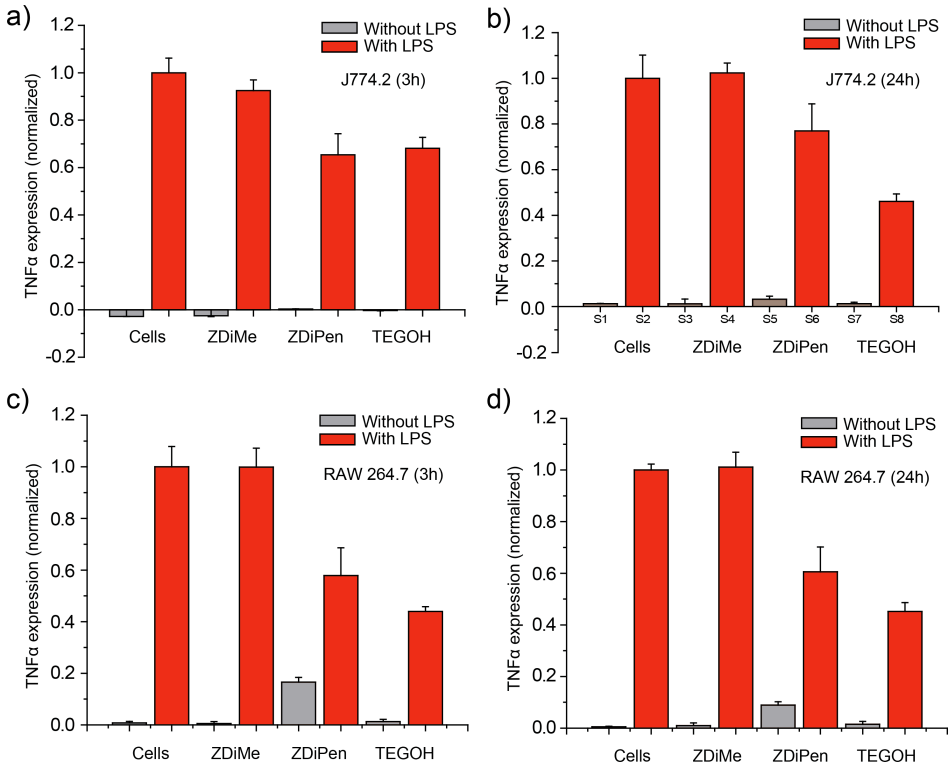

Figure 5.5. TNFα expression of J774.2 and RAW 264.7 cells at 3h and 24h.

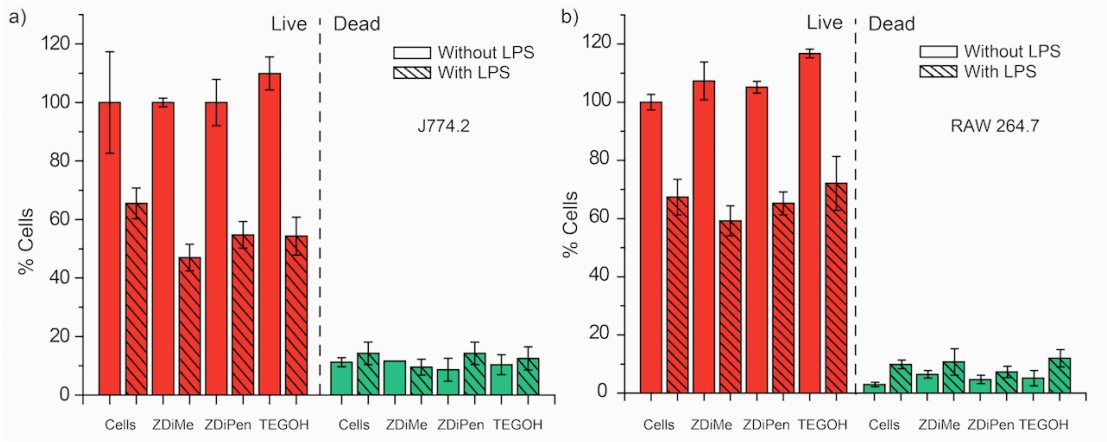

Figure 5.6. Cell viability of J774.2 and RAW 264.7 cells.

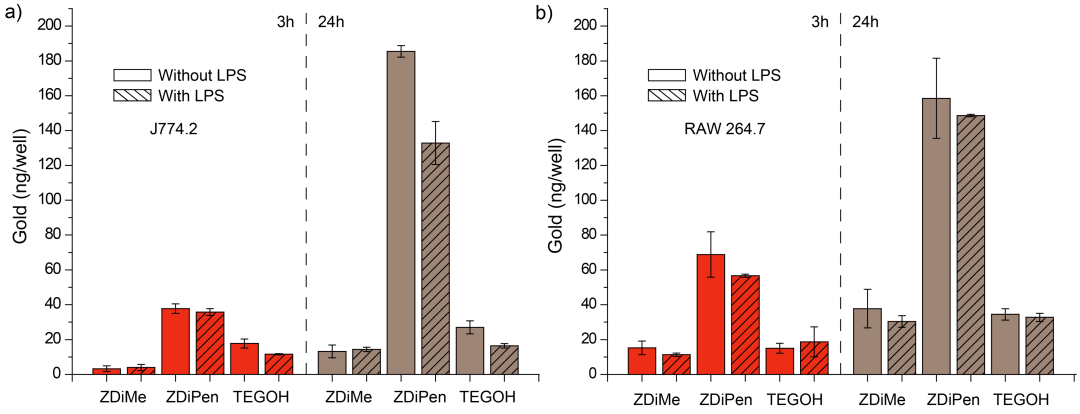

Figure 5.7. Cellular uptake of the NPs for both J774.2 and RAW 264.7 cells at 3h and 24h.

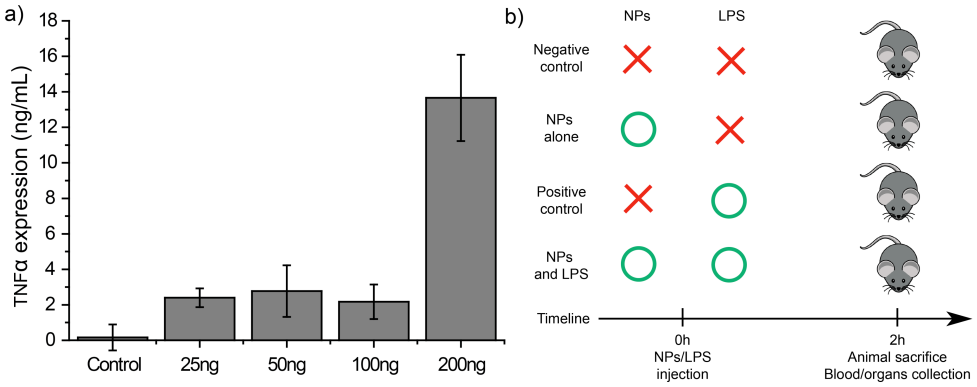

Figure 5.8. a) LPS dose study. b) Animal studies scheme

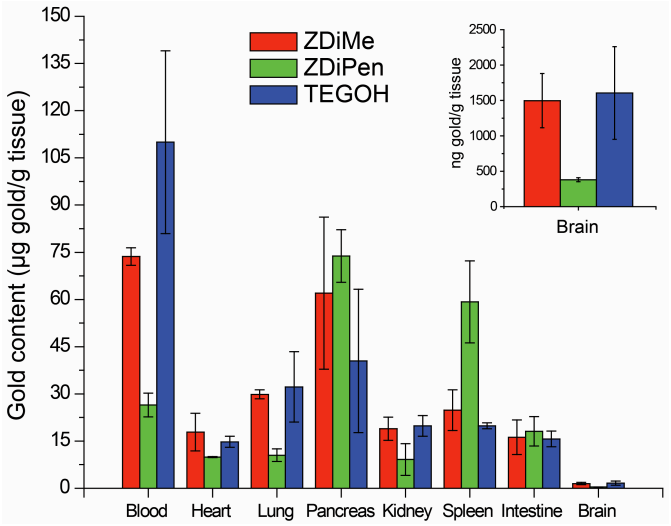

Figure 5.9. Biodistribution of the different nanoparticles.

5.6. References

1. a) Moon, J. J.; Huang, B.; Irvine, D. J. *Adv. Mater.* **2012**, *24*, 3724. b) Elsabahy, M.; Wooley, K. L. *Chem. Soc. Rev.* **2013**, *42*, 5552. c) Dobrovolskaia, M. A.; McNeil, S. E. *Nat. Nanotechnol.* **2007**, *2*, 469. d) Hubbell, J. A.; Thomas, S. N.; Swartz, M. A. *Nature* **2009**, *462*, 449.

2. Bastus, N. G.; Sanchez-Tillo, E.; Pujals, S.; Farrera, C.; Kogan, M. J.; Giralt, E.; Celada, A.; Lloberas, J.; Puntes, V. *Mol. Immunol.* **2009**, *46*, 743.

3. Serda, R. E. *Int. J. Nanomedicine* **2013**, *8*, 1683.

4. De Geest, B. G.; Willart, M. A.; Hammad, H.; Lambrecht, B. N.; Pollard, C.; Bogaert, P.; De Filette, M.; Saelens, X.; Vervaet, C.; Remon, J. P.; Grooten, J.; De Koker, S. *ACS Nano* **2012**, *6*, 2136.

5. Lewis, J. S.; Roy, K.; Keselowsky, B. G. *MRS Bulletin* **2014**, *39*, 25.

6. Juskewitch, J. E.; Platt, J. L.; Knudsen, B. E.; Knutson, K. L.; Brunn, G. J.; Grande, J. P. *Sci. Rep.* **2013**, *2*, 918.

7. Lorenz, E.; Patel, D. D.; Hartung, T.; Schwartz, D. A. *Infect. Immun.* **2002**, *70*, 4892.

8. Cao, Z.; Jiang, S. *Nano Today* **2012**, *7*, 404.

9. Shima, F.; Akagi, T.; Uto, T.; Akashi, M. *Biomaterials* **2013**, *34*, 9709.

10. Jones, K. J.; Perris, A. D.; Vernallis, A. B.; Worthington, T.; Lambert, P. A.; Elliott, T. S. J.; *J. Med. Microbiol.* **2005**, *54*, 315.

APPENDICES

The following sections illustrate additional work that I also performed during my PhD studies, related to structure-property relationship studies of the interaction of NPs and different biomacromolecules, such as proteins (Appendix 1) and glycosaminoglycans (Appendix 2). Although this work is not related to immunomodulation, it is included in this thesis as a way to illustrate the importance of engineering the NP surface chemistry to achieve desired properties (in this case sensing capabilities). In addition, this work also illustrates the central role of surface hydrophobicity in the interaction of NPs and biomacromolecules, demonstrating the importance of controlling this property at the nano-bio interface.

APPENDIX A

GOLD NANOPARTICLE-POLYMER/BIOPOLYMER COMPLEXES FOR PROTEIN SENSING: THE IMPORTANCE OF SURFACE HYDROPHOBICITY

A.1. Introduction

Nature has generated diverse mechanisms for sensing molecular systems and triggering appropriate responses. The majority of biological recognition processes occur via specific interactions such as antibody–antigen interactions.[1] However, sensory processes such as taste and smell use an array of cross-reactive receptors that use differential binding for analyte identification. These receptors bind to their analytes through interactions that are selective rather than specific.[2] Such array-based sensing platforms can be trained to create a response fingerprint for each analyte, enabling their detection and differentiation.[3] The potential of this method has been demonstrated in numerous biomacromolecule sensing including peptides,[4] proteins,[5] amino acids,[6,7] sugars,[8] bacteria,[9] and even mammalian cells.[10,11] Likewise, a number of synthetic biomolecular platforms including porphyrin,[12] oligopeptide functionalized resins,[13] polymers,[14] have been employed to create these sensor arrays.

Nanoparticles provide a versatile scaffold for array-based sensing of biomolecules.[15] Gold NPs (AuNPs) offer many advantages in terms of recognition and transduction of binding events.[16] The surface of AuNPs can be decorated easily with various ligands of interest. Hence, physicochemical properties including charge, hydrogen-bonding ability, hydrophobicity or hydrophilicity, and surface topology, can easily be modulated on the AuNP surface.[17] AuNPs can be readily fabricated in sizes comparable with biomacromolecules, facilitating high affinity interactions.[18] In addition, the extraordinary stability and high resistance to exchange by amines (e.g. lysine residues)[19] provide stable platforms for recognition. Finally, the strong quenching

ability of AuNPs[20] provides facile transduction of the recognition process, making AuNPs attractive candidates for application in differential sensing.[21]

In our research, we have used arrays of AuNPs featuring different ligand structures at their surface to detect and differentiate a diversity of analytes. As shown in Figure A.1a, the sensor unit is formed by adding a fluorescent probe to a supramolecularly complimentary NP, turning off the fluorescence. When analytes are incubated with the NP-probe complexes, there is competitive binding between analyte and NP probe complexes. Selective displacement of the probe from the particle by the analytes restores fluorescence, transducing the binding event in a ‘‘turn on’’ fashion. The NPs are chosen to possess different affinities for dissimilar analytes depending on the NP structure and analyte surfaces. As a result, each analyte generates a unique signature that allows differentiation and recognition.

Our initial biosensing studies involved proteins identification employing AuNPs as the receptors and conjugated polymers as the transducer.[14] Our strategy relied on the displacement of the fluorescent probe from the supramolecular complexes between cationic AuNPs and anionic polymers, generating distinct fluorescence response patterns. This system used six NPs, and was able to properly identify seven different proteins in buffer solution. Later studies showed that analogous arrays could differentiate cell state on the basis of cell surface properties.[22] However, aggregation problems of the polymers restricted their applicability in complex matrices such as serum. To overcome this issue, we used Green Fluorescent Protein (GFP) as the fluorophore, replacing the polymer transducer with a biopolymer analog. Not only that, the biocompatibility of the probe allowed us to use the system without affecting the target protein conformations. These GFP-AuNP sensor arrays were capable of differentiating bio-relevant changes (500 nM changes in 1 mM overall protein content) in human serum protein.[23]

Our efforts have concurrently been directed towards enhancing the stability and biocompatibility of synthetic polymers. Recently, we synthesized a new polymer specifically designed to avoid aggregation by introducing oligo(ethylene glycol) chains designed to prevent

aggregation. This polymer was used with three nanoparticles to successfully differentiate twelve bacteria including three strains of the same species.[24]

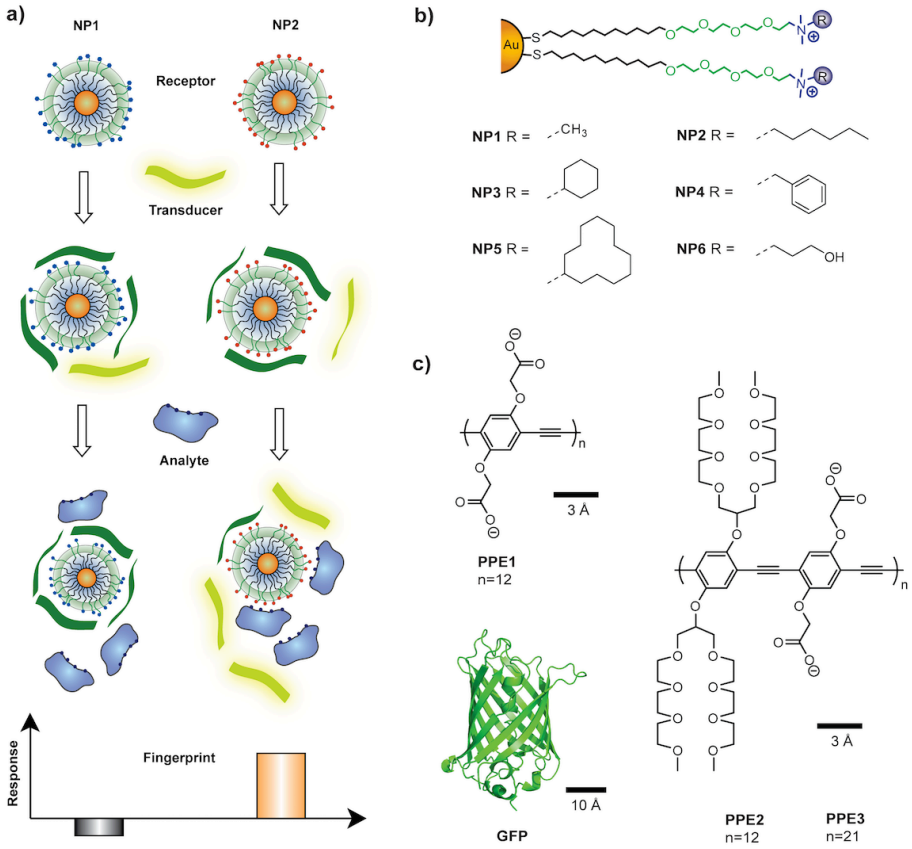

Figure A.1. a) Schematic illustration of NP/transducer sensor-array. Each nanoparticle and fluorescent probes are mixed followed by incubation with analytes. Depending on the nanoparticle/probe/analyte competitive binding, ‘‘lighting up’’ or further quenching of fluorescence can be observed. Such fluorescence response patterns are distinct and characteristics of each analyte, allowing differentiation. b) Structure of the nanoparticles and ligands used in the current study, featuring an aliphatic interior, a tetra(ethylene glycol) layer and the head group responsible for analyte recognition. c) Molecular structures and size of the different fluorescent probes including the conjugated polymers (PPE1, PPE2, PPE3) and GFP.

In this report, we analyze the structure–activity relationship of the particle–polymer/biopolymer sensing system, providing insight into how to enhance sensor efficiency. This study uses six AuNPs with variations in hydrophobicity, hydrogen bonding ability and

aromatic recognition unit (Figure A.1b). We analyzed the effect of structural variation and relative molar emissivity of the transducers using three fluorescent polymers (PPE1, PPE2, PPE3) and GFP as shown in Figure A.1c.

A.2. Results and discussion

Comparison of the fluorescent probes: Emissivity is a key determinate of fluorescence sensor design, dictating fluorophore concentrations required for sensing.[25] As shown in Figure A.2, the fluorescence intensity of PPE1, PPE2 and GFP are similar at 50 nM. However, PPE3 shows a drastic increase in emission. This difference in molar emissivity can be explained by polymer structure and length. The extended conjugation of the aromatic rings of PPE3 provides the possibility of multiple fluorescent units along the chain of the polymer.[26] Additionally, PPE3 carries more charges, potentially inhibiting self-quenching. For the below studies we employed concentrations of the probes that produced similar emission intensity (PPE1: 50nM, PPE2: 50nM, PPE3: 5nM, GFP: 150nM).

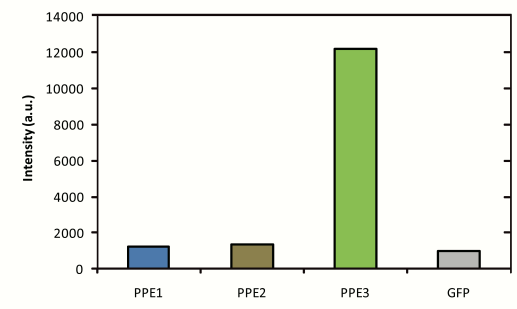

Figure A.2. Relative molar emissivity of different fluorescent probes used in the study with a concentration of 50 nM.

Next, we assessed the complexation between the fluorescent probes and the cationic NPs using fluorescence titrations. The fluorescence of GFP and the polymers were quenched significantly for all six AuNPs (Figure A.3 and Figures A.6-A.9). The complex stability constants (Ks) and association stoichiometries (n) obtained through nonlinear least-squares curve-fitting analysis are tabulated in Figure A.3. The variation in complex stabilities and the binding stoichiometry demonstrate the significant effect of AuNP head groups in the NP-probe affinity. Differences in the molecular structure and properties of the transducers also play a key role in the complex supramolecular interactions, as reflected in the parameters. From the binding curves it is apparent that PPE3 binds to the NPs with higher affinity and lower stoichiometries than the other polymers or GFP due to the increased contact area and size of PPE3. In addition to the lower amount of polymer required, the optimum NP concentration ranged from 1–7 nM for PPE3 and 5–25 nM for the other probes, demonstrating that PPE3 allows a more parsimonious use of materials.

Finally, we investigated the ability of the sensor arrays to differentiate analytes. Twelve proteins with diverse structural features including molecular weight and isoelectric point (pI) were used as the target analytes. In our protocol we used UV absorbance as a means of decoupling protein concentrations from sensor response. We used standard absorbance (A_{280} = 0.005) for the sensor studies, diluting stock solutions to obtain the desired levels. These protein solutions were added to the fluorescence-quenched supramolecular complexes using NP/probe ratios obtained from the titrations (Figure A.3). The changes in fluorescence (Figure A.10) upon addition of protein generate a pattern characteristic of the individual proteins. We used Linear Discriminant Analysis (LDA) to quantitatively differentiate the fluorescence response patterns. LDA is a statistical technique that maximizes the ratio of between-class variance to within-class variance, allowing response patterns to be differentiated. The 72 training cases (12 proteins x 6 replicates) were efficiently clustered into 12 separate groups with 95% confidence ellipses using

LDA. Distinction of the groups was reflected in the overall classification accuracy obtained from Jackknifed classification matrix.[27]

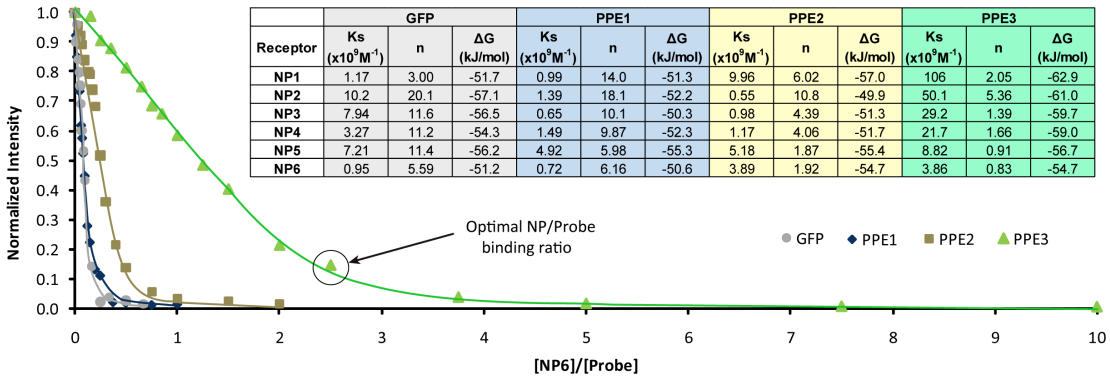

Receptor	GFP Ks ($x10^9 M^{-1}$)	GFP n	GFP ΔG (kJ/mol)	PPE1 Ks ($x10^9 M^{-1}$)	PPE1 n	PPE1 ΔG (kJ/mol)	PPE2 Ks ($x10^9 M^{-1}$)	PPE2 n	PPE2 ΔG (kJ/mol)	PPE3 Ks ($x10^9 M^{-1}$)	PPE3 n	PPE3 ΔG (kJ/mol)
NP1	1.17	3.00	-51.7	0.99	14.0	-51.3	9.96	6.02	-57.0	106	2.05	-62.9
NP2	10.2	20.1	-57.1	1.39	18.1	-52.2	0.55	10.8	-49.9	50.1	5.36	-61.0
NP3	7.94	11.6	-56.5	0.65	10.1	-50.3	0.98	4.39	-51.3	29.2	1.39	-59.7
NP4	3.27	11.2	-54.3	1.49	9.87	-52.3	1.17	4.06	-51.7	21.7	1.66	-59.0
NP5	7.21	11.4	-56.2	4.92	5.98	-55.3	5.18	1.87	-55.4	8.82	0.91	-56.7
NP6	0.95	5.59	-51.2	0.72	6.16	-50.6	3.89	1.92	-54.7	3.86	0.83	-54.7

Figure A.3. Titration curves of the different probes with NP6. The circle indicates the point of optimal NP/probe binding ratio chosen. The table shows the thermodynamic parameters calculated for NPs against the fluorescent probes.

Distinct canonical score plots were obtained from LDA analysis for each transducer and the most significant scores are plotted in Figure A.4. It is observed that the PPE1 and PPE2 show considerable differences in classification abilities in spite of their similar relative emissivities and size. In fact, PPE2 possesses the lowest identification efficiency among all the transducers. However, PPE3 features greater capability of differentiation, possibly due to higher binding affinity and molar emissivity. Although the classification accuracy of PPE3 is similar to PPE1, it possesses added advantages of biocompatibility and lack of aggregation in complex media. It is worth noting that PPE3 needs 10-fold less polymer concentration that the other two polymers, indicating much higher sensitivity.

In the present study, we achieved high efficiency of identification of the analyte proteins using GFP as well as with PPE1 and PPE3. Compared to the other transducers, GFP shows higher dispersion of clustering on LDA analysis suggesting greater possibility of differentiating multiple

analytes at the same time. However, GFP-based sensing required substantially more fluorophore and nanoparticle compared to PPE3.

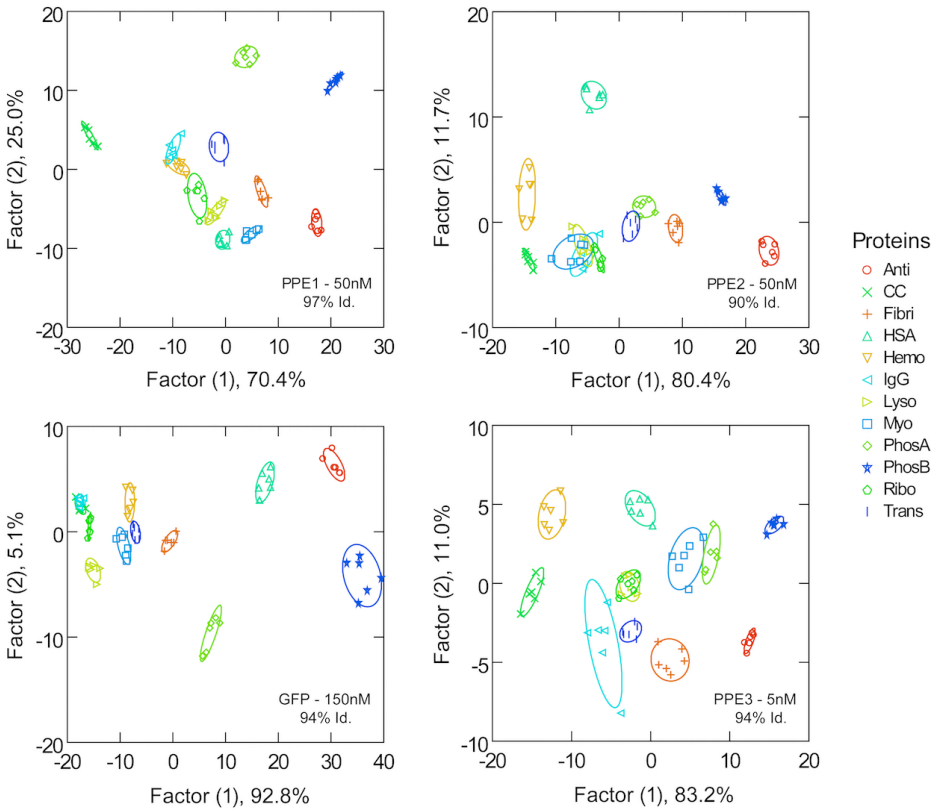

Figure A.4. Canonical score plots for the fluorescence patterns of the different probes as obtained from LDA use of six NP-probe complexes against twelve analyte proteins (analytes added in a concentration 10–500 nM, with absorbance of 0.005 at 280 nm). The 95% confidence ellipses for the each analyte, the concentration of the probe used and the percentage of identification accuracy are shown on the plots. Acronyms used: Anti = α-Antitrypsin, CC = Cytochrome C, Fibri = Fibrinogen, HSA = Human Serum Albumin, Hemo = Hemoglobin, IgG = Immunoglobulin G, Lyso = Lysozyme, Myo = Myoglobin, PhosA = Phosphatase acidic, PhosB = Phosphatase basic, Ribo = Ribonuclease A, Trans = Transferrin.

Nanoparticle surface functionality: structure–activity relationships in sensing: One of the goals for array-based sensor design is maximal differentiation with the minimal number of sensing elements. The head groups of the ligands used in this study were designed to exhibit different physicochemical properties such as hydrophobicity, hydrogen-bonding sites, and π-

stacking systems. The purpose of this structural diversity was to obtain clues about which interactions best generated selectivity in analyte binding. Insight into the nature of the multivalent interactions involved in the NP–protein interactions would help us in designing appropriate NP surfaces with enhanced selectivity.[28, 29]

We used a Jackknifed classification matrix to determine which particles were most effective at analyte differentiation. When using only two NPs as predictors the classification is poor, with accuracy below 80%. With a number of combinations, however, three NPs could be used to differentiate all 12 proteins. The accuracy, however, varies depending on the nature of NPs, as evident from Figure A.5. All possible combinations of three NPs presented in Figure A.5 reveal that the hydrophobic NPs contribute more towards the discrimination of proteins irrespective of the transducer. In general, the combinations containing NP4 and NP6 show poorer differentiation grouping (e.g. NP2–NP4–NP6; NP1–NP4–NP6 combinations). Interestingly, NP5 appears to be highly effective at differentiating analytes, as all highly efficient sets contained this NP.

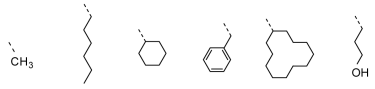

NP1	NP2	NP3	NP4	NP5	NP6	PPE1	PPE2	PPE3	GFP
■	■	■				83	86	74	92
	■	■	■			79	85	78	92
		■	■	■		97	89	92	90
			■	■	■	97	85	89	90
		■		■	■	97	85	85	93
	■			■	■	96	92	85	90
■				■	■	92	88	94	86
■			■		■	85	74	82	85
■		■			■	81	76	69	88
■	■				■	86	78	88	83
	■	■			■	89	86	79	89
		■	■		■	78	76	72	90
	■		■		■	81	79	81	89
■			■	■		99	88	92	94
	■		■	■		97	90	92	94
	■	■		■		97	90	82	96
■		■		■		97	82	93	93
■	■			■		97	89	92	94
■		■	■			74	76	72	93
■	■		■			86	85	81	88

Figure A.5. Jackknifed classification matrix for identification using selected combinations with three nanoparticles as predictors in LDA analysis. Combinations with hydrophobic changes on nanoparticle functionality show better identification accuracy.

A.3. Conclusions

In this study we demonstrate the versatility of AuNPs in array-based sensing, identifying twelve different proteins using a variety of polymer and biopolymer transducers. Of the transducers, PPE3 shows greatest sensitivity due to its higher intrinsic molar emissivity. The other polymers were equally effective in differentiation, and possess their respective advantages for sensing applications. From our studies, we also determined some general guidelines for nanoparticle design. First, we found that hydrophobic particles were better able to discriminate among analyte proteins. Second, structure is important, as the cyclododecyl-terminated NP5 was a very effective partner in protein differentiation. Taken together, these studies demonstrate that through tuning of receptor and transducer structure highly effective array based sensors for proteins can be produced.

A.4. Experimental section

Materials: The nanoparticles (Figure A.2) were synthesized as described in section 2.4. Three different fluorescent polymers were synthesized and characterized according to literature procedures.[30] GFP was expressed according to reported methodology,[31] starting from cultures of a glycerol stock of GFP in BL21(DE3) that was grown overnight in culture media at 37°C. These initial cultures were then added to a Fernbach flask that contained culture media and the mixture was shaken until the optical density at 600 nm was 0.6. GFP formation was then induced by adding isopropyl-b-D-thiogalactopyranoside, shaking at 28°C for three hours. The solution was centrifuged and the cells were resuspended, lysed and then the protein was purified using HisPur Cobalt columns and dialysis.

Sensor optimization: Nanoparticle titrations were performed to find the optimal nanoparticle/probe ratio for sensing purposes, measuring the change in fluorescence intensities after the addition of cationic nanoparticles (0–200 nM in 5mM sodium phosphate buffer pH 7.4). The measurement wavelengths were 465nm for the polymers (Ex. 430nm) and 510nm for GFP (Ex. 495nm). All the values were normalized using a neutral non-interacting nanoparticle as control (gold core functionalized with a ligand lacking the amine head group) to subtract the absorption effect of gold NP due to its optical properties. The curve fitting was done with Origin 8.0 using a previous reported algorithm[32] to find the physicochemical parameters of the binding process, namely binding constant (Ks) and binding sites per nanoparticle (n). The ultimate nanoparticle/probe ratio was chosen to balance sensitivity and dynamic range.

Sensing studies: Fluorescence of the samples was measured in a M5 SpectraMax Molecular Devices plate reader instrument using 96 well black plates. A stock solution of the each fluorescent probe was prepared in 5mM sodium phosphate buffer pH 7.4 with a concentration that gave 1000 a.u. of emission. This solution was then divided and nanoparticles added. The conjugates were added to microwell plates. After 15 min of incubation initial fluorescence was recorded, and 10 mL of a solution of the analyte proteins (with absorbance of 0.005 at 280 nm, Table 1) was added. After 15 min additional incubation the final fluorescence intensity was determined. For data analysis, the change in fluorescence was plotted against each descriptor to get the fingerprint patterns for all the analytes. The obtained data were analyzed by Linear Discriminant Analysis (LDA) applying Mahalonobis clustering analysis, using the software Systat 11.[33] Canonical score plots were obtained in order to parameterize each case, using the nanoparticle as predictors. A total of 12 different proteins were analyzed using 6 replicates in each case.

A.5. Supporting information

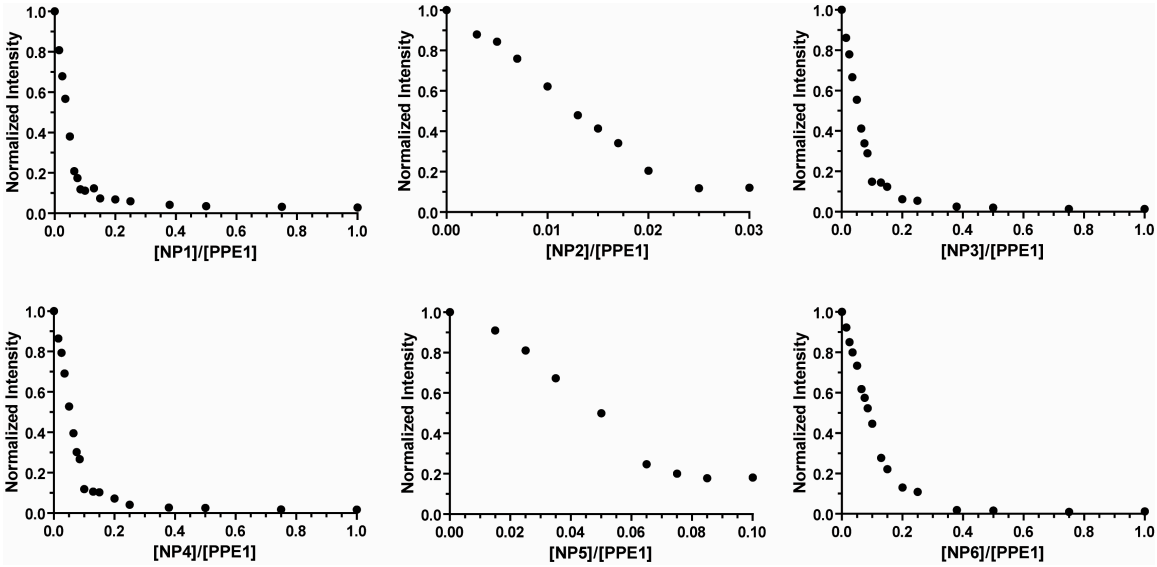

Figure A.6. Titration curves for PPE1 against six nanoparticles.

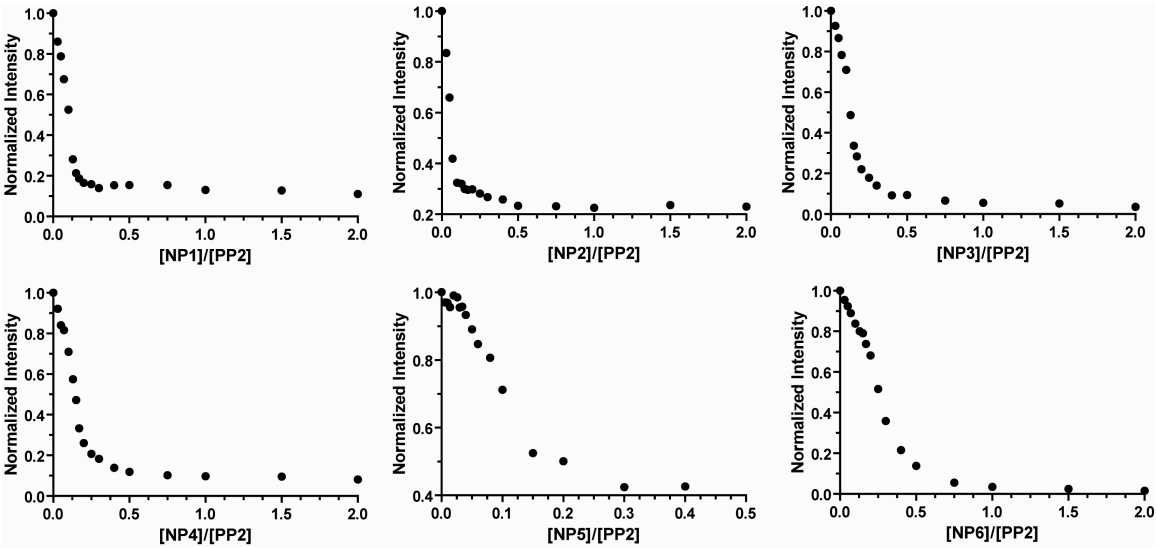

Figure A.7. Titration curves for PPE2 against six nanoparticles.

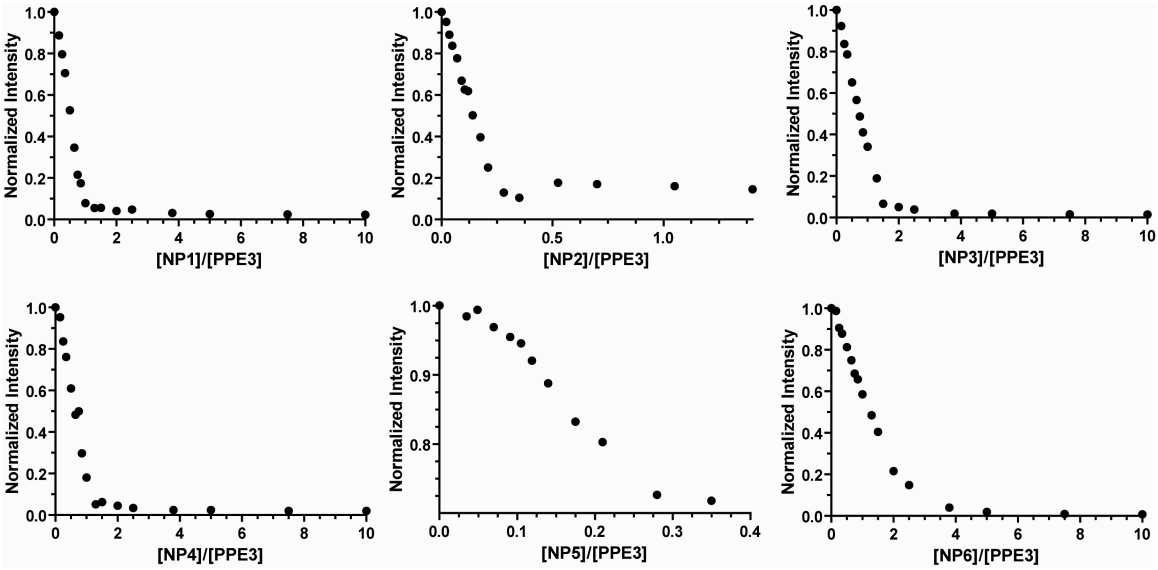

Figure A.8. Titration curves for PPE3 against six nanoparticles.

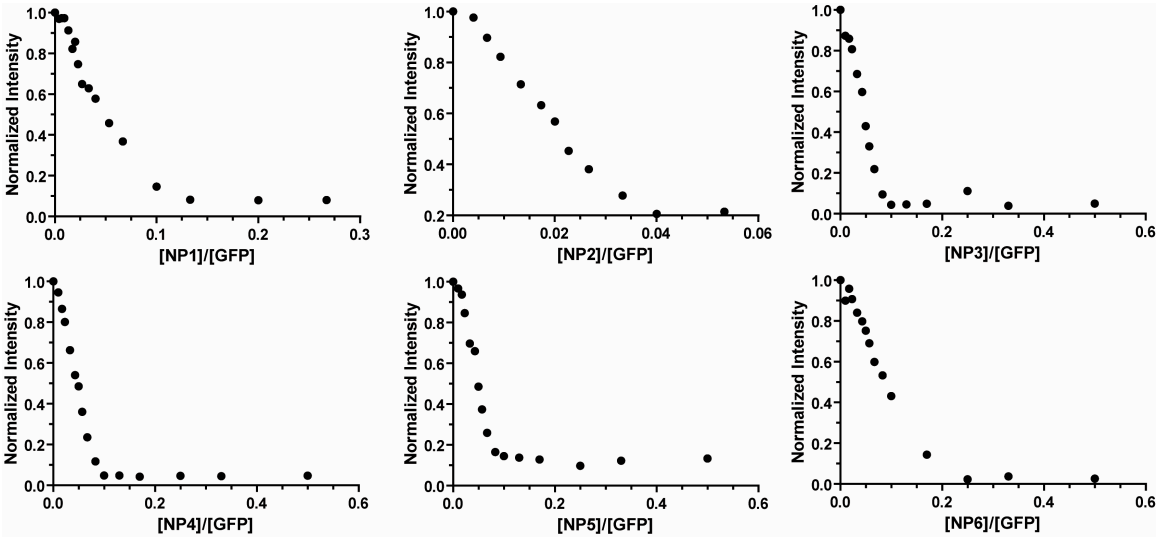

Figure A.9. Titration curves for GFP against six nanoparticles.

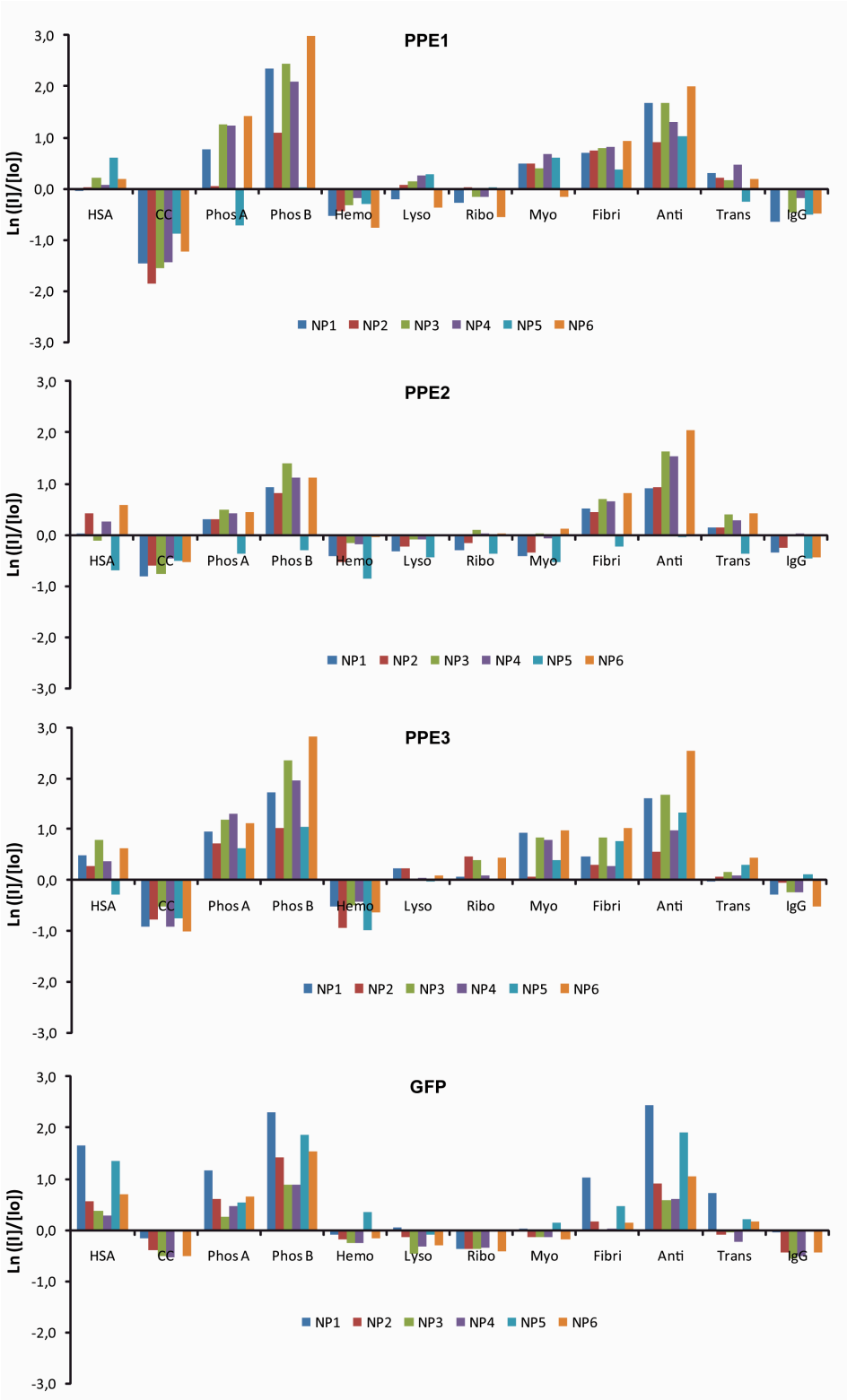

Figure A.10. Change in response expressed as the ratio of fluorescence after and before the addition of the analyte.

A.6. References

1. Raftos, D.; Raison, R. L. *Immunol. Cell Biol.* **2008**, *86*, 479.

2. Albert, K. J.; Lewis, N. S.; Schauer, C. L.; Sotzing, G. A.; Stitzel, S. E.; Vaid, T. P.; Walt, D. R. *Chem. Rev.* **2000**, *100,* 2595.

3. Umali, A. P.; Anslyn, E. V. *Curr. Opin. Chem. Biol*. **2010**, *14*, 685.

4. Zhang, T.; Edwards, N. Y.; Bonizzoni, M.; Anslyn, E. V. *J. Am. Chem. Soc.* **2009**, *131*, 11976.

5. Miranda, O. R.; You, C.-C.; Phillips, R.; Kim, I.-K.; Ghosh, P. S.; Bunz, U. H. F.; Rotello, V. M. *J. Am. Chem. Soc.* **2007**, *129*, 9856.

6. Folmer-Andersen, J. F.; Kitamura, M.; Anslyn, E. V. *J. Am. Chem. Soc.* **2006**, *128*, 5652.

7. Buryak, A.; Severin, K. *J. Am. Chem. Soc*. **2005**, *127*, 3700.

8. Lee, J. W.; Lee, J. S.; Chang, Y. T.; *Angew. Chem. Int. Ed.* **2006**, *45*, 6485.

9. Duarte, A.; Chworos, A.; Flagan, S. F.; Hanrahan, G.; Bazan, G. C. *J. Am. Chem. Soc.* **2010**, *132*, 12562.

10. Bajaj, A.; Rana, S.; Miranda, O. R.; Yawe, J. C.; Jerry, D. J.; Bunz, U. H. F.; Rotello, V. M. *Chem. Sci.* **2010**, *1*, 134.

11. El-Boubbou, K.; Zhu, D. C.; Vasileiou, C.; Borhan, B.; Prosperi, D.; Li, W.; Huang, X. F. *J. Am. Chem. Soc*. **2010**, *132*, 4490.

12. Baldini, L.; Wilson, A. J.; Hong, J.; Hamilton, A. D. *J. Am. Chem. Soc.* **2004**, *126*, 5656.

13. Wright, A. T.; Anslyn, E. V. *Chem. Soc. Rev.* **2006**, *35*, 14.

14. You, C.-C.; Miranda, O. R.; Gider, B.; Ghosh, P. S.; Kim, I.-B.; Erdogan, B.; Krovi,S. A.; Bunz, U. H. F.; Rotello, V. M. *Nat. Nanotechnol.* **2007**, *2*, 318.

15. Di Marco, M.; Shamsuddin, S.; Razak, K. A.; Aziz, A. A.; Devaux, C.; Borghi, E.; Levy, L.; Sadun, C. *Int. J. Nanomed*. **2010**, *5*, 37.

16. Rana, S.; Yeh, Y.; Rotello, V. M. *Curr. Opin. Chem. Biol.* **2010**, *14*, 828.

17. Moyano, D. F.; Rotello, V. M. *Langmuir* **2011**, *27*, 10376.

18. Lynch, I.; Dawson, K. A. *Nano Today* **2008**, *3*, 40.

19. Nath, S.; Ghosh, S. K.; Kundu, S.; Praharaj, S.; Panigrahi, S.; Pal, T. *J. Nanopart. Res.* **2006**, *8*, 111.

20. Fan, C.; Wang, S.; Bazan, G. C.; Plaxco, K. W.; Heeger, A. *J. Proc. Natl. Acad. Sci. U. S. A.* **2003**, *100*, 6297.

21. Miranda, O. R.; Creran, B.; Rotello, V. M. *Curr. Opin. Chem. Biol.* **2010**, *14*, 728.

22. Bajaj, A.; Miranda, O. R.; Kim, I.-B.; Phillips, R. L.; Jerry, D. J.; Bunz, U. H. F.; Rotello, V. M. *Proc. Natl. Acad. Sci. U. S. A.* **2009**, *106*, 10912.

23. De, M.; Rana, S.; Akpinar, H.; Miranda, O. R.; Arvizo, R. R.; Bunz, U. H. F.; Rotello, V. M. *Nat. Chem.* **2009**, *1*, 461.

24. Phillips, R. L.; Miranda, O. R.; You, C.-C.; Rotello, V. M.; Bunz, U. H. F. *Angew. Chem. Int. Ed.* **2008**, *47*, 2590.

25. Fu, J.; Li, G.; Qiin, Y.; Freeman, W. *J. Sens. Actuators B,* **2007**, *125*, 489.

26. Filatov, I.; Larsson, S. *Chem. Phys*. **2002**, *3*, 575.

27. Jurs, P. C.; Bakken G. A.; McClelland, H. E. *Chem. Rev.* **2000**, *100*, 2649.

28. Roan, J. R.; *Phys. Rev. Lett.* **2006**, *96*, 248301.

29. Wang, J.; Tian, S.; Petros, R. A.; Napier, M. E.; Desimone, J. M. *J. Am. Chem. Soc.* **2010**, *132*, 11206.

30. Kim, I.-B.; Phillips, R.; Bunz, U. H. F. *Macromolecules* **2007**, *40*, 5290.

31. De, M.; Rana S.; Rotello, V. M.; *Macromol. Biosci.* **2009**, *9*, 174.

32. Phillips, R. L.; Miranda, O. R.; Mortenson, D. E.; Subramani, C.; Rotello V. M.; Bunz, U. H. F. *Soft Matter* **2009**, *5*, 607.

33. SYSTAT11.0, SystatSoftware, Richmond, CA 94804, USA, **2004**.

APPENDIX B

RECOGNITION OF GLYCOSAMINOGLYCAN CHEMICAL PATTERNS USING AN UNBIASED SENSOR ARRAY

B.1. Introduction

Carbohydrates are a large, diverse, and functionally important class of polymeric biomacromolecules. They are involved in different biological functions including cell–cell recognition,[1] cell signaling[2] and microbial infection.[3] Glycosaminoglycans (GAGs) are a subfamily of polymeric carbohydrates composed solely of repeating disaccharide units. Due to their unbranched nature, chemical properties such as charge, size, acetylation, and sulfonation patterns dictate the functionality of GAGs. For example, GAGs with high charge density produce a local increase of viscosity, and can be naturally found in connective tissue.[4] Moreover, small changes in the GAG structure can dramatically affect their biological activity. Such is the case of sulfonation patterns that are used as specific molecular recognition elements of growth factors.[5]

Despite the significant impact of these subtle changes in the functionality of GAGs, the identification of these molecules is difficult to achieve. A classical example of this limitation is heparin, whose major contaminants are the structurally related chondroitin sulfate and hyaluronic acid.[6] Current analytical methods such as HPLC and mass spectrometry can quantify and identify GAGs,[7,8] but possess lengthy analysis times and complex protocols. Lectin arrays provide useful tools to identify glycan families through the interaction with specific sugar moieties.[9,10] However, structurally similar glycans can bind to the same arrays, complicating the analysis. Likewise, colorimetric[11,12] and fluorescent sensors[13,14] to identify heparin and other GAGs have been recently reported. However, no robust methodology has been developed as the analysis is limited

to either specific classes or very distant families. In addition, no correlation with the chemical parameters of the GAGs structure has been presented.

Unbiased array sensors provide an important tool for the recognition and identification of chemical signatures. In this approach, the interaction of a given compound with the sensor is selective rather than specific, mimicking the olfactory process.[15] Due to the nature of this recognition, there is no requirement of prior knowledge of the analytes being studied.[16] This selective recognition has been employed in various sensing applications, such as the detection of flavonoids,[17] carbohydrates,[18] and sugars.[19] In recent years we have developed a nanoparticle-based sensing platform following the unbiased principle.[20] The applicability of this methodology has been validated in complex matrices such as serum,[21] and its robustness has been observed using highly complex analytes such as cells and tissues.[22] Here we report the use of a systematic set of 11 glycosaminoglycans with variations in size, charge, chirality, sulfonation and acetylation profiles to explore both the differentiation of GAGs, and the structural correlation capabilities of the nanoparticle-based sensing platform.

B.2. Results and discussion

Platform design: The array system is composed of eight positively charged gold nanoparticles (AuNPs, Figure B.1a) acting as receptors, and a negatively charged fluorescent polymer (poly(para-phenyleneethynylene swallowtail), PPE, Figure B.1b)[23,24] as the transducer.[25] In this array, the fluorescence of the polymer is quenched upon formation of an electrostatic complex with the cationic AuNP. When the analyte is introduced to the AuNP–PPE complex, a competitive binding towards the AuNP occurs. Due to this competition, the polymer is displaced from the AuNP surface with concomitant recovery of the fluorescent signal (Figure B.1c). The

magnitude of the fluorescent signal depends on the nanoparticle–analyte affinity that is based on the nanoparticle surface chemistry and the structural features of the GAG.

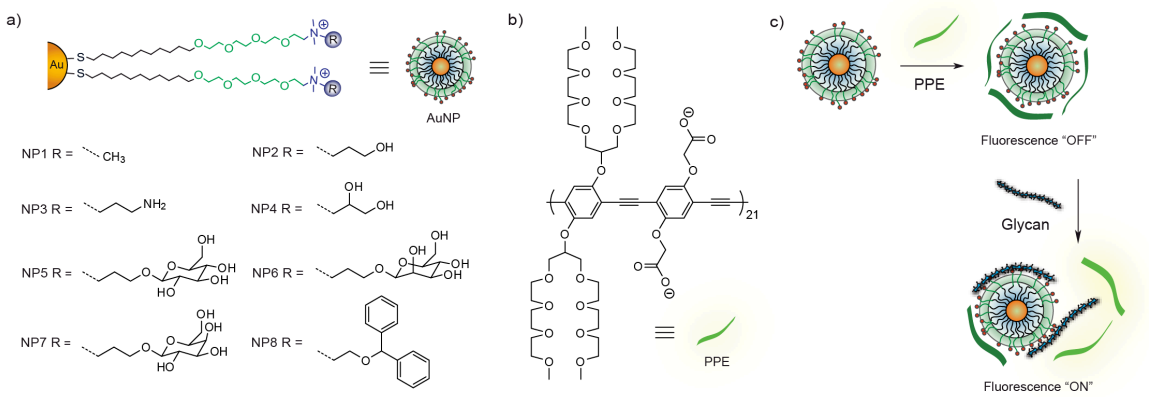

Figure B.1. Chemical structure of the (a) gold nanoparticles (receptors) and (b) fluorescent polymer (transducer) used in the sensor design. (c) Schematic illustration of the AuNP–PPE sensor array. Each nanoparticle is incubated with the polymer, quenching its fluorescence. After the analyte is added, PPE is displaced from the AuNP surface with concomitant recovery of the fluorescence that depends on nanoparticle–analyte affinity.

One of the principal limitations of array-based sensors is the lack of information regarding the analyte–receptor(s) interactions that drive the differentiation. This drawback can be overcome using a systematic set of analytes, while taking advantage of the structural uniformity of specific chemical functionalities on the receptors.[26] As a starting point to screen functionalities that are selective for GAGs, AuNPs featuring hydrogen bond elements (single and multiple donors and acceptors, NP2–NP4) were chosen, as the most prominent differences between the GAGs involve these types of functionalities (Figure B.1a).[4] Similarly, a nanoparticle with a p-system was included (NP8), given that amino–aromatic interactions are commonly involved in biomolecular recognition.[27] Finally a series of glycoside nanoparticles was synthetized (NP5–NP7), as glycan–glycoside interactions are believed to be involved in the specific recognition of GAGs.[28] A large fluorescent polymer PPE (n = 21) was chosen to obtain smaller AuNP–PPE ratios, where subtle

variations in the chemical residues at the AuNP surface account for significant changes in the properties of the system.[29]

Figure B.2 shows the set of GAGs used in this work, featuring systematic changes of their structures. Heparin and its related compounds (G1–G4) were selected as the model to analyze changes in the acetylation and sulfonation profiles while maintaining the same backbone. Likewise, chondroitin sulfate B (G7) and chondroitin sulfate A (G8) were chosen to investigate if a small chiral change could be identified by the sensor platform. Finally, chitosan (G5), hyaluronic acid (G6), and various dextran sulfates of different molecular weights (G9A–C) were selected to observe the effect of charge and size, and to further test the structural parameters involved in the differentiation process. Glycosaminoglycans G2–G4 were purchased from VLabs Inc., and G1, G5–G9C from Sigma-Aldrich, and used without further purification. Heparin was chosen to estimate the limit of detection (Figure B.12), and based on this analysis all the GAGs were detected at a concentration of 140 ng mL^{-1}

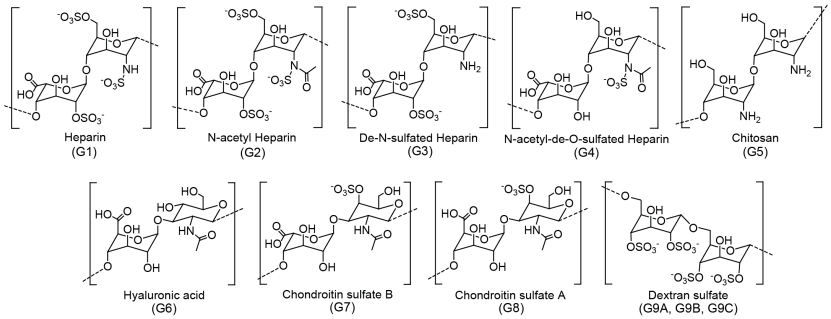

Figure B.2. Chemical structures of the GAGs, featuring differences in acetylation and sulfonation profiles (G1, G2, G3 and G4), charge (G5, G6 and G9), chirality (G7 and G8) and size (G9A, G9B and G9C).

Identification results: We obtained characteristic fluorescence response patterns for all the GAGs in this study (Figure B.11). These responses were then analyzed using three different statistical methods: hierarchical clustering analysis (HCA) to determine the relationships among the analytes, linear discriminant analysis (LDA) to facilitate identification and separation, and

principal component analysis (PCA) to evaluate receptor/analyte correlations. First, the differentiation capability of the array was tested using LDA. Figure B.13 depicts the LDA plot of all the GAGs, obtaining a variance of 86.8% in the first linear discriminant and 7.0% variance on the second one. LDA was able to classify all the GAGs with 92% accuracy. To validate the recognition efficiency of the 11 different GAGs, unknown samples were tested against the training set, achieving 88% of identification accuracy for a randomly selected group of samples (58 correct cases out of 66).

After validating the sensing platform, HCA was employed to understand the structural origins of the response pattern. HCA clusters the analytes according to the smallest distance between the different vectors (in this case GAGs), creating a dendrogram as shown in Figure B.3a. It is evident that GAGs with high negative charge cluster together (cyan colored trees), while the neutral and positively charged ones form a separate group (red colored trees). This trend reveals the importance of the analyte charge as the principal property that drives the discrimination. PCA analysis reveals a similar behavior, where analytes are separated according to charge (Figure B.3b). However, in this case we can observe that specific nanoparticles cluster together with certain GAGs. Important attention is drawn to NP6, NP7 and NP8 that cluster with the less negative GAGs (left side of the biplot) while NP1–NP5 are located with the rest of the GAGs.

Jackknifed classification analysis evaluates the contribution of each receptor in the overall discrimination, and was applied to understand better the significance of the nanoparticle clustering. The analysis reveals a behavior similar to the one observed in PCA for the nanoparticles. As shown in Figure B.3c, NP8 (featuring aromatic functionality) accounts for the highest classification among all the AuNPs (52% of differentiation). This selectivity can be rationalized by the possibility of π-dipole interactions that should affect the AuNP–GAG binding. The PCA biplot (Figure B.3b) shows that NP8 clusters with the less negative GAGs, an expected result as aromatic rings interact more with positive systems. On the other hand, it is important to

note that glycan–glycoside interactions do not seem to drive the separation, as NP6 and NP7 have the lowest values of identification. Such behavior is not surprising, as nanoparticles surrounded by glycoside moieties are known to avoid interactions with different biosystems.[30] Interestingly it is important to note that despite the fact that NP5 has the same chemical nature as NP6 and NP7, it is found in a different cluster. This nanoparticle also presents the highest degree of differentiation among the glycoside nanoparticles, indicating the involvement of spatial geometry in the discrimination process.

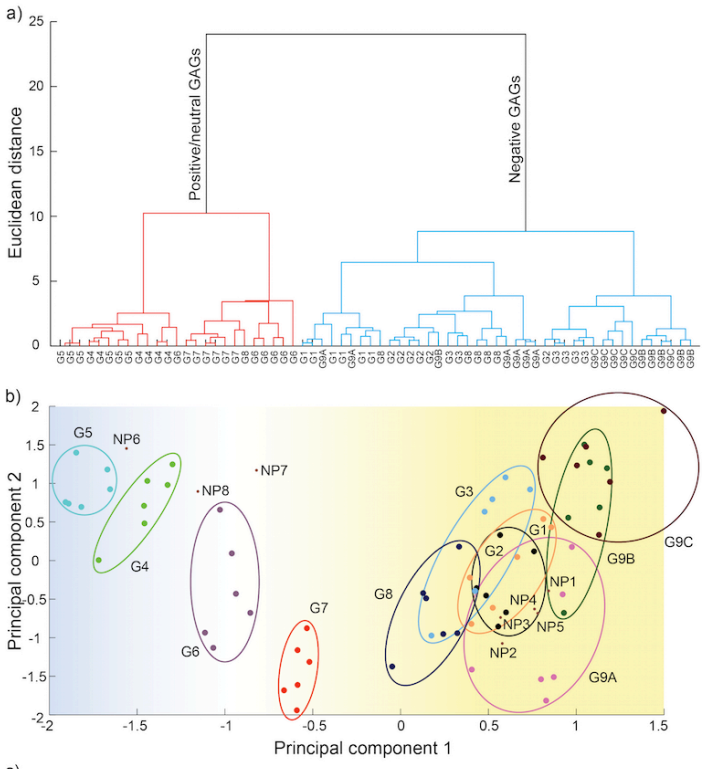

NP1	NP2	NP3	NP4	NP5	NP6	NP7	NP8	%
■								39
	■							36
		■						42
			■					38
				■				36
					■			24
						■		18
							■	52
■	■	■	■	■	■	■	■	92

Figure B.3. (a) HCA dendrogram based on the Euclidean distance along with Ward method for clustering. (b) PCA biplot of the 11 GAGs showing a charge-based discrimination (from positive at the left to negative on the right, passing through the more neutral GAGs). (c) The Jackknifed classification matrix showing the contribution of each nanoparticle in the differentiation.

We further investigated the capabilities of our sensor to test if chemical changes in the GAG structure can be readily identified. For this purpose, specific subsets of the GAGs were analyzed separately using LDA. In the first subset, G1 to G4 were studied to analyze how the variations in the functional groups of the glycoside units affect the discrimination of closely related analytes. Figure B.4a shows the LDA clustering results for this subset, where G4 (de-O-sulfated) is located on the left quadrants of the plot while G1, G2 and G3 cluster apart, owing to the sulfonation profiles. Similarly, acetylation profiles provided the second factor of discrimination, separating G2 and G4 (both N-acetylated) from G1 and G3 (non-acetylated). The size of the analyte can also be recognized by the sensor. This can be observed by the analysis of subset 2 (G5, G6 and G9A–G9C), where GAGs of different sizes (G9A, G9B and G9C) are discriminated according to their molecular weight by the second factor on the LDA plot (Figure B.4b). In this subset it is also evident that charge is the principal factor of differentiation, separating G5 and G6 from the G9A/G9B/G9C group (clustered together in the right quadrants).

Finally, we were interested in observing if a change in the epimeric structure of the GAGs (chirality of one stereocenter) can be detected by the sensor array. This detection represents a significant challenge given that low throughput techniques are the current standard to observe such subtle changes.[31] For this purpose, the epimers G7 and G8 (Figure B.2) were analyzed as a third subset. The set was completed with G2 and G6, of similar chirality to G7 and G8 respectively. As seen in Figure B.4c, this small change can also be recognized, and G7 and G8 are clearly differentiated. Moreover, G2 and G7 cluster together, away from G6 and G8, generating a separation by the nature of the stereocenter (this discrimination can also be seen on the HCA analysis, Figure B.16). These results evidence the robustness of the nanoparticle-based sensor array for the detection of GAGs, being able to detect changes as significant as charge, and as subtle as epimeric nature.

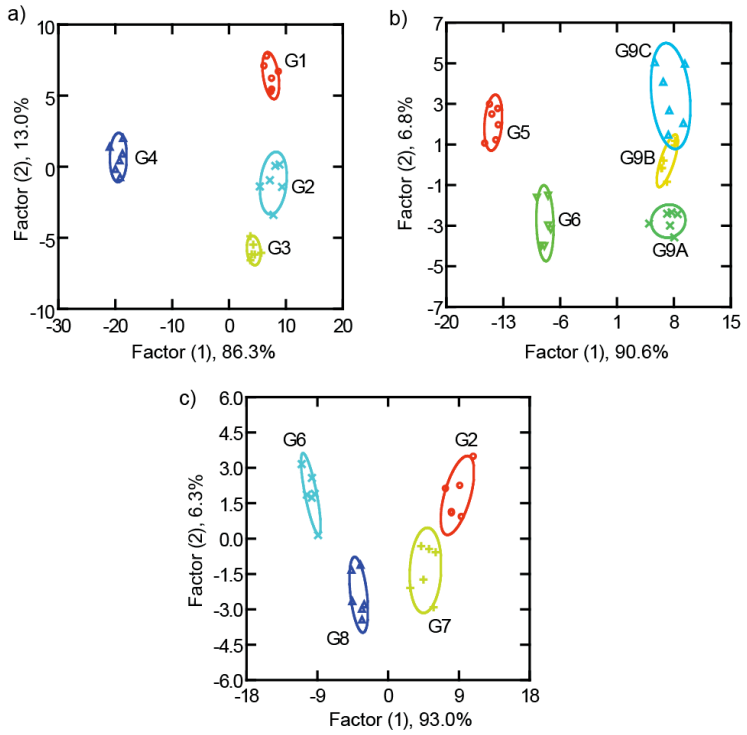

Figure B.4. LDA canonical score plots. The graphs summarize the differentiation by changes in (a) sulfonation and acetylation, (b) size and charge, and (c) epimeric nature.

B.3. Conclusions

We were able to discriminate between 11 different GAGs using their specific chemical profiles. Multiple chemical signatures of the GAGs such as sulfonation, acetylation, epimeric form, size and charge were recognized in the differentiation process. The use of aromatic and specific sugars moieties on the AuNP surface contributed significantly in the differentiation process. This study not only demonstrates the sensing capabilities of the array, but also provides fundamental insight into the supramolecular chemistry of GAGs with synthetic receptors.

B.4. Experimental section

Nanoparticle synthesis: Gold nanoparticles were synthesized according to the method described in Section 2.4. The ligands for NP1-NP4 and NP8 were synthesized according to the reported procedure. The ligands for NP5, NP6 and NP7 were synthesized as follows (Figure B.5):

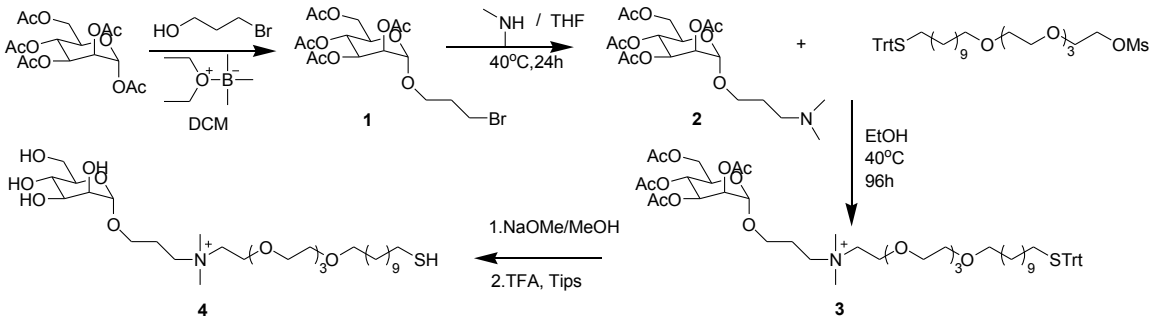

Figure B.5. Synthetic route of glycan-functionalized ligands.

Compound 1: Boron trifluoride etherate (8 mL, 65 mmol) was added to a solution of 1,2,3,4,6-penta-O-acetyl-alpha-D-glucopyranose (6.5 g, 16.65 mmol) and 3-bromo-1-propanol (1.8 mL, 20 mmol) in dry CH_2Cl_2 (100ml). The reaction mixture was stirred under a nitrogen atmosphere overnight. The reaction mixture was neutralized by adding 100 mL of a saturated solution of sodium bicarbonate and then washed with distilled water (2x100 mL). The combined organic layers were dried over sodium sulfate, filtered and concentrated under reduced pressure. The resulting oil was then purified using column chromatography (ethyl acetate/hexane (1:1, v/v)). After collecting the relevant fractions, the solvent was evaporated and 3'-bromopropyl 2,3,4,6-tetra-O-acetyl-alpha-D-glucopyranose was obtained as a light yellow oil (4.4 g, 56%). Compound 2: Compound 1 (730 mg, 1.556 mmol) was dissolved into 2M dimethylamine solution in THF (15 ml). The reaction mixture was stirred at ~40°C overnight. The crude product was

checked by TLC and THF was evaporated at reduced pressure. The light yellowish residue was washed with hexanes using sonication and centrifugation, and it was further dried at high vacuum. The product formation was quantitative (>95%). Compound 3: Compound 2 (550 mg, 1.27 mmol) was added to a solution in ethanol of 1,1,1-triphenyl-14,17,20,23-tetraoxa-2-thiapentacosan-25-yl methanesulphonate (2.67 g, 3.81 mmol). The reaction mixture was stirred at ~40°C for 96 h. When the reaction was finally completed (according to TLC), the ethanol was evaporated. The crude product was washed three times with hexane and six times with diethylether to afford compound 3 (yellowish oil, 1.55 g, 79 %). Compound 4: To a solution of compound 3 (300mg, 0.29 mmol) in dry and deoxygenated MeOH (5ml), NaOMe was added. After 10 minutes the reaction was neutralized with H+ Dowex resin, filtered and the solvent was removed, giving the product without any other purification. The product was then dissolved in dry dichloromethane (5 mL) and an excess of trifluoroacetic acid (TFA, ~20 equivalents) was added. The color of the solution turned yellow immediately. Subsequently, triisopropylsilane (TIPS, ~1.5 equivalents) was added to the reaction mixture. The reaction mixture was stirred overnight under N2 at room temperature. The solvent, TFA and TIPS were distilled off under reduced pressure. The pale yellow residue was purified washing with hexanes (3 times) and ether (6 times) combining successive sonication and centrifugation. The product formation was quantitative (>95%). NMRs in Figures B.6, B.7 and B.8. MALDI-MS spectrum in Figure B.9.

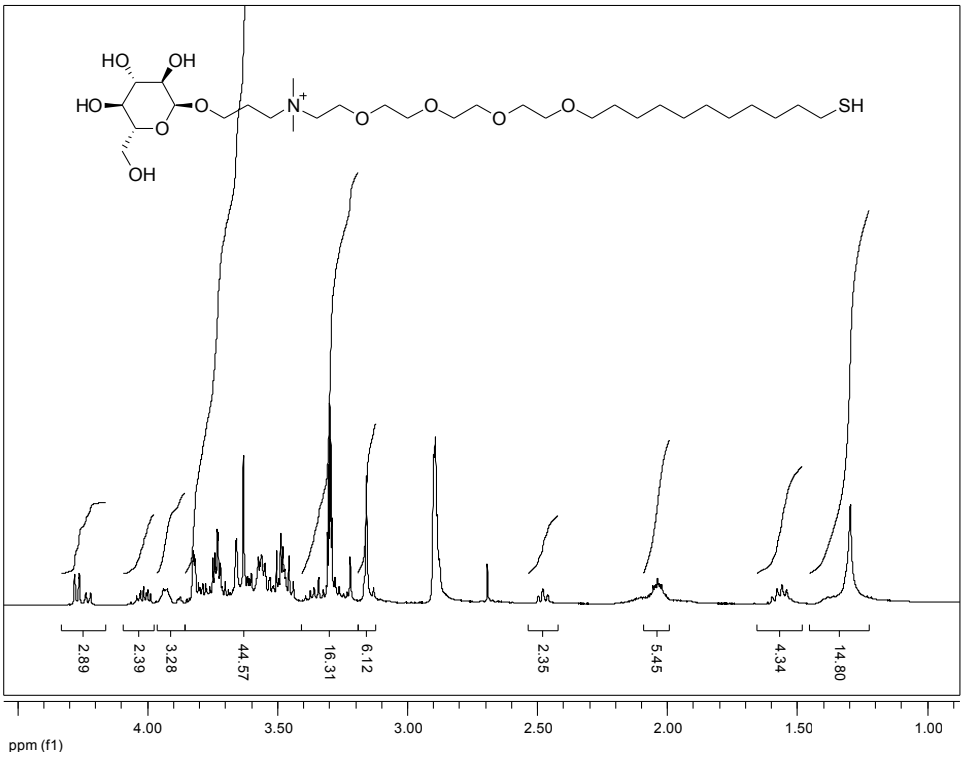

Figure B.6. 400 MHz 1H NMR spectra of the glucose ligand in MeOD (D, 99.8%).

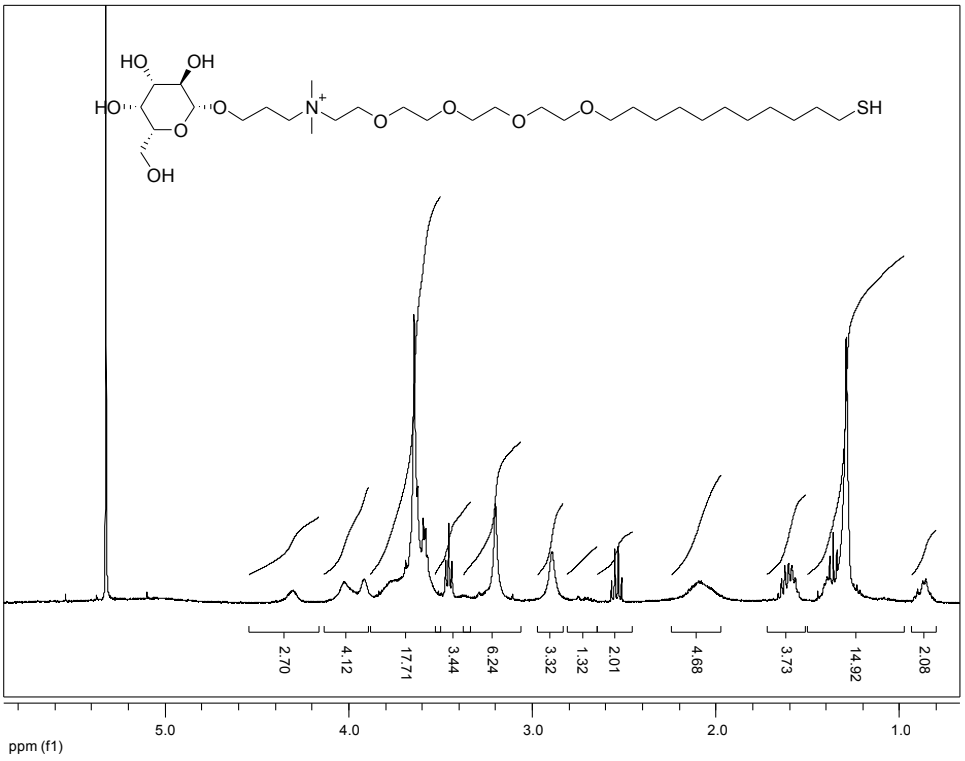

Figure B.7. 400 MHz 1H NMR spectra of the galactose ligand in MeOD (D, 99.8%).

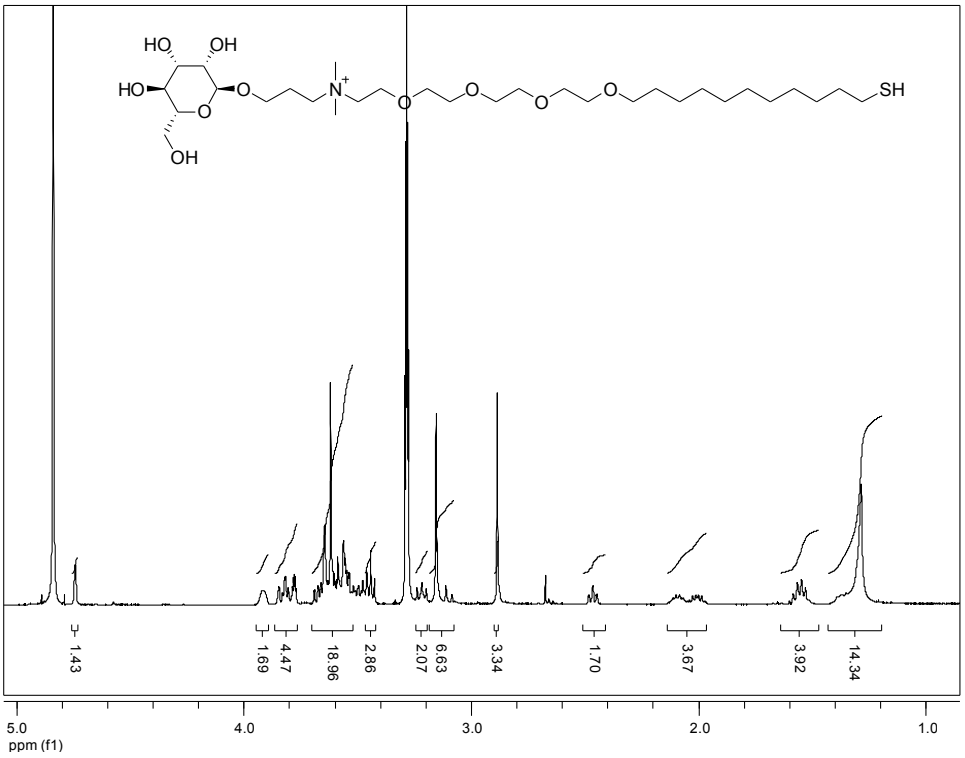

Figure B.8. 400 MHz 1H NMR spectra of the mannose ligand in MeOD (D, 99.8%).

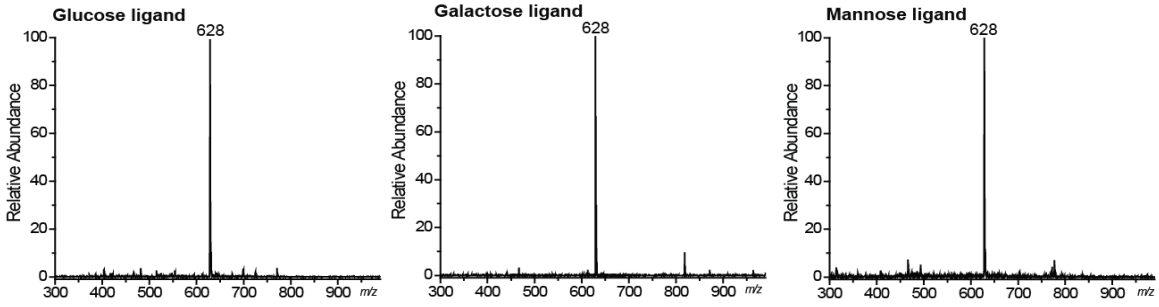

Figure B.9. Matrix-assisted laser desorption/ionization mass spectroscopy (MALDI-MS) spectrum of three glycan ligands.

Sensor design and other materials: For a detailed description of the glycosaminoglycans used in the study (including source) and the development of the sensor arrays, please refer to section B2.

B.5. Supporting information

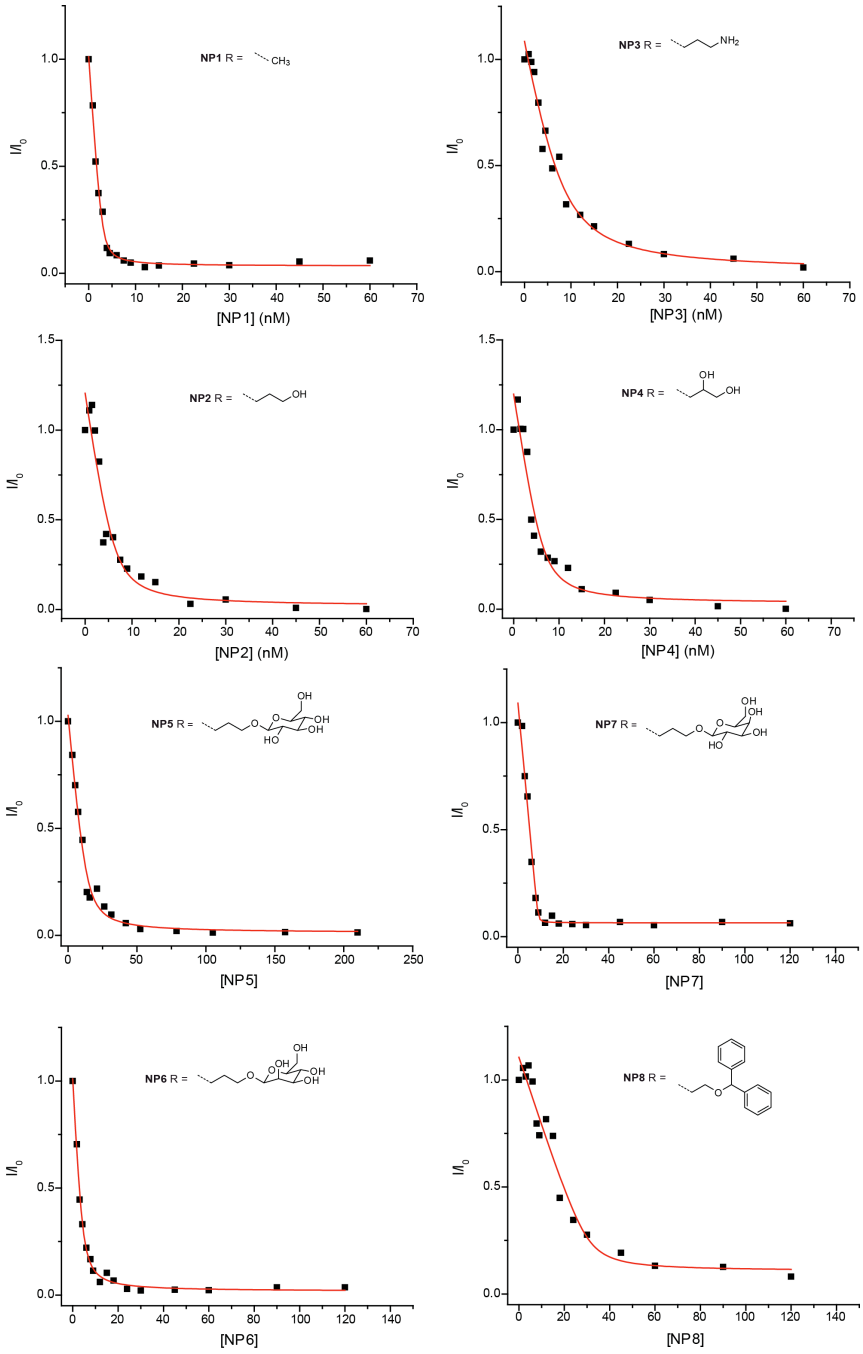

Figure B.10. Fluorescence titration curves of the gold nanoparticles with the polymer PPE.

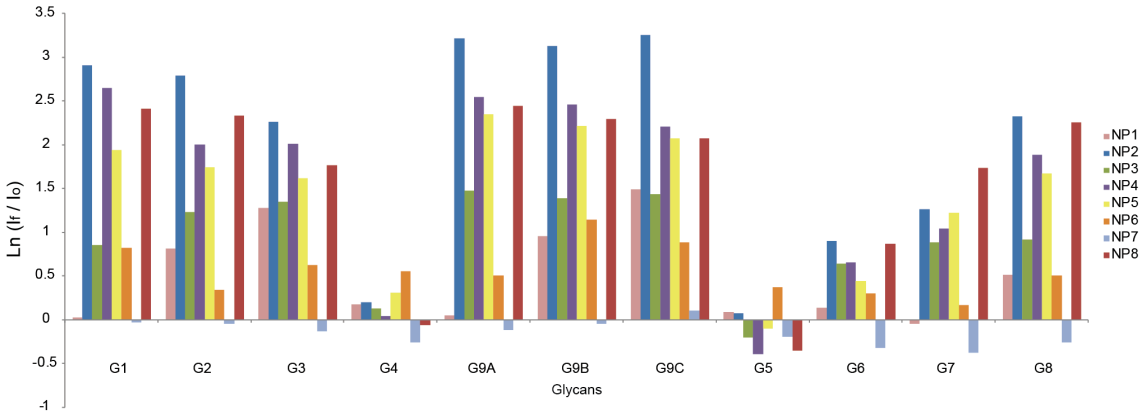

Figure B.11. Fluorescence response patterns for all the glycosaminoglycans under study.

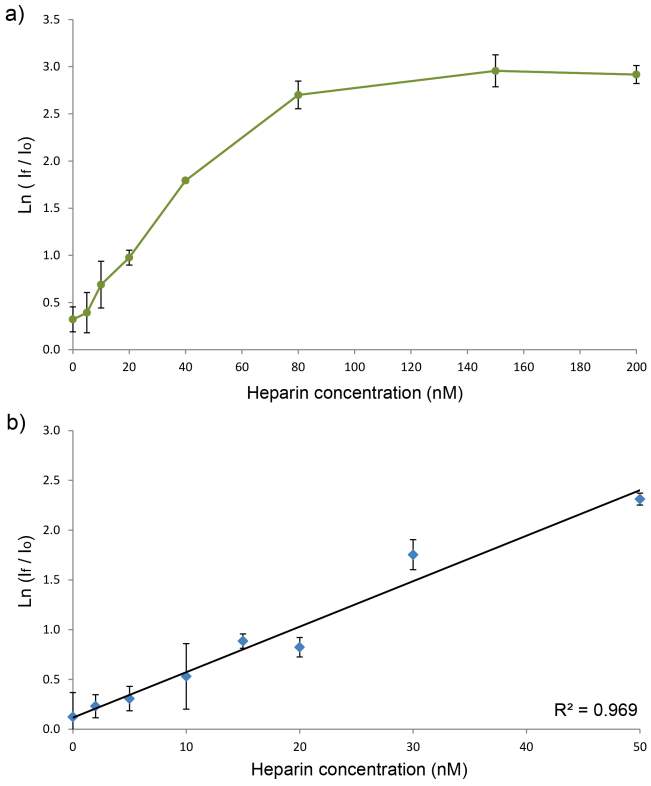

Figure B.12. Dose response curve of (a) heparin concentration from 0 to 200 nM, and (b) dynamic range of the response curve from 0 to 50 nM of heparin.

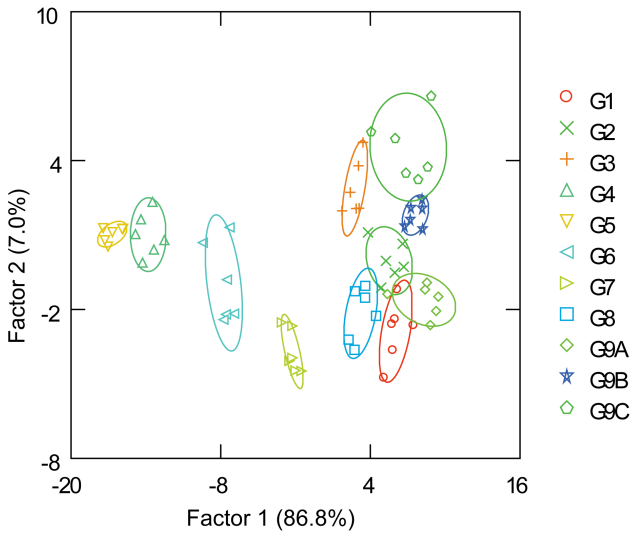

Figure B.13. LDA canonical score plots for all the glycosaminoglycans under study.

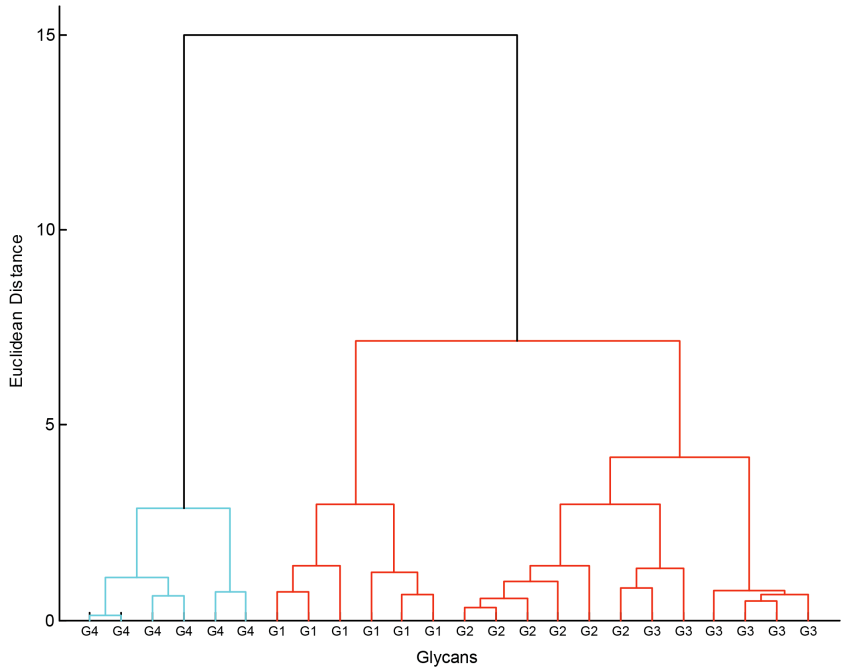

Figure B.14. HCA of structurally different heparin molecules (G1:Heparin, G2:N-acetyl Heparin, G3: De-N-sulfated Heparin and G4: N-acetyl-de-O-sulfated Heparin).

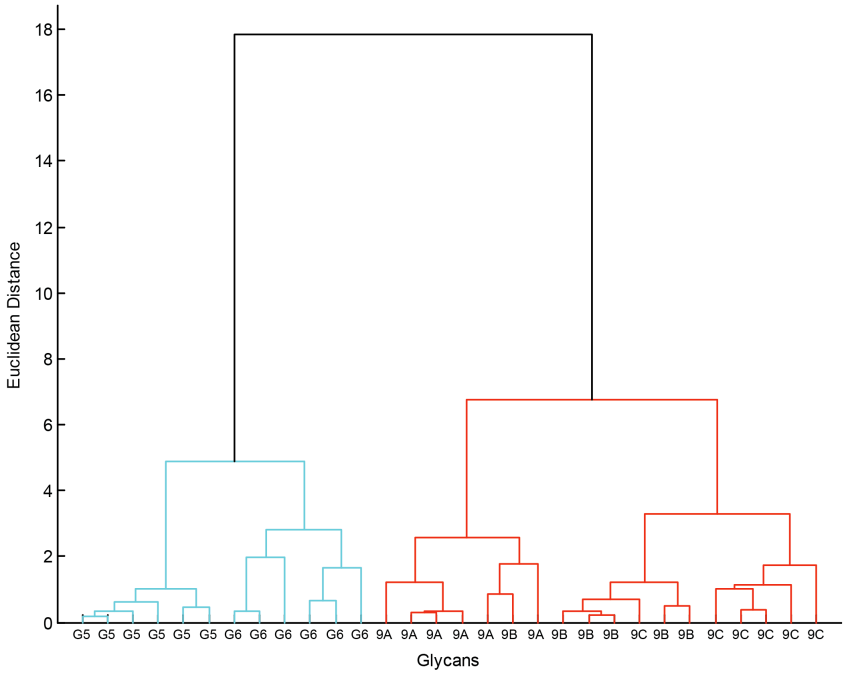

Figure B.15. HCA of glycans with different size and charge. (G5:Chitosan, G6: Hyaluronic Acid, 9A: Dextran Small (8kDa), 9B: Dextran Medium (15kDa) and 9C: Dextran Large (500kDa)).

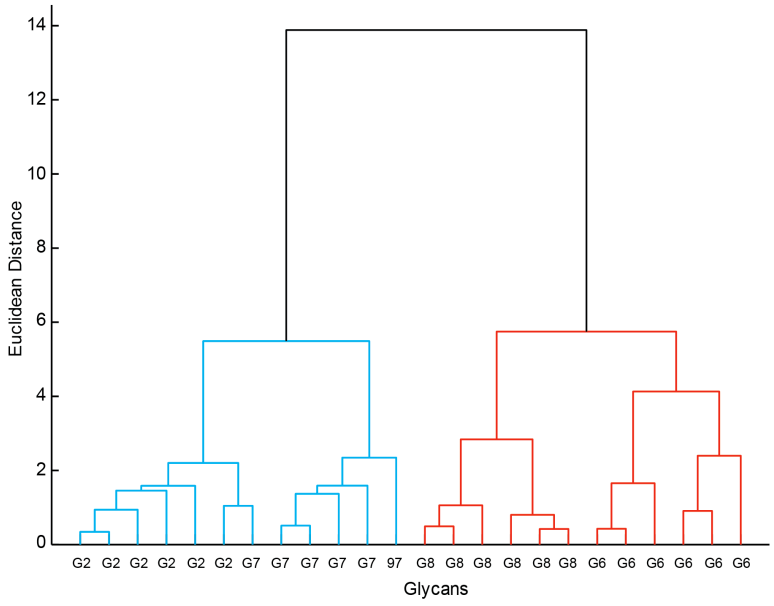

Figure B.16. HCA of glycans with different chirality. (G7: Chondroitin sulfate B, G8: Chondroitin sulfate A, G2: N-acetyl Heparin and G6: Hyaluronic acid).

B.6. References

1. Varki, A.; Cummings, R. D.; Esko, J. D.; Freeze, H. H.; Stanley, P.; Bertozzi, C. R.; Hart, G. W.; Etzler, M. E. *Essentials of Glycobiology, Cold Spring Harbor Laboratory Press, New York, 2nd Ed.,* **2009**.

2. Ghandi, N. S.; Mancera, R. L. *Chem. Biol. Drug Des.* **2008**, *72*, 455.

3. Bernardes, G. J. L.; Castagner, B.; Seeberger, P. H. *ACS Chem. Biol.* **2009**, *4*, 703.

4. Scott, J. E. *FASEB J.* **1992**, *6*, 2639.

5. Gama, C. I.; Tully, S. E.; Sotogaku, N.; Clark, P. M.; Rawat, M.; Vaidehi, N.; Goddard III, W. A.; Nishi, A.; HsiehWilson, L. C. *Nat. Chem. Biol.* **2006**, *2*, 467.

6. Guerrini, M.; Zhang, Z.; Shriver, Z.; Naggi, A.; Masuko, S.; Langer, R.; Casu, B.; Linhardt, R. J.; Torri, G.; Sasisekharan, R. *Proc. Natl. Acad. Sci. U. S. A.* **2009**, *106*, 16956.

7. Studelska, D. R.; Giljum, K.; McDowell, L. M.; Zhang, L. *Glycobiology* **2006**, *16*, 65.

8. Zhang, Z.; Xie, J.; Liu, H.; Liu J.; Lindhardt, R. J. *Anal.Chem.* **2009**, *81*, 4349.

9. Gupta, G.; Surolia, A.; Sampathkumar, S. G. OMICS: *J. Integr. Biol.* **2010**, *14*, 419.

10. Zuo, Y.; Broughton, D. L.; Bicker, K. L.; Thompson, P. R.; Lavigne, J. J. *ChemBioChem* **2007**, *8*, 2048.

11. Zhong, Z.; Anslyn, E. V. *J. Am. Chem. Soc.* **2002**, *124*, 9014.

12. Muller-Graff, P. K.; Szelke, H.; Severin, K.; Kramer, R. *Org. Biomol. Chem.* **2010**, *8*, 2327.

13. Sun, W.; Bandmann, H.; Schrader, T. *Chem.–Eur. J.* **2007**, *13*, 7701.

14. Nyren-Erickson, E. K.; Haldar, M. K.; Gu, Y.; Qian, S. Y.; Friesner, D. L.; Malik, S. *Anal. Chem.* **2011**, *83*, 5989.

15. Wright, A. T.; Anslyn, E. V. *Chem. Soc. Rev.* **2006**, *35*, 14.

16. Duncan, B.; Elci, S. G.; Rotello, V. M. *Nano Today* **2012**, *7*, 228.

17. Umali, A. P.; LeBoeuf, S. E.; Newberry, R. W.; Kim, S.; Tran, L.; Rome, W. A.; Tian, T.; Taing, D.; Hong, J.; Kwan, M.; Heymann, H.; Anslyn, E. V. *Chem. Sci*. **2011**, *2*, 439.

18. Lee, J. W.; Lee, J. S.; Chang, Y. T. *Angew. Chem., Int. Ed.* **2006**, *45*, 6485.

19. Musto, J. C.; Suslick, K. S. *Curr. Opin. Chem. Biol.* **2010**, *14*, 758.

20. Miranda, O. R.; Creran B.; Rotello, V. M. *Curr. Opin. Chem. Biol.* **2010**, *14*, 728.

21. De, M.; Rana, S.; Akpinar, H.; Miranda, O. R.; Arvizo, R. R.; Bunz, U. H. F.; Rotello, V. M. *Nat. Chem.* **2009**, *1*, 461.

22. Rana, S.; Singla, A. K.; Bajaj, A.; Elci, S. G.; Miranda, O. R.; Mout, R.; Yan, B.; Jirik F. R.; Rotello, V. M. *ACS Nano* **2012**, *6*, 8233.

23. Kim, I. B.; Phillips, R.; Bunz, U. H. F. *Macromolecules* **2007**, *40*, 5290.

24. McRae, R. L.; Phillips, R. L.; Kim, I. B.; Bunz, U. H. F.; Fahrni, C. J. *J. Am. Chem. Soc.* **2008**, *130*, 7851.

25. Bunz, U. H. F.; Rotello, V. M. *Angew. Chem., Int. Ed.* **2010**, *49*, 3268.

26. Moyano D. F.; Rotello, V. M. *Langmuir* **2011**, *27*, 10376.

27. Laughrey, Z. R.; Kiehna, S. E.; Riemen, A. J.; Waters, M. L. *J. Am. Chem. Soc.* **2008**, *130*, 14625.

28. Pincet, F.; Le Bauer, T.; Zhang, Y.; Esnault, J.; Mallet, J.-M.; Perez, E.; Sinay, P. *Biophys. J.* **2001**, *80*, 1354.

29. Moyano, D. F.; Rana, S.; Bunz U. H. F.; Rotello, V. M. *Faraday Discuss.* **2011**, *152*, 33.

30. Rojo, J.; Diaz, V.; de la Fuente, J. M.; Segura, I.; Barrientos, A. G.; Riese, H. H.; Bernad, A.; Penades, S. *ChemBioChem* **2004**, *3*, 291.

31. Wolff, J. J.; Chi, L.; Linhardt, R. J.; Amster, I. J.; *Anal. Chem.* **2007**, *79*, 2015.

APPENDIX C

CURRICULUM VITAE

DANIEL FERNANDO MOYANO MARIÑO
(04/22/15)
Department of Chemistry, University of Massachusetts Amherst
dfmoyanom@gmail.com / Cel: 413-695-5725

EDUCATION

• **Ph.D. in Chemistry.**

University of Massachusetts Amherst, MA, USA (2015).

• **B.Sc. in Chemistry (Honors)**.

National University of Colombia, Bogotá, Colombia (2009).

DISTINCTIONS AND AWARDS

• Dr. Paul Hatheway Terry Graduate Scholarship Award (2013)
University of Massachusetts Amherst, MA, USA

• William E. McEwen Fellowship Award (2012)
University of Massachusetts Amherst, MA, USA.

• *Summa Cum Laude* - Honors Degree in Science (2009).
National University of Colombia, Science Faculty, Bogotá, Colombia.

• Outstanding Honor Student Scholarship (granted 9 times, 2003-2008).
National University of Colombia, Department of Chemistry, Bogotá, Colombia.

• Bronze Medal - VIII Iberoamerican Chemistry Olympiad (2003 – Continental level).
National Autonomous University of Mexico, Cuernavaca, Mexico.

• Gold Medal – X Colombian Chemistry Olympiad (2002 – National level).
National University of Colombia, Bogotá, Colombia.

PUBLICATIONS

33. Mizuhara, T.; Saha, K.; **Moyano, D. F.**; Kim, C. S.; Yan, B.; Kim, Y.-K.; Rotello, V. M. "Acylsulfonamide-Functionalized Zwitterionic Gold Nanoparticles for Enhanced Cellular Uptake at Tumor pH" *Angew. Chem. Int. Ed.* **2015**, DOI: 10.1002/anie.201411615.

32. Bera, M. K.; Chan, H.; **Moyano, D. F.**; Yu, H.; Tatur, S.; Amoanu, D.; Bu, W.; Rotello, V. M.; Meron, M.; Kral, P.; Lin, B.; Schlossman, M. L. "Interfacial localization and voltage-tunable arrays of charged nanoparticles" *Nano Lett.* **2014**, *14*, 6816.

31. **Moyano, D. F.**; Ray, M.; Rotello, V. M. "Nanoparticle-protein interactions: water is the key" *MRS Bulletin* **2014**, *39*, 1069.
30. Li, X.; Kong, H.; Mout, R.; Saha, K.; **Moyano, D. F.**; Robinson, S. M.; Rana, S.; Zhang, X.; Riley, M. A.; Rotello, V. M. "Rapid Identification of Bacterial Biofilms and Biofilm Wound Models Using a Multichannel Nanosensor" *ACS Nano* **2014**, *8*, 12014.
29. Creran, B.; Li, X.; Duncan, B.; Kim, C. S.; **Moyano, D. F.**; Rotello, V. M. "Detection of Bacteria Using Inkjet-Printed Enzymatic Test Strips" *ACS Appl. Mater. Inter.* **2014**, *6*, 19525.
28. Ekmekci, Z.; Saha, K.; **Moyano, D. F.**; Tonga, G. Y.; Wang, H.; Mout, R.; Rotello, V. M. "Probing the Protein-Nanoparticle Interface: The Role of Aromatic Substitution Pattern on Affinity" *Supramol. Chem.* **2015**, *27*, 123.
27. Manshian, B. B.; **Moyano, D. F.**; Corthout, N.; Munck, S.; Himmelreich, U.; Rotello, V. M. Soenen, S. J. "High-content imaging and gene expression analysis to study cell-nanomaterial interactions: The effect of surface hydrophobicity" *Biomaterials* **2014**, *35*, 9941.
26. Li, X.; Robinson, S. M.; Gupta, A.; Saha, K.; Jiang, Z.; **Moyano, D. F.**; Sahar, A.; Riley, M. A.; Rotello, V. M. "Functional Gold Nanoparticles as Potent Antimicrobial Agents against Multi-Drug-Resistant Bacteria" *ACS Nano* **2014**, *8*, 10682. (Featured by Nanotechweb: http://nanotechweb.org/cws/article/tech/58690).
25. **Moyano, D. F.**; Rotello, V. M. "Gold Nanoparticles: Testbeds for Engineered Protein-Particle Interactions" *Nanomedicine* **2014**, *9*, 1905.
24. Mout, R.; Tonga, G. Y.; Ray, M.; **Moyano, D. F.**; Rotello, V. M. "Environmentally Responsive Histidine-Carboxylate Zipper Formation between Proteins and Nanoparticles" *Nanoscale* **2014**, *6*, 8873.
23. **Moyano, D. F.**; Saha, K.; Prakash, G.; Yan, B.; Kong, H.; Yazdani, M.; Rotello, V. M. "Fabrication of Corona-Free Nanoparticles with Tunable Hydrophobicity" *ACS Nano* **2014**, *8*, 6748. (Selected as ACS Editor's choice 07/11/14 and Featured by Science: http://www.sciencemag.org/content/345/6198/783.5).
22. Tonga, G. Y.; **Moyano, D. F.**; Kim, C. S.; Rotello, V. M. "Inorganic Nanoparticles for Therapeutic Delivery: Trials, Tribulations and Promise" *Curr. Opin. Colloid Interface Sci.* **2014**, *19*, 49.
21. Chen, K.; Rana, S.; **Moyano, D. F.**; Xu, Y.; Guo, X.; Rotello, V. M. "Optimizing the selective recognition of protein isoforms through tuning of nanoparticle hydrophobicity" *Nanoscale* **2014**, *6*, 6492.

20. Tang, R.; **Moyano, D. F.**; Subramani, C.; Yan, B.; Jeoung, E.; Tonga, G. Y.; Duncan, B.; Yeh, Y.-C.; Jiang, Z.; Kim, C.; Rotello, V. M. "Rapid Coating of Surfaces with Functionalized Nanoparticles for Regulation of Cell Behavior" *Adv. Mater.* **2014**, *26*, 3310.
19. Saha, K.; **Moyano, D. F.**; Rotello, V. M. "Protein coronas suppress the hemolytic activity of hydrophilic and hydrophobic nanoparticles" *Mater. Horiz.* **2014**, *1*, 102.
18. Arvizo, R. R.; **Moyano, D. F.**; Saha, S.; Thompson, M. A.; Bhattacharya, R.; Rotello, V. M.; Prakash, Y. S.; Mukherjee, P. "Probing Novel Roles of the Mitochondrial Uniporter in Ovarian Cancer Cells Using Nanoparticles" *J. Biol. Chem.* **2013**, *288*, 17610. (Featured by Sciencedaily: http://www.sciencedaily.com/releases/2013/05/130521105059.htm and the journal cover).
17. Yan, B.; Kim, S. T.; Kim, C. S.; Saha, K.; **Moyano, D. F.**; Xing, Y.; Jiang, Y.; Roberts, A. L.; Alfonso, F. S.; Rotello, V. M., Vachet, R. W. "Multiplexed Imaging of Nanoparticles in Tissues using Laser Desorption/Ionization Mass Spectrometry" *J. Am. Chem. Soc.* **2013**, *135*, 12564.
16. **Moyano, D. F.**; Duncan, B.; Rotello, V. M. "Preparation of 2 nm Gold Nanoparticles for In vitro and In vivo Applications" *Methods Mol. Biol.* **2013**, *1025*, 3.
15. Xu, Y.; Engel, Y.; Yan, Y.; Chen, K.; **Moyano, D. F.**; Dubin, P. L.; Rotello, V. M. "Enhanced Electrostatic Discrimination of Proteins at Nanoparticle-Coated Surfaces" *J. Mater. Chem. B* **2013**, *1*, 5230-5234. (Featured in the JMCB News Blog: http://blogs.rsc.org/jm/2013/09/04/hot-articles-for-september).
14. Elci, S. G.; **Moyano, D. F.**; Rana, S.; Tonga, G. Y.; Phillips, R. L.; Bunz, U. H. F.; Rotello, V. M. "Recognition of glycosaminoglycan chemical patterns using an unbiased sensor array" *Chem. Sci.* **2013**, *4*, 2076.
13. **Moyano, D. F.**; Rotello, V. M. "Nanoparticle-GFP 'chemical nose' sensor for cancer cells identification" *Methods Mol. Biol*. **2013**, *991*, 1.
12. Creran, B.; Yan, B.; **Moyano, D. F.**; Gilbert, M. M.; Vachet, R. W.; Rotello, V. M. "Laser Desorption Ionization Mass Spectrometric Imaging of Inkjet Patterned Gold Nanoparticles for Security Applications" *Chem. Commun.* 2012, *48*, 4543. (Featured by Chemistry World: http://www.rsc.org/chemistryworld/2012/05/mass-spectrometry-imaging-new-tool-counterfeit-security and the journal cover).
11. Zhu, Z.-J.; Posati, T.; **Moyano, D. F.**; Tang, R.; Yan, B.; Vachet, R. W.; Rotello, V. M. "The Interplay of Monolayer Structure and Serum Protein Interactions on the Cellular Uptake of Gold Nanoparticles" *Small* **2012**, *8*, 2659-2663.

10. **Moyano, D. F.**; Goldsmith, M.; Solfiell, D. J.; Landesman-Milo, D.; Miranda, O. R.; Peer, D.; Rotello, V. M. "Nanoparticle Hydrophobicity Dictates Immune Response" *J. Am. Chem. Soc.* **2012**, *134*, 3965. (Featured by Sciencedaily: http://www.sciencedaily.com/releases/2012/03/120326160907.htm).
9. Arvizo, R. R.; Giri, K.; **Moyano, D.**; Miranda, O. R.; Madden, B.; McCormick, D. J.; Bhattacharya, R.; Rotello, V. M.; Kocher, J.-P.; Mukherjee, P. "Identifying New Therapeutic Targets via Modulation of Protein Corona Formation by Engineered Nanoparticles" *PLoS One* **2012**, *7*, e33650.
8. Subramani, C.; Saha, K.; Creran, B.; Bajaj, A.; **Moyano, D. F.**; Wang, H.; Rotello, V. M. "Cell Alignment using Patterned Biocompatible Gold Nanoparticle Templates" *Small* **2012**, *8*, 1209.
7. Mout, R.; **Moyano, D. F.**; Rana, S.; Rotello, V. M. "Surface functionalization of nanoparticles for nanomedicine" *Chem. Soc. Rev.* **2012**, *41*, 2539. (Featured in the CSR News Blog: http://blogs.rsc.org/cs/2012/02/07/surface-functionalization-of-nanoparticles-for-nanomedicine/).
6. Rana, S.; Yu, X.; Patra, D.; **Moyano, D. F.**; Miranda, O. R.; Hussain, I.; Rotello, V. M. "Control of Surface Tension at Liquid-Liquid Interfaces using Nanoparticles and Nanoparticle-Protein Complexes" *Langmuir* **2012**, *28*, 2023.
5. **Moyano, D. F.**; Rana, S.; Bunz, U. H. F.; Rotello, V. M. "Gold Nanoparticle-Polymer/Biopolymer Complexes for Protein Sensing" *Faraday Discuss.* **2011**, *152*, 33.
4. Arvizo, R. R.; Miranda, O. R.; **Moyano, D. F.**; Walden, C. A.; Giri, K.; Bhattacharya, R.; Robertson, J. D.; Rotello, V. M.; Reid, J. M.; Mukherjee, P. "Modulating Pharmacokinetics, Tumor Uptake and Biodistribution by Engineered Nanoparticles" *PLoS One* **2011**, *6*, e24374.
3. **Moyano, D. F.**; Rotello, V. M. "Nano Meets Biology: Structure and Function at the Nanoparticle Interface" *Langmuir* **2011**, *27*, 10376. (Featured on the journal cover).

---

2. **Moyano, D. F.**; Murcia, L. E.; Parra, D. A.; Burgos, A. E.; Aristizabal, F. A. "Evaluation of the cytotoxicity and antimicrobial activity of the [Ag(phen)2]SalH compound" *Rev. Colomb. Quim.* **2012**, *41*, 47.
1. Rivera, A.; **Moyano, D.**; Maldonado, M.; Ríos-Motta, J.; Reyes, A. "FTIR and DFT studies of the proton affinity of small aminal cages" *Spectrochim. Acta A* **2009**, *74*, 588.

PROFESSIONAL EXPERIENCE

Research Experience

• Graduate Research Assistant. **06/2010 – *Present***.

University of Massachusetts Amherst. Department of Chemistry.

- Synthesis and characterization of monolayer functionalized gold nanoparticles for biological applications.

- Comprehensive studies of the interplay of the nanoparticle surface chemistry and the protein corona on the innate immune responses, cellular uptake, and toxicity.

- Development of nanoparticle-based unbiased sensor arrays for the differentiation and identification of biomacromolecular signatures (proteins, glycosaminoglycans, cells/tissues).

• Undergraduate Research Assistant. **01/2008 – 02/2009**.

National University of Colombia. Department of Chemistry.

- Experimental and computational studies of the proton affinity of macrocyclic aminal cages.

- Synthesis, characterization and cytotoxic assays of Silver coordination compounds.

Industrial Experience

• PPG Industries (Pittsburgh, PA, USA).

Research Chemist. **2015**.

• AQM Laboratories (Bogotá, Colombia).

Scientist / Analyst. **2009 – 2009**.

- Coordinated with clients and evaluated quality control profiles of pharmaceutical products.

- Analyzed different pharmaceutical products to comply with USP standards.

Invited talks

• Gordon Research Conference - Noble Metal Nanoparticles.

"Tabula Rasa: Nanoparticles interacting with proteins the way we want"

2014, Mount Holyoke College, South Hadley MA, USA.

• Chalk Talk - Chemistry-Biology Interface Program.

"Exploring the immune system: the role of hydrophobicity"

2012, University of Massachusetts Amherst, MA, USA.

Poster in conferences

- Cancer Nanotechnology - Gordon Research Conference. **2013**, West Dover, VT, USA.
- Boston Symposium on Organic and Bioorganic Chemistry. **2012**, Boston, MA, USA.
- 244th American Chemical Society National Meeting. **2012**, Philadelphia, PA, USA.
- Polymer Science and Engineering Symposium. **2011**, Amherst, MA, USA.
- XXIX Latin American Chemistry Congress. **2010**, Cartagena de Indias, Colombia.
- XII National Chemistry Students Encounter ENEQUIM. **2008**, Cartagena de Indias, Colombia.

Teaching Experience

- Teaching Assistant. **09/2009 - 05/2010** & **09/2011 - 12/2011** (Undergraduate students).
  Physical/General Chemistry. Department of Chemistry, University of Massachusetts.
- Teaching Assistant. **02/2007 - 06/2008** (Undergraduate students).
  General Chemistry. Department of Medicine, National University of Colombia.
- Teaching Assistant. **02/2006 - 12/2006** (High school students).
  Chemistry and Biology. Instituto Pedagógico Arturo Ramírez Montúfar (IPARM)
- Private Tutor. **08/2004 - 10/2008** (High school and undergraduate students).
  Chemistry, Physics, Biology and Mathematics.

LIST OF ORIGINAL PUBLICATIONS

The present thesis is based on the work of the following first author/co-author publications:

1) **Moyano, D. F.**; Goldsmith, M.; Solfiell, D. J.; Landesman-Milo, D.; Miranda, O. R.; Peer, D.; Rotello, V. M. "Nanoparticle Hydrophobicity Dictates Immune Response" *J. Am. Chem. Soc.* (2012) *134*, 3965-3967.

2) Saha, K.; **Moyano, D. F.**; Rotello, V. M. "Protein coronas suppress the hemolytic activity of hydrophilic and hydrophobic nanoparticles" *Mater. Horiz*. (2014) *1*, 102-105.

3) **Moyano, D. F.**; Saha, K.; Prakash, G.; Yan, B.; Kong, H.; Yazdani, M.; Rotello, V. M. "Fabrication of Corona-Free Nanoparticles with Tunable Hydrophobicity" *ACS Nano* (2014) *8*, 6748-6755.

4) **Moyano, D. F.**; Rana, S.; Bunz, U. H. F.; Rotello, V. M. "Gold nanoparticle-polymer/biopolymer complexes for protein sensing" *Faraday Discuss.* (2011) *152*, 33-42.

5) Elci, S. G.; **Moyano, D. F.**; Rana, S.; Tonga, G. Y.; Phillips, R. L.; Bunz, U. H. F., Rotello, V. M. "Recognition of glycosaminoglycan chemical patterns using an unbiased sensor array" *Chem. Sci.* (2013) *4*, 2076-2080.

During the course of my Ph.D. studies, several other original publications were obtained in other research projects that were not included in the present document. For a complete list, please refer to http://goo.gl/z7jWHJ or Appendix C (curriculum vitae).

The papers were reprinted (adapted) in chapters 2 to 4 and appendices A and B with permission from the American Chemical Society (papers 1 and 3), and The Royal Society of Chemistry (papers 2, 4 and 5). Similarly, the research described in Chapter 5 and the overview illustrated in Chapter 1, were being prepared for publication in scientific journals as this thesis was written.

BIBLIOGRAPHY

Aggarwal, P.; Hall, J. B.; McLeland, C. B.; Dobrovolskaia, M. A.; McNeil, S. E. *Adv. Drug Delivery Rev.* **2009**, *61*, 428.

Akagi, T.; Wang, X.; Uto, T.; Baba, M.; Akashi, M. *Biomaterials* **2007**, *28*, 3427.

Akira, S.; Takeda, K. *Nat. Rev. Immunol*. **2004**, *4*, 499.

Albanese, A.; Tang, P. S.; Chan, W. C. W. *Annu. Rev. Biomed. Eng.* **2012**, *14*, 1.

Albert, K. J.; Lewis, N. S.; Schauer, C. L.; Sotzing, G. A.; Stitzel, S. E.; Vaid, T. P.; Walt, D. R. *Chem. Rev.* **2000**, *100,* 2595.

Andreeva, Z. I.; Nesterenko, V. F.; Fomkina, M. G.; Ternovsky, V. I.; Suzina, N. E.; Bakulina, A. Y.; Solonin, A. S.; Sineva, E. V. *Biochim. Biophys. Acta* **2007**, *1768*, 253.

Arvizo R. R.; Giri K.; Moyano D.; Miranda O. R.; Madden B.; McCormick D. J.; Bhattacharya R.; Rotello V. M.; Kocher J. P.; Mukherjee P. *PLoS One*, **2012**, *7*, e33650.

Arvizo, R. R.; Miranda, O. R.; Moyano, D. F.; Walden, C. A.; Giri, K.; Bhattacharya, R.; Robertson, J. D.; Rotello, V. M.; Reid, J. M.; Mukherjee, P. *PLoS One* **2011**, *6*, e24374.

Baier, G.; Costa, C.; Zeller, A.; Baumann, D.; Sayer, C.; Araujo, P. H. H.; Mailander, V.; Musyanovych, A.; Landfester, K. *Macromol. Biosci.* **2011**, *11*, 628.

Bajaj, A.; Miranda, O. R.; Kim, I.-B.; Phillips, R. L.; Jerry, D. J.; Bunz, U. H. F.; Rotello, V. M. *Proc. Natl. Acad. Sci. U. S. A.* **2009**, *106*, 10912.

Bajaj, A.; Rana, S.; Miranda, O. R.; Yawe, J. C.; Jerry, D. J.; Bunz, U. H. F.; Rotello, V. M. *Chem. Sci.* **2010**, *1*, 134.

Baldini, L.; Wilson, A. J.; Hong, J.; Hamilton, A. D. *J. Am. Chem. Soc.* **2004**, *126*, 5656.

Barran-Berdon, A. L.; Pozzi, D.; Caracciolo, G.; Capriotti, A. L.; Caruso, G.; Cavaliere, C.; Riccioli, A.; Palchetti, S.; Lagana, A.; *Langmuir* **2013**, *29*, 6485.

Bastós, N. G.; Sanchez-Tillo, E.; Pujals, S.; Farrera, C.; López, C.; Giralt, E.; Celada, A.; LIoberas, J.; Puntes, V. *ACS Nano* **2009**, *3*, 1335.

Bastós, N. G.; Sanchez-Tillo, E.; Pujals, S.; Farrera, C.; Kogan, M. J.; Giralt, E.; Celada, A.; Lloberas, J.; Puntes, V. *Mol. Immunol.* **2009**, *46*, 743.

Bernardes, G. J. L.; Castagner, B.; Seeberger, P. H. *ACS Chem. Biol.* **2009**, *4*, 703.

Brust, M.; Walker, M.; Bethell, D.; Schiffrin, D. J.; Whyman, R. *J. Chem. Soc., Chem. Commun.* **1994**, 801.

Bunz, U. H. F.; Rotello, V. M. *Angew. Chem., Int. Ed.* **2010**, *49*, 3268.

Buryak, A.; Severin, K. *J. Am. Chem. Soc*. **2005**, *127*, 3700.

Cao, Z. Q.; Jiang, S. Y. *Nano Today* **2012**, *7*, 404.

Casals, E.; Puntes, V. F. *Nanomedicine* **2012**, *7*, 1917.

Chen, Z.; Ward, R.; Tian, Y.; Baldelli, S.; Opdahl, A.; Shen, Y.-R.; Somorjai, G. A. *J. Am. Chem. Soc*. **2000**, *122*, 10615.

Chevallet, M.; Luche, S.; Rabilloud, T. *Nat. Protoc*. **2006**, *1*, 1852

Cho, E. C.; Xie, J.; Wurm, P. A.; Xia, Y. *Nano Lett*. **2009**, *9*, 1080.

Cho, W.; Cho, M.; Jeong, J.; Choi, M.; Cho, H.; Han, B.; Kim, S.; Kim, H.; Lim, Y.; Chung, B.; Jeong, J. *Toxicol. Appl. Pharm.* **2009**, *236*, 16.

Choi J.; Reipa V.; Hitchins V. M.; Goering P. L.; Malinauskas R. A. *Toxicol. Sci*. **2011**, *123*, 133.

Connor, E. E.; Mwamuka, J.; Gole, A.; Murphy, C. J.; Wyatt, M. D. *Small* **2005**, *1*, 325.

Daniel, M.-C.; Astruc, D. *Chem. Rev.* **2004**, *104*, 293.

De, M.; Rana, S.; Akpinar, H.; Miranda, O. R.; Arvizo, R. R.; Bunz, U. H. F.; Rotello, V. M. *Nat. Chem.* **2009**, *1*, 461.

De, M.; Rana S.; Rotello, V. M.; *Macromol. Biosci.* **2009**, *9*, 174.

De Geest, B. G.; Willart, M. A.; Hammad, H.; Lambrecht, B. N.; Pollard, C.; Bogaert, P.; De Filette, M.; Saelens, X.; Vervaet, C.; Remon, J. P.; Grooten, J.; De Koker, S. *ACS Nano* **2012**, *6*, 2136.

Dell'Orco, D.; Lundqvist, M.; Oslakovic, C.; Cedervall, T.; Linse, S. *PLoS One* **2010**, *5*, e10949.

Del Pino, P.; Pelaz, B.; Zhang, Q.; Maffre, P.; Nienhausbc, G. U.; Parak, W. J. *Mater. Horiz.* **2014**, *1*, 301.

Di Marco, M.; Shamsuddin, S.; Razak, K. A.; Aziz, A. A.; Devaux, C.; Borghi, E.; Levy, L.; Sadun, C. *Int. J. Nanomed*. **2010**, *5*, 37.

Ding, Y.; Jiang, Z.; Saha, K.; Kim, C. S.; Kim, S. T.; Landis, R. F.; Rotello, V. M. *Mol. Ther.* **2014**, *22*, 1075.

Dobrovolskaia, M. A.; McNeil, S. E. *Nat. Nanotechnol.* **2007**, *2*, 469.

Duarte, A.; Chworos, A.; Flagan, S. F.; Hanrahan, G.; Bazan, G. C. *J. Am. Chem. Soc.* **2010**, *132*, 12562.

Duncan, B.; Elci, S. G.; Rotello, V. M. *Nano Today* **2012**, *7*, 228.

El-Boubbou, K.; Zhu, D. C.; Vasileiou, C.; Borhan, B.; Prosperi, D.; Li, W.; Huang, X. F. *J. Am. Chem. Soc*. **2010**, *132*, 4490.

Elci, S. G.; Moyano, D. F.; Rana, S.; Tonga, G. Y.; Philips, R. L.; Bunz, U. H. F.; Rotello, V. M. *Chem. Sci.* **2013**, *4*, 2076.

Elsabahy, M.; Wooley, K. L. *Chem. Soc. Rev.* **2013**, *42*, 5552.

Fan, C.; Wang, S.; Bazan, G. C.; Plaxco, K. W.; Heeger, A. *J. Proc. Natl. Acad. Sci. U. S. A.* **2003**, *100*, 6297.

Faraday, M. *Phil. Trans. R. Soc. Lond.* **1857**, *147*, 145.

Filatov, I.; Larsson, S. *Chem. Phys*. **2002**, *3*, 575.

Fleischer, C. C.; Kumar, U.; Payne, C. K. *Biomater. Sci.* **2013**, *1*, 975.

Folmer-Andersen, J. F.; Kitamura, M.; Anslyn, E. V. *J. Am. Chem. Soc.* **2006**, *128*, 5652.

Fong, A. M.; Premont, R. T.; Richardson, R. M.; Yu, Y.-R. A.; Lefkowitz, R. J.; Patel, D. D. *Proc. Natl. Acad. Sci. U.S.A.* **2002**, *99*, 7478.

Fourches, D.; Pu, D.; Tassa, C.; Weissleder, R.; Shaw, S. Y.; Mumper, R. J.; Tropsha, A. *ACS Nano* **2010**, *4*, 5703.

Fu, J.; Li, G.; Qiin, Y.; Freeman, W. *J. Sens. Actuators B,* **2007**, *125*, 489.

Gallucci, S.; Lolkema, M.; Matzinger, P. *Nat. Med*. **1999**, *5*, 1249.

Gama, C. I.; Tully, S. E.; Sotogaku, N.; Clark, P. M.; Rawat, M.; Vaidehi, N.; Goddard III, W. A.; Nishi, A.; HsiehWilson, L. C. *Nat. Chem. Biol.* **2006**, *2*, 467.

Gessner, A.; Waicz, R.; Lieske, A.; Paulke, B. R.; Mader, K.; Muller, R. H *Int. J. Pharm.* **2000**, *196*, 245.

Ghandi, N. S.; Mancera, R. L. *Chem. Biol. Drug Des.* **2008**, *72*, 455.

Ghosh, P.; Han, G.; De, M.; Kim, C. K.; Rotello, V. M. *Adv. Drug Deliver. Rev.* **2008**, *60*, 1307.

Giljohann, D. A.; Seferos, D. S.; Daniel, W. L.; Massich, M. D.; Patel, P. C.; Mirkin, C. A. *Angew. Chem. Int. Ed.* **2010**, *49*, 3280.

Gronbeck, H.; Curioni, A.; Andreoni, W. *J. Am. Chem. Soc.* **2000**, *122*, 3839.

Grzelczak, M.; Pérez-Juste, J.; Mulvaney, P.; Liz-Marzán, L. M. *Chem. Soc. Rev.* **2008**, *37*, 1783.

Guerrini, M.; Zhang, Z.; Shriver, Z.; Naggi, A.; Masuko, S.; Langer, R.; Casu, B.; Linhardt, R. J.; Torri, G.; Sasisekharan, R. *Proc. Natl. Acad. Sci. U. S. A.* **2009**, *106*, 16956.

Gupta, G.; Surolia, A.; Sampathkumar, S. G. OMICS: *J. Integr. Biol.* **2010**, *14*, 419.

Hamad, I.; Al-Hanbali, O.; Hunter, A. C.; Rutt, K. J.; Andresen, T. L.; Moghimi, S. M. *ACS Nano* **2010**, *4*, 6629.

Hong, R.; Fischer, N. O.; Verma, A.; Goodman, C. M.; Emrick, T. S.; Rotello, V. M. *J. Am. Chem. Soc.* **2004**, *126*, 739.

Hubbell, J. A.; Thomas, S. N.; Swartz, M. A. *Nature* **2009**, *462*, 449.

Hühn, D.; Kantner, K.; Geidel, C.; Brandholt, S.; Cock, I. D.; Soenen, S. J. H.; Rivera_Gil, P.;Montenegro, J.-M.; Braeckmans, K.; Müllen, K.; Nienhaus, G. U.; Klapper, M.; Parak, W. J. *ACS Nano* **2013**, *7*, 3253.Iwasaki, A.; Medzhitov, R. *Science* **2010**, *327*, 292.

Janeway, C. A. Jr. *Cold Spring Harb. Symp. Quant. Biol*. **1989**, *54*, 1.

Janeway, C. A. Jr.; Medzhitov, R. Annu. Rev. *Immunol.* **2002**, *20*, 197.

Joglekar, M.; Roggers, R. A.; Zhao, Y. N.; Trewyn, B. G. *RSC Adv*. **2013**, *3*, 2454.

Jokerst, J. V.; Lobovkina, T.; Zare, R. N.; Gambhir, S. S. *Nanomedicine* **2011**, *6,* 715.

Jones, K. J.; Perris, A. D.; Vernallis, A. B.; Worthington, T.; Lambert, P. A.; Elliott, T. S. J.; *J. Med. Microbiol.* **2005**, *54*, 315.

Jordan, B. J.; Hong, R.; Han, G.; Rana, S.; Rotello, V. M. *Nanotechnology* **2009**, *20*, 43004.

Jurs, P. C.; Bakken G. A.; McClelland, H. E. *Chem. Rev.* **2000**, *100*, 2649.

Juskewitch, J. E.; Platt, J. L.; Knudsen, B. E.; Knutson, K. L.; Brunn, G. J.; Grande, J. P. *Sci. Rep.* **2013**, *2*, 918.

Karakoti, A. S.; Das, S.; Thevuthasan, S.; Seal, S. Angew. Chem., Int. Ed. **2011,** 50, 1980.

Kedmi, R.; Ben-Arie,N.; Peer, D. *Biomaterials* **2010**, *31*, 6867.

Kim, C. K.; Ghosh, P.; Pagliuca, C.; Zhu, Z.-J.; Menichetti, S.; Rotello, V. M. *J. Am. Chem. Soc.* **2009**, *131*, 1360.

Kim, I.-B.; Phillips, R.; Bunz, U. H. F. *Macromolecules* **2007**, *40*, 5290.

Kimbrell, D. A.; Beutler, B. *Nat. Rev. Genet.* **2001**, *2*, 256.

Kono, H.; Rock, K. L. *Nat. Rev. Immunol*. **2004**, *8*, 279.

Kumar, M. N. V. R. *J. Pharm. Pharm. Sci.* **2000**, *3*, 234.

Kwon, T.; Woo, H. J.; Kim, Y. H.; Lee, H. J.; Park, K. H.; Park, S.; Youn, B. *J. Nanosci. Nanotechnol*. **2012**, *12*, 6168.

Lai, W.-F.; Lin, M. C.-M. *J. Control. Release* **2009**, *134*, 158.

Laughrey, Z. R.; Kiehna, S. E.; Riemen, A. J.; Waters, M. L. *J. Am. Chem. Soc.* **2008**, *130*, 14625.

LaVan, D. A.; McGuire, T.; Langer, R. *Biotechnology* **2003**, *21*, 1184.

Lee, J. W.; Lee, J. S.; Chang, Y. T.; *Angew. Chem. Int. Ed.* **2006**, *45*, 6485.

Leeson, P. D.; Springthorpe, B. Nat. *Rev. Drug Discovery* **2007**, *6*, 881.

Lesniak, A.; Fenaroli, F.; Monopoli, M. R.; Aberg, C.; Dawson, K. A.; Salvati, A. *ACS Nano* **2012**, *6*, 5845.

Leszczynski, J. *Nat. Nanotechnol.* **2010**, *5*, 633.

Lewin, M.; Carlesso, N.; Tung, C.-H.; Tang, X.-W.; Cory, D.; Scadden, D. T.; Weissleder, R. *Nat. Biotechnol.* **2000**, *18*, 410.

Lewis, J. S.; Roy, K.; Keselowsky, B. G. *MRS Bulletin* **2014**, *39*, 25.

Li, W.; Szoka Jr., F. C. *Pharm. Res.* **2007**, *24*, 438.

Li, Y. T.; Liu, J.; Zhong, Y. J.; Zhang, J.; Wang, Z. Y.; Wang, L.; An, Y. L.; Lin, M.; Gao, Z. Q.; Zhang, D. S. *Int. J. Nanomed.* **2011**, *6*, 2805.

Liu, Y.; Yin, Y.; Wang, L.; Zhang, W.; Chen, X.; Yang, X.; Xu, J.; Ma, G. *J. Mater. Chem. B* **2013**, *1*, 3888.

Lin, Y. S.; Haynes, C. L. *Chem. Mater*. **2009**, *21*, 3979.

Lin, Y. S.; Haynes, C. L. *J. Am. Chem. Soc.* **2010**, *132*, 4834

Liu, X.; Atwater, M.; Wang, J.; Huo, Q. *Colloid. Surface. B* **2007**, *58*, 3.

Lonez, C.; Vandenbranden, M.; Ruysschaert, J.-M. *Adv. Drug Deliver. Rev.* **2012**, *64*, 1749.

Lonez, C.; Vandenbranden, M.; Ruysschaert, J.-M. *Prog. Lip. Res*. **2008**, *47*, 340.

Lorenz, E.; Patel, D. D.; Hartung, T.; Schwartz, D. A. *Infect. Immun.* **2002**, *70*, 4892.

Love, S. A.; Thompson, J. W.; Haynes, C. L. *Nanomedicine* **2012**, *7*, 1355.

Lu, S. L.; Duffin, R.; Poland, C.; Daly, P.; Murphy, F.; Drost, E.; MacNee, W.; Stone, V.; Donaldson, K. *Environ. Health Perspect.* **2009**, *117*, 241.

Lundqvist, M.; Stigler, J.; Elia, G.; Lynch, I.; Cedervall, T.; Dawson, K. A. *Proc. Natl. Acad. Sci. U.S.A*. **2008**, *105*, 14265.

Lynch, I.; Dawson, K. A.; *Nano Today* **2008**, *3*, 40.

Mahmoudi, M.; Lynch, I.; Ejtehadi, M. R.; Monopoli, M. P.; Bombelli, F. B.; Laurent, S. *Chem. Rev.* **2011**, *111*, 5610.

Maltzahn, G. V.; Park, J.-H.; Lin, K. Y.; Singh, N.; Schwoppe, C.; Mesters, R.; Berdel, W. E.; Ruoslahti, E.; Sailor, M. J.; Bhatia, S. N. *Nat. Mater.* **2011**, *10*, 545.

Ma, Z.; Li, J.; He, F.; Wilson, A.; Pitt, B.; Li, S. *Biochem. Biophys. Res. Commun*. **2005**, 3*30*, 755.

Massich, M. D.; Giljohann, D. A.; Seferos, D. S.; Ludlow, L. E.; Horvath, C. M.; Mirkin, C. A. *Mol. Pharm*. **2009**, *6*, 1934.

Matyjaszewski, K. *Macromolecules* **2012**, *45*, 4015.

Matzinger, P. Annu. *Rev. Immunol*. **1994**, *12*, 991.

Matzinger, P.; Kamala, T. *Nat. Rev. Immunol*. **2011**, *11*, 221.

McCormick, C. L.; Lowe, A. B. *Acc. Chem. Res.* **2004**, *37*, 312.

McRae, R. L.; Phillips, R. L.; Kim, I. B.; Bunz, U. H. F.; Fahrni, C. J. *J. Am. Chem. Soc.* **2008**, *130*, 7851.

Milani, S.; Bombelli, F. B.; Pitek, A. S.; Dawson, K. A.; Rädler, J. *ACS Nano* **2012**, *6*, 2532.

Miranda, O. R.; Chen, H.-T.; You, C.-C.; Mortenson, D. E.; Yang, X.-C.; Bunz, U. H. F.; Rotello, V. M. *J. Am. Chem. Soc*. **2010**, *132*, 5285.

Miranda, O. R.; Creran, B.; Rotello, V. M. *Curr. Opin. Chem. Biol.* **2010**, *14*, 728.

Miranda, O. R.; You, C.-C.; Phillips, R.; Kim, I.-K.; Ghosh, P. S.; Bunz, U. H. F.; Rotello, V. M. *J. Am. Chem. Soc.* **2007**, *129*, 9856.

Mirshafiee, V.; Mahmoudi, M.; Lou, K. Y.; Cheng, J. J.; Kraft, M. L. *Chem. Commun.* **2013**, *49*, 2557.

Mizrahy, S.; Raz, S. B.; Hasgaard, M.; Liu, H.; Soffer-Tsur, N.;Cohen, K.; Dvash, R.; Landsman-Milo, D.; Bremer, M. G. E. G.; Moghimi, S. M.; Peer, D. J. *Controlled Release* **2011**, *156*, 231

Monopoli, M. P.; Aberg, C., Salvati, A; Dawson, K. A. *Nat. Nanotechnol*. **2012**, *7*, 779.

Monopoli, M. P.; Pitek, A. S.; Lynch, I.; Dawson, K. A. *Methods Mol. Biol*. **2013**, *1025*, 137.

Monopoli, M. P.; Walczyk, D.; Campbell, A.; Elia, G.; Lynch, I.; Bombelli, F. B.; Dawson, K. A. *J. Am. Chem. Soc.* **2011**, *133*, 2525.

Moon, J. J.; Huang, B.; Irvine, D. J. *Adv. Mater.* **2012**, *24*, 3724.

Mortimer, G. M.; Butcher, N. J.; Musumeci, A. W.; Deng, Z. J.; Martin, D. J.; Minchin, R. F. *ACS Nano* **2014**, *8*, 3357.

Mout, R.; Moyano, D. F.; Rana, S.; Rotello, V. M. *Chem. Soc. Rev*. **2012**, *41*, 2539.

Moyano, D. F.; Duncan, B.; Rotello, V. M. *Method. Mol. Biol.* **2013**, *1025*, 3.

Moyano, D. F.; Goldsmith, M.; Solfiell, D. J.; Landesman-Milo, D.; Miranda, O. R.; Peer, D.; Rotello, V. M. *J. Am. Chem. Soc.* **2012**, *134*, 3965.

Moyano, D. F.; Rana, S.; Bunz, U. H. F.; Rotello, V. M. *Faraday Discuss.* **2011**, *152*, 33.

Moyano, D. F.; Rotello, V. M. *Langmuir* **2011**, *27*, 10376.

Moyano, D. F.; Saha, K.; Prakash, G.; Yan, B.; Kong, H.; Yazdani, M.; Rotello, V. M. *ACS Nano* **2014**, *8*, 6748.

Muller-Graff, P. K.; Szelke, H.; Severin, K.; Kramer, R. *Org. Biomol. Chem.* **2010**, *8*, 2327.

Murthy, A. K.; Stover, R. J.; Hardin, W. G.; Schramm, R.; Nie, G. D.; Gourisankar, S.; Truskett, T. M.; Sokolov, K. V.; Johnston, K. P. *J. Am. Chem. Soc.* **2013**, *135*, 7799.

Musto, J. C.; Suslick, K. S. *Curr. Opin. Chem. Biol.* **2010**, *14*, 758.

Nath, S.; Ghosh, S. K.; Kundu, S.; Praharaj, S.; Panigrahi, S.; Pal, T. *J. Nanopart. Res.* **2006**, *8*, 111.

Nobs, L.; Buchegger, F.; Gurny, R.; Allémann, E. *J. Pharm. Sci.* **2004**, *93*, 1980.

Niemeyer, C. M. *Angew. Chem. Int. Ed.* **2001**, *40*, 4128.

Nyren-Erickson, E. K.; Haldar, M. K.; Gu, Y.; Qian, S. Y.; Friesner, D. L.; Malik, S. *Anal. Chem.* **2011**, *83*, 5989.

Owens, D. E.; Peppas, N. A.; *Int. J. Pharm.* **2006**, *307*, 93.

Patel, P. C.; Giljohann, D. A.; Daniel, W. L.; Zheng, D.; Prigodich, A. E.; Mirkin, C. A.; *Bioconjugate Chem.* **2010**, *21*, 2250.

Patil, S.; Sandberg, A.; Heckert, E.; Self, W.; Seal, S. *Biomaterials* **2007**, *28*, 4600.

Pike, J. K.; Ho, T.; Wynne, K. J. *Chem. Mater.* **1996**, *8*, 856.

Peer, D.; Park, E. J.; Morishita, Y.; Carman, C. V.; Shimaoka, M. *Science* **2008**, *319*, 627.

Pelaz, B.; Charron, G.; Pfeiffer, C.; Zhao, Y.; de la Fuente, J. M.; Liang, X.-J.; Parak, W. J.; Del Pino, P. *Small* **2013**, *9*, 1573.

Peng, G.; Hakim, M.; Broza, Y. Y.; Brillan, S.; Abdah-Bortnyak, R.; Kuten, A.; Tisch, U.; Haick, H. *Br. J. Cancer* **2010**, *103*, 542.

Perkins, J.; *Asian J. Transfus. Sci.* **2008**, *2*, 20.

Phillips, R. L.; Miranda, O. R.; Mortenson, D. E.; Subramani, C.; Rotello V. M.; Bunz, U. H. F. *Soft Matter* **2009**, *5*, 607.

Phillips, R. L.; Miranda, O. R.; You, C.-C.; Rotello, V. M.; Bunz, U. H. F. *Angew. Chem. Int. Ed.* **2008**, *47*, 2590.

Pincet, F.; Le Bauer, T.; Zhang, Y.; Esnault, J.; Mallet, J.-M.; Perez, E.; Sinay, P. *Biophys. J.* **2001**, *80*, 1354.

Puzyn, T.; Leszczynska, D.; Leszczynski, J. *Small* **2009**, *5*, 2494.

Puzyn, T.; Rasulev, B.; Gajewicz, A.; Hu, X.; Dasari, T. P.; Michalkova, A.; Hwang, H.-M.; Toropov, A.; Leszczynska, D.; Leszczynski, J. *Nat. Nanotechnol.* **2011**, *6*, 175.

Raftos, D.; Raison, R. L. *Immunol. Cell Biol.* **2008**, *86*, 479.

Rana, S.; Singla, A. K.; Bajaj, A.; Elci, S. G.; Miranda, O. R.; Mout, R.; Yan, B.; Jirik F. R.; Rotello, V. M. *ACS Nano* **2012**, *6*, 8233.

Rana, S.; Yeh, Y.; Rotello, V. M. *Curr. Opin. Chem. Biol.* **2010**, *14*, 828.

Rana, S.; Yu, X.; Patra, D.; Moyano, D. F.; Miranda, O. R.; Hussain, I.; Rotello, V. M. *Langmuir* **2012**, *28*, 2023.

Reddy, S.; Van Der Vlies, A. J.; Simeoni, E.; Angeli, V.; Randolph, G. J.; O'Neil, G. P.; Lee, L. K.; Swartz, M. A.; Hybbell, J. A. *Nat. Biotechnol.* **2007**, *25*, 1159.

Roan, J. R.; *Phys. Rev. Lett.* **2006**, *96*, 248301.

Rodriguez, P. L.; Harada, T.; Christian, D. A.; Pantano, D. A.; Tsai, R. K.; Discher, D. E. *Science* **2013**, *339*, 971.

Rojo, J.; Dıaz, V.; de la Fuente, J. M.; Segura, I.; Barrientos, A. G.; Riese, H. H.; Bernad, A.; Penades, S. *ChemBioChem* **2004**, *3*, 291.

Rose, G. D.; Wolfenden, R. *Annu. Rev. Biopharm. Biomed*. **1993**, *22*, 381.

Rosen, J. E.; Gu, F. X *Langmuir* **2011**, *27*, 10507.

Rother, R. P.; Bell, L.; Hillmen, P.; Gladwin, M. T. *JAMA, J.Am. Med. Assoc.* **2005**, *293*, 1653.

Saha, K.; Agasti, S. S.; Kim, C.; Li, X.; Rotello, V. M. *Chem. Rev.* **2012**, *112*, 2739.

Saha, K.; Bajaj, A.; Duncan, B.; Rotello, V. M. *Small* **2011**, *7*, 1903.

Saha, K.; Moyano, D. F.; Rotello, V. M. *Mater. Horiz.* **2014**, *1*, 102.

Saitoh, D.; Kadota, T.; Senoh, A.; Takahara, T.; Okada, Y.; Mimura, K.; Yamashita, H.; Ohno, H.; Inoue, M. *Am. J. Emerg. Med.* **1993**, *11*, 355.

Salvador-Morales, C.; Flahaut, E.; Sim, E.; Sloan, J.; Green, M. L. H.; Sim, R. B. *Mol. Immunol*. **2006**, *43*, 193

Salvati, A.; Pitek, A. S.; Monopoli, M. P.; Prapainop, K.; Bombelli, F. B.; Hristov, D. R.; Kelly, P. M.; Aberg, C.; Mahon, E.; Dawson, K. A. *Nat. Nanotechnol*. **2013**, *8*, 137.

Sapsford, K. E.; Algar, W. R.; Berti, L.; Gemmill, K. B.; Casey, B. J.; Oh, E.; Stewart, M. H.; Medintz, I. L. *Chem. Rev*. **2013**, *113*, 1904.

Scharte, M.; Fink, M. P. *Crit. Care Med*. **2003**, *31*, S651.

Scott, J. E. *FASEB J.* **1992**, *6*, 2639.

Sekiguchi, S.; Niikura, K.; Matsuo, Y.; Ijiro, K. *Langmuir* **2012**, *28*, 5503.

Seong, S.-Y.; Matzinger, P. *Nat. Rev. Immunol*. **2004**, *4*, 469.

Serda, R. E. *Int. J. Nanomedicine* **2013**, *8*, 1683.

Shahbazi, M.-A.; Fernández, T. D.; Mäkilä, E. M.; Guével, X. L.; Mayorga, C.; Kaasalainen, M. H.; Salonen, J. J.; Hirvonen, J. T.; Santos, H. A. *Biomaterials* **2014**, *35*, 9224.

Sharrna, P.; Brown, S.; Walter, G.; Santra, S.; Moudgil, B. *Adv. Colloid Interface Sci.* **2006**, *123*, 471.

Shebl, F. M.; Pinto, L. A.; García-Piñeres, A.; Lempicki, R.; Williams, M.; Harro, C.; Hildesheim, A. *Cancer Epidem. Biomar*. **2010**, *19*, 978.

Shima, F.; Akagi, T.; Uto, T.; Akashi, M. *Biomaterials* **2013**, *34*, 9709.

Smith, D. M.; Simon, J. K.; Baker Jr, J. R. *Nat. Rev. Immunol.* **2013**, *13*, 592-605.

Sperling, R. A.; Gil, P. R.; Zhang, F.; Zanella, M.; Parak, W. J. *Chem. Soc. Rev.* **2008**, *37*, 1896.

Stroncek, D.; Procter, J. L.; Johnson, J. *Am. J. Hematol.* **2000**, *64*, 67.

Studelska, D. R.; Giljum, K.; McDowell, L. M.; Zhang, L. *Glycobiology* **2006**, *16*, 65.

Sun, W.; Bandmann, H.; Schrader, T. *Chem.–Eur. J.* **2007**, *13*, 7701.

SYSTAT11.0, SystatSoftware, Richmond, CA 94804, USA, **2004**.

Tao, A. R.; Habas, S.; Yang, P. *Small* **2008**, *4*, 310.

Templeton, A. C.; Wuelfing, W. P.; Murray, R. W. *Accounts Chem. Res.* **2000**, *33*, 27.

Tenzer, S.; Docter, D.; Kuharev, J.; Musyanovych, A.; Fetz, V.; Hecht, R.; Schlenk, F.; Fischer, D.; Kiouptsi, K.; Reinhardt, C.; Landfester, K.; Schild, H.; Maskos, M.; Knauer, S. K.; Stauber, R. H. *Nat. Nanotechnol*. **2013**, *8*, 772.

Tonga, G. Y.; Moyano, D. F.; Kim, C. S.; Rotello, V. M. *Curr. Opin. Coll. Inter. Sci.* **2014**, *19*, 49.

Toropov, A. A.; Leszczynska, D.; Leszczynski, J. *Comput. Biol.Chem.* **2007**, *31*, 127.

Umali, A. P.; LeBoeuf, S. E.; Newberry, R. W.; Kim, S.; Tran, L.; Rome, W. A.; Tian, T.; Taing, D.; Hong, J.; Kwan, M.; Heymann, H.; Anslyn, E. V. *Chem. Sci*. **2011**, *2*, 439.

Umali, A. P.; Anslyn, E. V. *Curr. Opin. Chem. Biol*. **2010**, *14*, 685.

Varki, A.; Cummings, R. D.; Esko, J. D.; Freeze, H. H.; Stanley, P.; Bertozzi, C. R.; Hart, G. W.; Etzler, M. E. *Essentials of Glycobiology, Cold Spring Harbor Laboratory Press, New York, 2nd Ed.,* **2009**.

Verma, A.; Stellacci, F. *Small* **2010**, *6*, 12.

Walkey, C. D.; Chan, W. C. W. *Chem. Soc. Rev*. **2012**, *41*, 2780.

Walkey, C. D.; Olsen, J. B.; Guo, H.; Emili, A.; Chan, W. C. *J. Am. Chem. Soc.* **2012**, *134*, 2139.

Wang, J.; Tian, S.; Petros, R. A.; Napier, M. E.; Desimone, J. M. *J. Am. Chem. Soc.* **2010**, *132*, 11206.

Wang, Z.; Jiang, J.; Li, Z.; Zhang, J.; Wang, H.; Qin, Z. J. *Immunother*. **2010**, *33*, 167.

Weintraub, K. *Nature* **2013**, *495*, S14.

Wolff, J. J.; Chi, L.; Linhardt, R. J.; Amster, I. J.; *Anal. Chem.* **2007**, *79*, 2015.

Wright, A. T.; Anslyn, E. V. *Chem. Soc. Rev.* **2006**, *35*, 14.

Xia, X.-R.; Monteiro-Riviere, N. A.; Riviere, J. E. *Nat. Nanotechnol*. **2011**, *5*, 671.

Xiao, W. C.; Lin, J.; Li, M. L.; Ma, Y. J.; Chen, Y. X.; Zhang, C. F.; Li, D.; Gu, H. C. *Contrast Media Mol. Imaging* **2012,** *7*, 320.

Xiao, Y.; Wiesner, M. R. *J. Hazard. Mater*. **2012**, *215*, 146.

Yang, H.; Zhou, Y.; Fung, S.; Wu, L.; Tsai, K.; Tan, R.; Turvey, S. E.; Machuca, T.; De Perrot, M.; Waddell, T. K.; Liu, M. *Part. Syst. Charact.* **2013**, *30*, 1039.

Yang, W.; Liu, S.; Bai, T.; Keefe, A. J.; Zhang, L.; Ella-Menye, J.; Li, Y.; Jiang, S. *Nano Today* **2014**, *9*, 10.

Yang, W.; Zhang, L.; Wang, S.; White, A. D.; Jiang, S. Y. *Biomaterials* **2009**, *30*, 5617.

Yoo, J. W.; Chambers, E.; Mitragotri, S. *Curr. Pharm. Des*. **2010**, *16*, 2298.

You, C. C.; De, M.; Miranda, O. R.; Gider, B.; Ghosh, S. P.; Kim, I.; Erdogan, B.; Krovi, S. A.; Bunz, U. H. F.; Rotello, V. M. *Nat. Nanotechnol.* **2007**, *2*, 318.

You, C.-C.; De, M.; Rotello, V. M. *Org. Lett.* **2005**, *7*, 5685.

Yuerek, S.; Riess, H.; Kreher, S.; Doerken, B.; Salama, A. *Transfus. Med*. **2010**, *20*, 265.

Zhang, C.; Macfarlane, R. J.; Young, K. L.; Choi, C. H. J.; Hao, L.; Auyeung, E.; Liu, G.; Zhou, X.; Mirkin, C. A. *Nat. Mater*. **2013**, *12*, 741.

Zhang, G.; Yang, Z.; Lu, W.; Zhang, R.; Huang, Q.; Tian, M.; Li, L.; Liang, D.; Li, C. *Biomaterials* **2009**, *30*, 1928.

Zhang, T.; Edwards, N. Y.; Bonizzoni, M.; Anslyn, E. V. *J. Am. Chem. Soc.* **2009**, *131*, 11976.

Zhang, Z.; Xie, J.; Liu, H.; Liu J.; Lindhardt, R. J. *Anal.Chem.* **2009**, *81*, 4349.

Zhao, Y. N.; Sun, X. X.; Zhang, G. N.; Trewyn, B. G., Slowing, I. I.; Lin, V. S. Y. *ACS Nano* **2011**, *5*, 1366.

Zhong, Z.; Anslyn, E. V. *J. Am. Chem. Soc.* **2002**, *124*, 9014.

Zhu, Z.-J.; Carboni, R.; Quercio, M. J. Jr.; Yan, B.; Miranda, O. R.; Anderton, D. L.; Arcaro, K. F.; Rotello, V. M.; Vachet, R. W. *Small* **2010**, *6*, 2261.

Zhu, Z.-J.; Ghosh, P.; Miranda, O. R.; Vachet, R. W.; Rotello, V. M. *J. Am. Chem. Soc.* **2008**, *130*, 14139.

Zhu, Z. J.; Posati, T.; Moyano, D. F.; Tang, R.; Yan, B.; Vachet, R. W.; Rotello, V. M. *Small* **2012**, *8*, 2659.

Zuo, Y.; Broughton, D. L.; Bicker, K. L.; Thompson, P. R.; Lavigne, J. J. *ChemBioChem* **2007**, *8*, 2048.